Australian Government
Geoscience Australia

3D Map and Supporting Geophysical Studies in the North Queensland Region

Richard Chopping and Paul A. Henson (Editors)

Record
2009/29

GeoCat #
69581

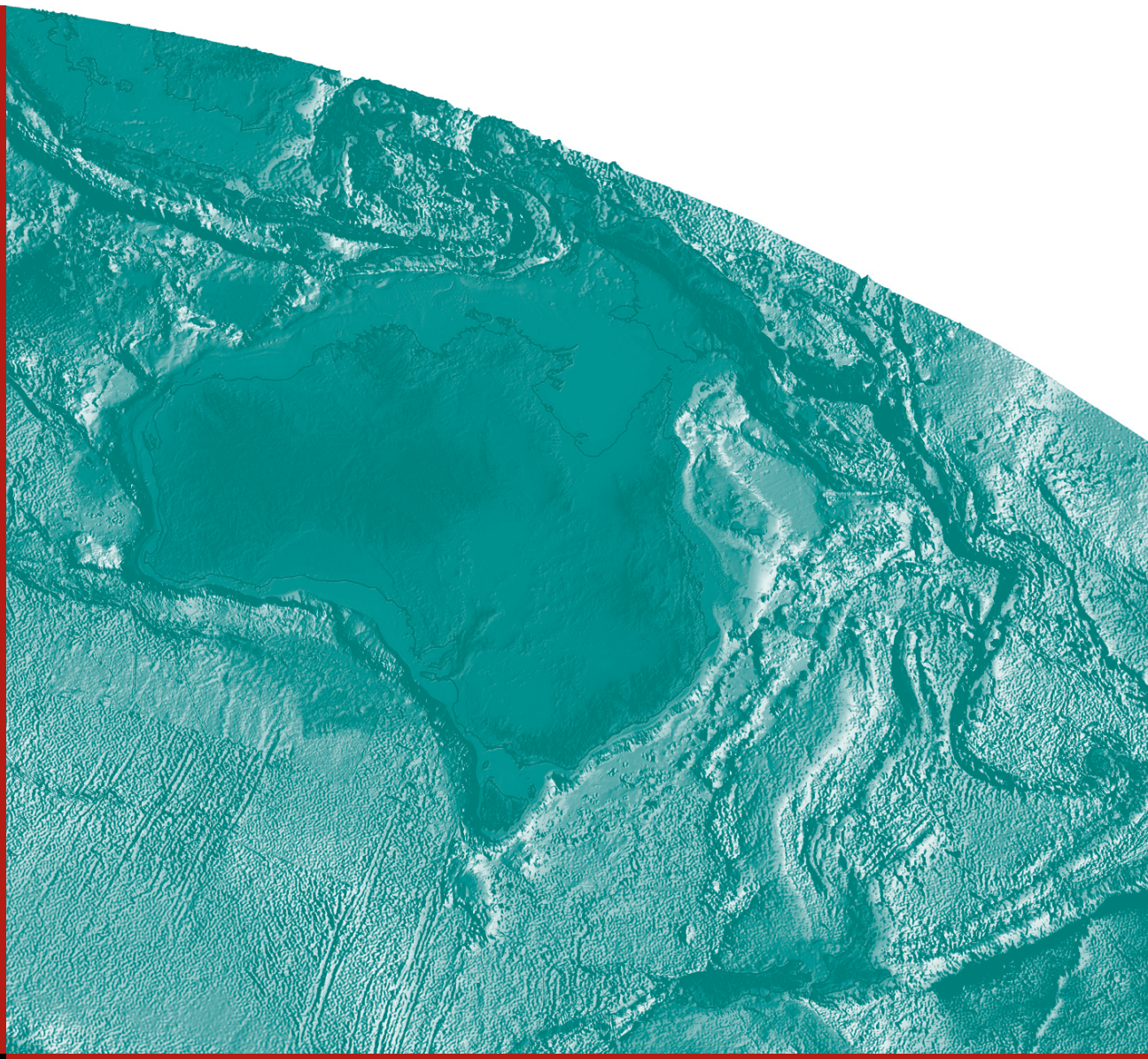

3D map and supporting geophysical studies in the North Queensland region

GEOSCIENCE AUSTRALIA
RECORD 2009/29

Edited by
R. Chopping[1]
P.A. Henson[1]

Contributions from
T. Brennan[1]
D.C. Champion[1]
R. Chopping[1]
R.D. Costelloe[1]
M.A. Craig[1]
P.A. Henson[1]
J. Holzschuh[1]
D.L. Huston[1]
R.J. Korsch[1]
S.F. Liu[1]
A.J. Meixner[1]
P.R. Milligan[1]
A. Nakamura[1]
M.G. Nicoll[1]
I.G. Roy[1]
E. Saygin[1]
N.C. Williams[1]

Australian Government
Geoscience Australia

1. Onshore Energy and Minerals Division, Geoscience Australia, GPO Box 378, Canberra ACT 2601.

Department of Resources, Energy and Tourism
Minister for Resources and Energy: The Hon. Martin Ferguson, AM MP
Secretary: Mr John Pierce

Geoscience Australia
Chief Executive Officer: Dr Neil Williams, PSM

ISSN 1448-2177
ISBN 978 1 921672 19 4 web
ISBN 978 1 921672 20 0 print

GeoCat # 69581

Bibliographic reference: Chopping, R. and Henson, P.A. (Eds.), 2009. *3D map and supporting geophysical studies in the North Queensland region*. Geoscience Australia, Record 2009/29, 82p.

Contents

1. Introduction

R. Chopping and P.A. Henson

1.1 INTRODUCTION, AIMS AND OBJECTIVES

Spatial geoscience data collected at the Earth's surface can provide numerous insights into the three dimensional nature of the underlying geology. The data from geological interpretations, drilling and geophysics can be used to determine the 3D architecture of geological regions. The 3D map is a medium where multidisciplinary data can be viewed and manipulated in a georeferenced space. It enables the relationships between multidisciplinary data to be analysed in 3D, and subsurface interpretations to be constructed into physical objects that can be populated with a variety of properties such as densities from inversions, or proportions of minerals from alteration mapping. Solid volumes representing individual objects can be used for statistical spatial analyses and numerical modelling, allowing the simulation of different geological processes. A 3D map provides a virtual representation of all the spatial data within a geological region and can be used as the basis for a variety of analytical processes. These can vary depending on the available data and the specific hypothesis that is required to be tested.

3D maps are at the forefront of mineral exploration technology and have the capability of greatly improving our understanding of 4D crustal architecture, mineral systems and energy potential. The great advantage of 3D mapping is that all the geological data must be integrated seamlessly within a single environment with all data located spatially correctly. The result is that one must consider the connectivity of the data whereby one area may affect the region as a whole. No longer will research be able to concentrate on an isolated small region, selectively leaving out data that does not fit the model. To put it bluntly, there is nowhere to hide in 3D space!

The recent widespread availability of three dimensional software packages has changed the way we view and analyse geological data. Although geological data have traditionally been interpreted and delivered using 2D technologies, all geological data are inherently 3D and there are many benefits in using the new 3D technologies. Geological and geophysical data collected at the Earth's surface can provide numerous insights into the depth component of the surface geology. These data, combined with seismic reflection and magnetotelluric data, are capable of being used to determine subsurface architecture, and differentiation of major crustal components.

The Australian Government's Onshore Energy Security Program, combined with the Queensland Government's Smart Mining and Smart Exploration initiatives, have enabled significant new geophysical and geological data to be acquired in the North Queensland region. These data include:

- Six new deep crustal seismic reflection lines acquired in 2006 in the Mount Isa Province, covering the region from the Century Mine to the Cannington Mine;
- Two lines acquired in 1994 which were reprocessed;
- Four new seismic reflection lines, acquired in 2007 by Geoscience Australia, the Geological Survey of Queensland and AuScope, that link with the 2006 seismic survey to the northeast of Cloncurry and cover the region through to Georgetown and Charters Towers; and
- Three magnetotelluric lines acquired and processed by Quantec Geoscience for Geoscience Australia and the Geological Survey of Queensland along three of the 2007 seismic reflection lines.

Geoscience Australia, along with its partners, have used these data and pre-existing geological and geophysical data, to provide new insights into the 3D architecture, geodynamics, mineral and the energy potential of this region. The 3D architecture was constrained using all available data leading

to an improved understanding of the North Queensland region. Innovative 3D geophysical techniques have been adopted to provide new understandings of the 3D alteration patterns associated with potential mineralisation and energy potential of the region.

The body of this report comprises three sections:
Section 2: Data used in the study. In this section, we discuss the seismic, magnetotelluric, potential field, geology, isotope geochemistry, regolith and rock property data available in the North Queensland region.
Section 3: Supporting geophysical studies. This section is a discussion on the methods used for accompanying geophysical studies. Depth to basement mapping, forward-modelling seismic interpretations against gravity data, potential field worms and their interpretations, and inverse modelling of the available gravity and magnetic data are discussed.
Section 4: 3D map and interpretations. This section contains a discussion on the constraints applied to the 3D map, the 4D evolution of the North Queensland region, as well as a discussion on the use of potential field inversions to define mineralised zones. A preliminary interpretation of the properties of the granites beneath the Millungera Basin, which may have implications for energy resources in the region, is also discussed.

Area of interest and geographic projection

The area of interest was selected to encompass the region of the 2007 seismic lines 07GA-IG1, 07GA IG2, 07GA-GC1 and 07GA-A1. Accordingly, the area of interest is between 139°30' and 147°E and 17°S to 22°S.

This area spans two Map Grid of Australia zones, namely zones 54 and 55. To minimise distortion in the 3D map and supporting studies, a customised projection, named TM144 (refer Table 1.1), has been used. This projection uses the GDA94 spheroid and a universal transverse Mercator projection, just as the Map Grid of Australia uses, but a central meridian of 144°E, approximately halfway between the central meridian for zone 54 (141°E) and zone 55 (147°E). All other features of the projection, such as false easting and northing, are identical to MGA zones.

Table 1.1: TM144 projection information.

PARAMETER	VALUE
Projection	Transverse Mercator
False easting	500 000.0
False northing	10 000 000.0
Central meridian	141° E
Scale factor	0.99960
Latitude of origin	0°
Linear unit	Metre
Datum	Geocentric Datum of Australia, 1994 (GDA94)
Spheroid	GRS 1980

Acknowledgements

The work in this study was conducted as part of the Australian Government's Onshore Energy Security Program. The following reviewers, who reviewed all or part of this report, significantly improved its quality: A. Barnicoat, E. Gerner, D. Huston, A. Kirkby, R. Korsch, N. Kositcin, A. Meixner, P. Milligan, N. Neumann, A. Schofield, S. van der Wielen and N. Williams.

2. Data used in the North Queensland region

2.1 SEISMIC REFLECTION AND MAGNETOTELLURIC DATA

P.A. Henson, R.J. Korsch, R.D. Costelloe, J. Holzschuh, A. Nakamura, E. Saygin, P.R. Milligan, M.G. Nicoll and T. Brennan

Introduction

The North Queensland region has a relatively extensive coverage of deep crustal seismic reflection lines (Figure 2.1.1). Two explosive-source lines were acquired in 1994: 94MTI-01 and 94MTI-02. A series of six vibroseis source lines were acquired in 2006: 06GA-M1 through 06GA-M6. Four additional vibroseis lines were acquired in 2007: 07GA-IG1, 07GA-IG2, 07GA-GC1 and 07GA-A1. These data were acquired collaboratively by Geoscience Australia, the Geological Survey of Queensland, the Predictive Mineral Discovery Cooperative Research Centre (pmd*CRC), Zinifex and AuScope, using the resources of ANSIR (Australian National Facility for Earth Sounding). Magnetotelluric data were acquired coincident with lines 07GA-IG1, 07GA-IG2 and 07GA-GC1; these data were acquired and processed by Quantec Geoscience. The seismic reflection and MT data are discussed in more detail in the North Queensland Seismic and MT Workshop notes (Camuti and Young, 2009).

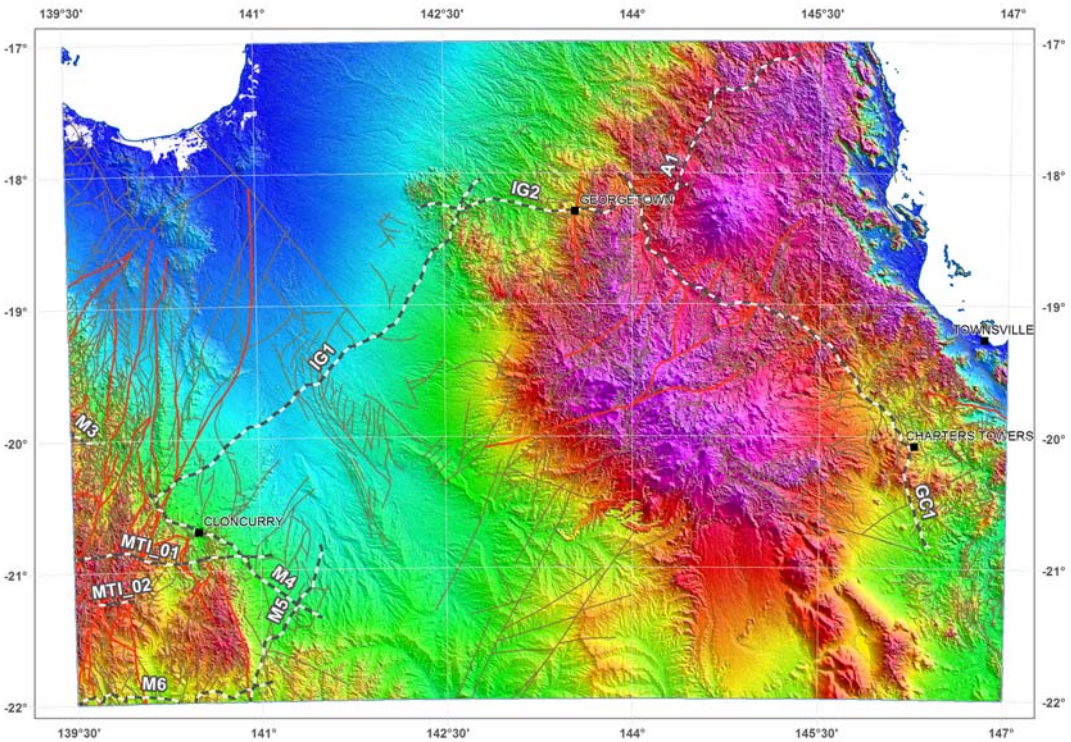

Figure 2.1.1: *Location of seismic lines 94MTI-01 and -02 (MTI_01 and MTI_02, respectively), 06GA-M3, -M4, -M5 and –M6 (M3, M4, M5 and M6, respectively) and 07GA-IG1, -IG2, -GC1 and –A1 (IG1, IG2, GC1 and A1, respectively) displayed on a digital elevation model derived from Shuttle Radar Topographic Mission (SRTM) data. Map projection is GDA94 TM144 projection, a Universal Transverse Mercator projection, central meridian 144°E. The majority of maps in this report are displayed in this projection.*

Note that the 3D map area of interest covered by the North Queensland 3D map was selected to cover the area bounded by the 2007 lines. This area also contains portions of all of the lines 94MTI-01, 06GA-M3, 06GA-M4, 06GA-M5 and 06GA-M6.

Seismic reflection interpretations

A series of large-scale crustal features can be identified in the seismic reflection and magnetotelluric data that have not previously been imaged using other geophysical techniques. The 3D architecture derived from these data has significant implications for the geodynamic understanding of the region and for identifying potential sites of mineralisation. The following summarises some of the significant components identified along the four new 2007 seismic lines that were used as constraints in the 3D interpretations. Further details can be found in Camuti and Young (2009). Seismic reflection data provided the majority of subsurface constraints, while the magnetotelluric data were used as an independent dataset at selected locations along the seismic lines.

The westernmost extremity of the 2007 survey, on the 07GA-IG1 seismic line, is within the Eastern Fold Belt of the Mount Isa Province and ties to the 06GA-M4 seismic line, which forms part of the 2006 Mount Isa Seismic Survey. These data provided new insights into the crustal architecture from the Mount Isa Province through to Charters Towers, and were used to constrain the geometries of faults, lithologies and terrane boundaries at depth.

07GA-IG1

The western extremity of the Mount Isa Eastern Province-Eastern Fold Belt marks the site of a major crustal feature that is imaged in the 07GA-IG1 seismic line as a change in reflectivity and abrupt thickening of the Moho to the west. Reflections dipping to the west in the seismic data, correspond with a major conductive zone that dips at a similar angle in the magnetotelluric 2D conductivity section (Korsch et al., 2009). Additionally, a major gradient occurs in the magnetic inversion data, closely corresponding with this structure (Chopping et al., 2009). This geometry, interpreted as a suture by Korsch et al. (2009) places the IOCG deposits of the Mount Isa Eastern Succession in the hangingwall of this structure.

To the west of this structure, reflectivity is relatively homogenous through the crust. In contrast, the seismic data images a highly reflective lower crust to the east, termed the Numil Seismic Province, overlain by a less reflective upper crust, termed the Kowanyama Province. The upper crust also images a relatively flat-lying, mildly inverted stratigraphic succession of undetermined age, termed the Millungera Basin (Korsch et al., 2009) which lies below the Eromanga Basin. This basin is also imaged in the magnetotelluric data as a conductive region. Economically, this basin may provide potential for geothermal energy based on a series of granites interpreted beneath the basin succession.

The northeastern end of the 07GA-IG1 seismic line images a major crustal structure that continues from the mid-crust into the mantle and offsets the Moho by ~6 km. Korsch et al. (2009) interpret this to be a possible relic subduction zone similar to examples in Canada (Cook et al., 2001) and north of Scotland (Morgan et al., 1994). This structure is the eastern termination of the Numil Seismic Province. The magnetotelluric 2D conductivity section also images a major change in the upper crust at this locality, with the region to the east showing significantly lower conductivity. The crust to the east of this zone contains a highly reflective lower crust and a less reflective upper crust that continues to the intersection with the 07GA-IG2 line.

07GA-IG2

The east-west trending 07GA-IG2 line images two distinctive crustal layers, with the upper less reflective crust interpreted to be the Etheridge Province and the underlying highly reflective zone interpreted as possible Archean or Paleoproterozoic age, termed the Numil and Abingdon Seismic Provinces (Hutton et al., 2009). These terranes display similar reflectivity and are juxtaposed by the apparent west dipping structure that offsets the Moho and terminates against the base of the Georgetown Province. A west-dipping structure imaged to the west of Georgetown displays possible extensional displacement which is spatially coincident with a change in isotopic signature in the exposed Etheridge Group (A. Lambeck, unpublished data). This locality is also imaged in the magnetotelluric as a west-dipping, highly-conductive zone.

07GA-GC1 and 07GA-A1

Both 07GA-GC1 and 07GA-A1 seismic lines image the eastward-tapering termination of the highly reflective Abingdon Seismic Province (Henderson et al., 2009; Withnall et al., 2009). This interpretation is consistent with the Sm-Nd isotopic data (Section 2.4), which shows old model crustal ages in the west, intermediate ages above the tapering Abingdon Seismic Province and younger ages further east. To the southeast of the exposed Etheridge Province, the mid to lower crustal reflectivity is similar to that of the Etheridge Province, whereas the Sm-Nd isotopic data suggests more juvenile crust in this region and hence it has been referred to as the Agwamin Seismic Province (Withnall et al., 2009). This has important implications for evolution of the Neoproterozoic to Phanerozoic terranes to the east and will be described in detail in the following sections.

06GA-M4, 06GA-M5, 06GA-M6 and 94MTI-01 seismic lines

Four additional lines, namely the 06GA-M4, 06GA-M5, 06GA-M6 lines acquired in 2006 and the 94MTI-01 seismic line acquired in 1994, were used to constrain the eastern edge of the Mount Isa Province. The previous seismic interpretations of these lines were used to define the architecture within this study.

Magnetotelluric data

The 2007 magnetotelluric data were acquired and processed by Quantec Geoscience, along the 07GA-IG1, 07GA-IG2, 07GA-GC1 seismic reflection lines, for Geoscience Australia and the Geological Survey of Queensland. Magnetotellurics (MT) is a natural source electromagnetic method which measures variations in the Earth's magnetic and electric fields. These data were processed to produce a series of interpreted 2D conductivity sections that model the conductivity to a depth of ~80 km. The role of magnetotelluric data in this study was to compare the geometries of the conductivity profiles against the interpreted geometries of the seismic reflection data. Some of the significant relationships that occurred are highlighted in this report.

From a qualitative interpretation, the magnetotelluric data appear to clearly delineate upper crustal basins, including the Millungera and Drummond basins, as conductive zones, whereas the regions that are dominated by granites at surface generally represent regions of low conductivity.

References

Camuti, K., and Young, D. (Eds.), 2009. *Northern Queensland Exploration and Mining 2009 and North Queensland Seismic and MT Workshop.* Australian Institute of Geoscientists Bulletin 49, 202p.

Chopping, R., Henson, P., Meixner, T., Roy, I.G. and Milligan, P., 2009. Use of potential field data sets to support the North Queensland seismic interpretations. In: Camuti, K., and Young, D. (Eds.). *Northern Queensland Exploration and Mining 2009 and North Queensland Seismic and MT Workshop.* Australian Institute of Geoscientists Bulletin 49, pp. 143-147.

Cook, F.A., van der Velden, A.J., Hall, K.W. and Roberts, B.J., 1998. Tectonic delamination and subcrustal imbrication of the Precambrian lithosphere in northwestern Canada mapped by LITHOPROBE. *Geology*, **26**(9), pp. 839-842.

Henderson, R.A., Fergusson, C.L., Collins, W.J., Henson, P.A., Korsch, R.J., Blewett, R.S., Withnall, I.W., Hutton, L.J., Costelloe, R.D., Champion, D.C., Blenkinsop, T.G., Wormald, R. and Nicoll, M.G., 2009. Geological interpretation of deep seismic reflection line 07GA-A1: The AuScope Mt Surprise to Mareeba transect. In: Camuti, K., and Young, D. (Eds.). Northern Queensland Exploration and Mining 2009 and North Queensland Seismic and MT Workshop. Australian Institute of Geoscientists Bulletin 49, pp. 169-173.

Hutton, L.J, Blewett, R.S., Henson, P.A., Withnall, I.W., Korsch, R.J., Nakamura, A., Collins, W.J., Henderson, R.A., Fergusson, C.L., Huston, D.L., Champion, D.C., Meixner, A.J., Nicoll, M.G., Blenkinsop, T.G. and Wormald, R., 2009. Geological interpretation of deep seismic reflection line 07GA-IG2: The Croydon to Mt Surprise transect. In: Camuti, K., and Young, D. (Eds.). Northern Queensland Exploration and Mining 2009 and North Queensland Seismic and MT Workshop. Australian Institute of Geoscientists Bulletin 49, pp. 159-162.

Korsch, R.J., Withnall, I.W., Hutton, L.J., Henson, P.A., Blewett, R.S., Huston, D.L., Champion, D.C., Meixner, A.J., Nicoll, M.G., and Nakamura, A., 2009. Geological interpretation of deep seismic reflection line 07GA-IG1: The Cloncurry to Croydon transect. In: Camuti, K., and Young, D. (Eds.). Northern Queensland Exploration and Mining 2009 and North Queensland Seismic and MT Workshop. Australian Institute of Geoscientists Bulletin 49, pp. 153-157.

Morgan, J.V., Hadwin, M, Warner, M.R., Barton, P.J. and Morgan, R.P.L.I., 1994. The polarity of deep seismic reflections from the lithospheric mantle: evidence for a relict subduction zone. Tectonophysics, 232(1-4), pp. 319-328.

Withnall, I.W., Korsch, R.J., Blewett, R.S., Henson, P.A., Hutton, L.J., Holzschuh, J., Saygin, E., Fergusson, C.L., Collins, W.J., Henderson, R.A., Huston, D.L., Champion, D.C., Nicoll, M.G., Blenkinsop, T.G. and Wormald, R., 2009. Geological interpretation of deep seismic reflection line 07GA-GC1: The Georgetown to Charters Towers transect. In: Camuti, K., and Young, D. (Eds.). Northern Queensland Exploration and Mining 2009 and North Queensland Seismic and MT Workshop. Australian Institute of Geoscientists Bulletin 49, pp. 163-167.

2.2 POTENTIAL FIELD DATA

R. Chopping, P.R. Milligan and T. Brennan

Relatively high resolution and high quality gravity and total magnetic intensity data are available for the North Queensland region. These data are available through national compilations of gravity (Bacchin et al., 2008) and magnetic (Milligan and Franklin, 2004) data, accessible on the Geophysical Archive Data Delivery System (GADDS: Geoscience Australia, 2009).

Gravity data

Gravity data in the North Queensland region are derived from the national gravity database. Most of these data were acquired by the Geological Survey of Queensland and Geoscience Australia although the database includes data acquired by other sources such as universities or mineral explorers. These data are variable in their spacing (Figure 2.2.1) but the majority of the region is covered by ~4 km spaced gravity data. Some regions, such as around Cloncurry and Charters Towers, have gravity stations spaced between 1 and 2 km apart. Finally, some regions such as that north of 18°S and east of 144°E have gravity station spacings of ~10 km.

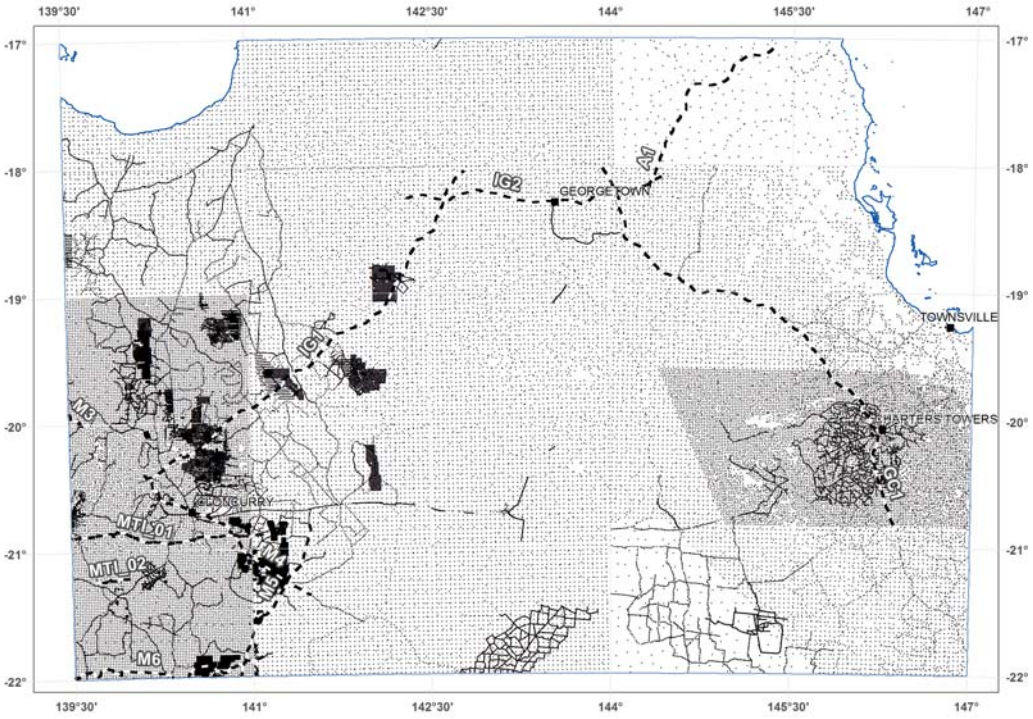

Figure 2.2.1: *Gravity stations in the North Queensland region.*

These data were gridded nationally (Bacchin et al., 2008) using the Variable Sampling Density Gridding (from Intrepid Geophysics) method to a nominal 800 m cell resolution, and were extracted for the North Queensland region (Figure 2.2.2).

Magnetic intensity data

In the North Queensland region, the majority of aeromagnetic data have been acquired at line spacings of 500 m or better. Some data, however, are spaced up to 3 km apart (Figure 2.2.3). The current national magnetic data have been gridded using variable sampling density gridding at a nominal cell resolution of 400 m (Milligan and Franklin, 2004). The data for North Queensland have been extracted from this national coverage (Figure 2.2.4).

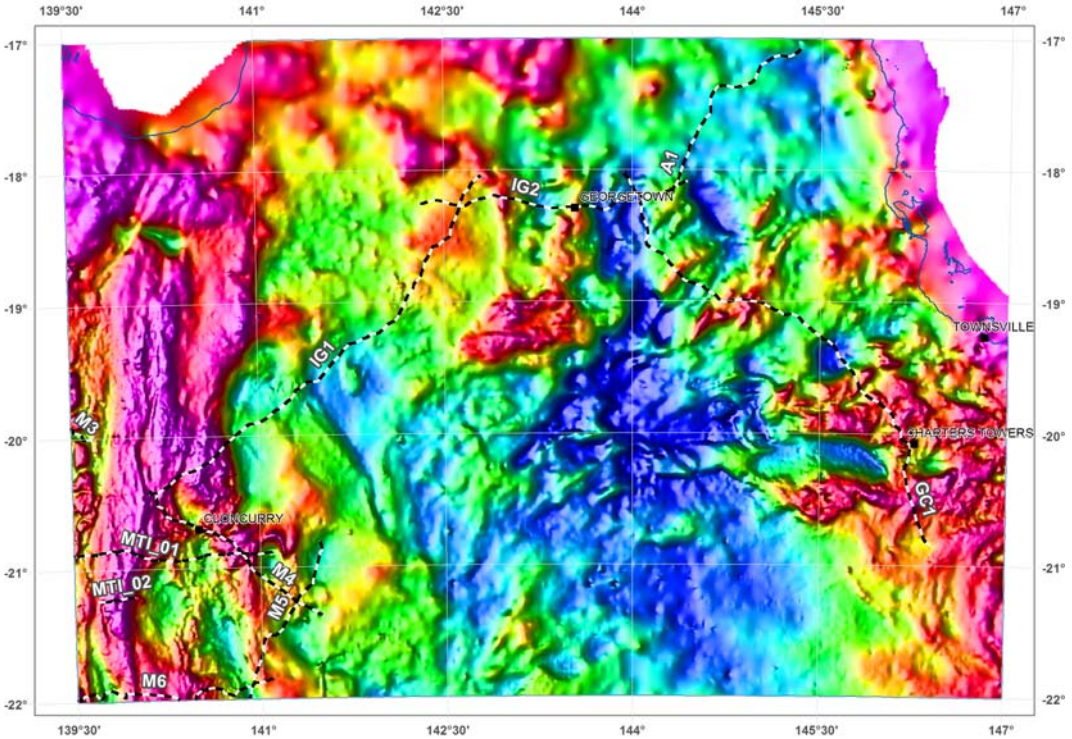

Figure 2.2.2: *Bouguer gravity in the North Queensland region.*

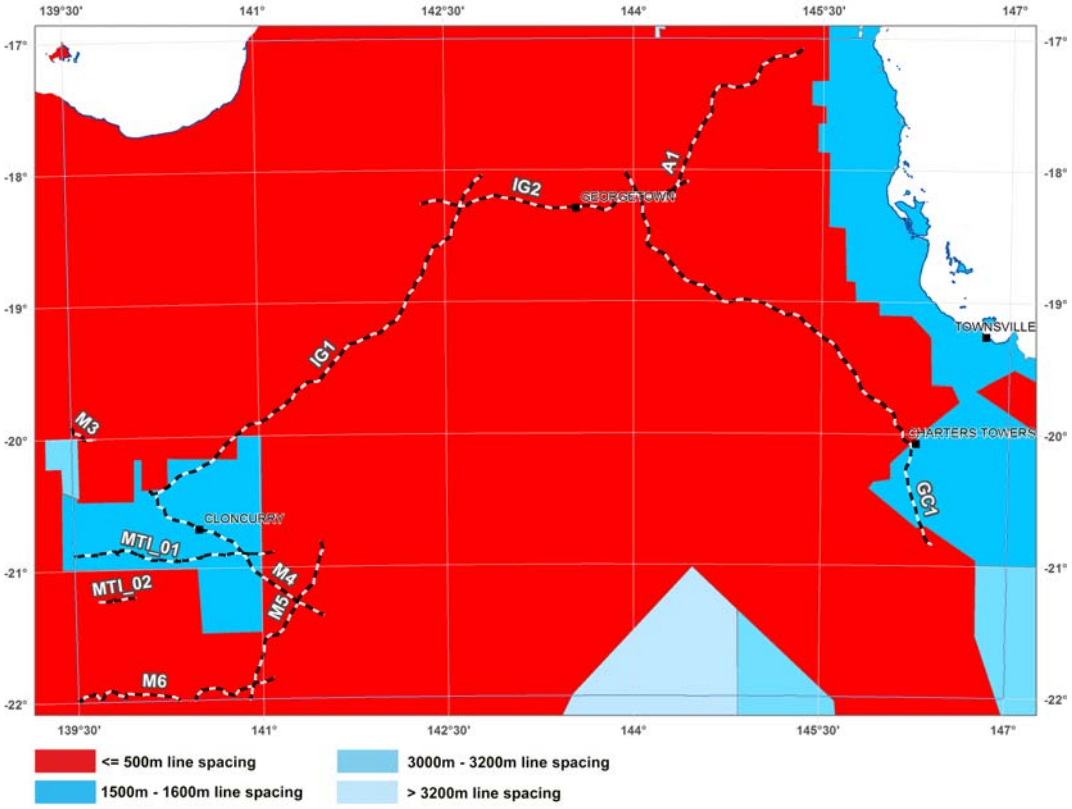

Figure 2.2.3: *Aeromagnetic survey coverage in the North Queensland region.*

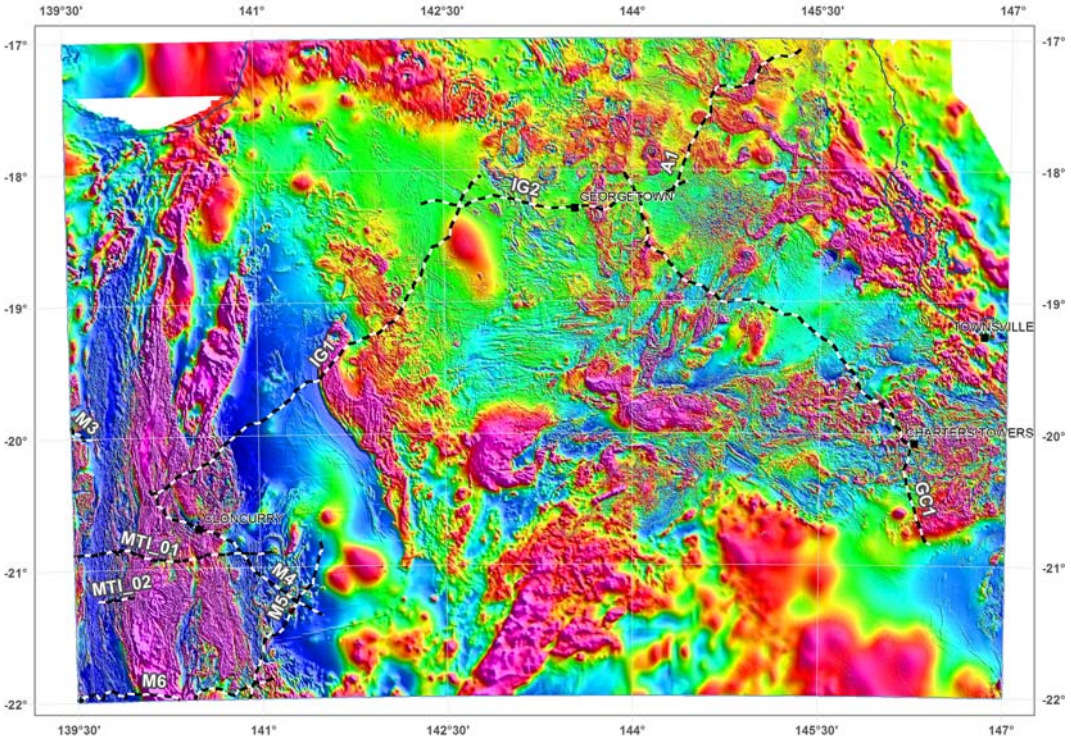

Figure 2.2.4: *Total magnetic intensity in the North Queensland region.*

References

Bacchin M., Milligan, P.R., Wynne, P. and Tracey, R., 2008. *Gravity anomaly map of the Australian region (Third Edition)*. Geoscience Australia, Canberra.

Geoscience Australia, 2009. Geophysical Archive Data Delivery System (GADDS). http://www.geoscience.gov.au/gadds/.

Milligan, P.R. and Franklin, R., 2004. *Magnetic Anomaly Map of Australia (Fourth Edition)*. Geoscience Australia, Canberra.

2.3 SOLID GEOLOGY DATA

S.F. Liu

The solid geology used in the North Queensland region (Liu et al., 2009) drew extensively on published 1:100 000, 1:250 000 and smaller-scale regional geological maps and analysis of regional aeromagnetic data. Gravity and borehole data were also used to complement the interpretation.

Flat-lying Cenozoic and Mesozoic cover materials have been excluded across the map area, and Paleozoic sediment have also been removed in the Mount Isa area in the west (north of the Diamantina Fault or northwest of the Thomson Orogen).

The digital data that accompanies this map contain lithostratigraphic units compiled at 1:1 000 000 scale. Approximately 900 mapped units are described in the Australian Stratigraphic Units Database (Geoscience Australia, 2009). The hard copy map (Liu, 2009) is simplified from the digital data to show the distribution of major lithology groups of different ages. The user is encouraged to use the publicly available digital data, included in the electronic version of Liu (2009), for more information.

Geological interpretation and compilation by S.F. Liu (Geoscience Australia), 2007-2008, with contributions from I.W. Withnall, L.J. Hutton (Geological Survey of Queensland), D.C. Champion, G.M. Gibson, and D.L. Huston (Geoscience Australia).

References

Geoscience Australia, 2009. Australian Stratigraphic Units Database. http://www.ga.gov.au/oracle/stratnames/index.jsp.

Liu, S.F., 2009. Basement Geology of Northern Queensland (First Edition), 1:1 000 000 scale. Geoscience Australia, Canberra, GeoCat #: 68592. https://www.ga.gov.au/products/servlet/controller?event=GEOCAT_DETAILS&catno=68592.

2.4 Sm-Nd DATA

D.C. Champion, P.A. Henson and T. Brennan

Samarium-neodynium (Sm-Nd) is an isotopic system often used to study the evolution of igneous rocks (DePaolo and Wasserburg, 1976; Champion and Cassidy, 2008). Sm-Nd data can also be used to produce a map of relative crustal ages, using Sm-Nd model ages (T_{DM}).

Sm-Nd data for felsic gneisses, granites and volcanics show that this region has a range of crustal model ages (Figure 2.4.1). These variations are interpreted to largely reflect the relative ages of the underlying crustal units, and hence can be used as a discriminator of different crustal components. The data indicate a broad younging trend to the east, with a gradient occurring within the Eastern Fold Belt of the Mount Isa Province and a major transition occurring to the east of Georgetown.

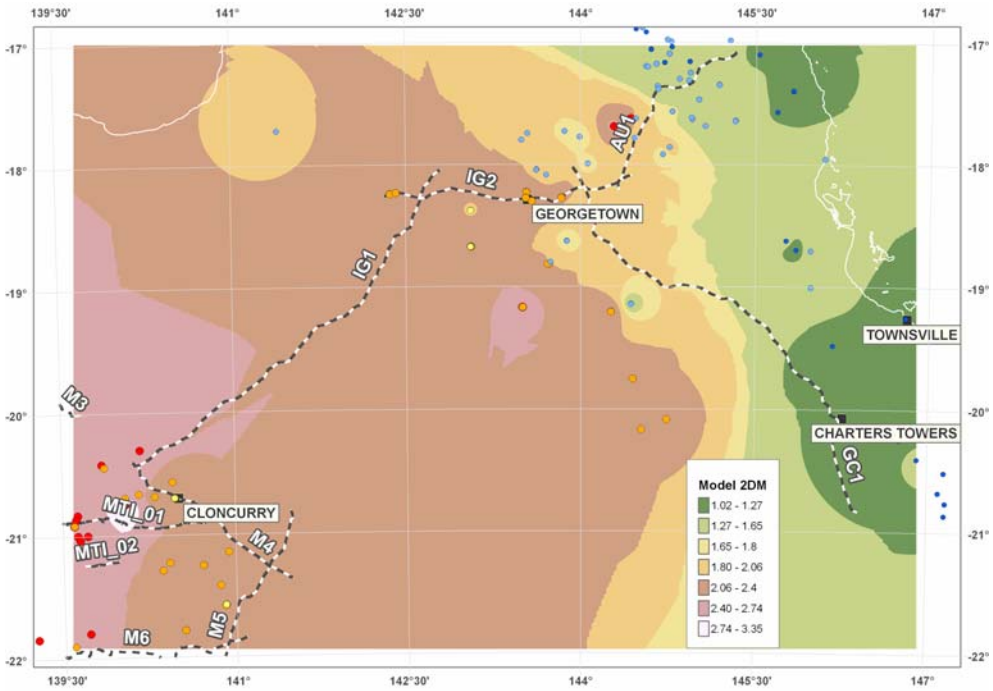

Figure 2.4.1: *Gridded image of Sm-Nd isotopic data showing the model crustal ages in the Mount Isa, Georgetown and Charters Towers region. Coloured dots (coloured by age) indicate sample locations.*

These Sm-Nd data were compared spatially with the seismic reflection and magnetotelluric data in order to derive an understanding of the different crustal components and relative ages of the middle to lower crust where these melts would have been formed. In parallel, inherited zircon ages were compared against the Sm-Nd model ages and showed very similar trends.

References

Champion, D.C. and Cassidy, K.F., 2008. Geodynamics: Using geochemistry and isotopic signatures of granites to aid mineral systems studies: and example from the Yilgarn Craton. In: Korsch, R.J. and Barnicoat, A.C., (Eds.), 2008, *New Perspectives: the foundations and future of Australian exploration – Abstracts for the June 2008 pmd*CRC Conference.* Geoscience Australia, Canberra, Record 2008/09, pp. 7-16.

DePaolo, D.J. and Wasserburg, G.J., 1976. Nd isotopic variations and petrogenetic models. *Geophysical Research Letters*, **3**(5), pp. 249–252.

2.5 REGOLITH

M.A. Craig

Introduction

This report provides a summary of the distribution and characteristics of regolith materials that occur within the area of the North Queensland 3D map. Regolith units for this study were extracted from the 1:2 500 000 and 1:250 000 scale regolith-landform map of Queensland (Craig, 2008; Craig et al., 2008). For convenience of description, the area of the North Queensland 3D map has been divided into major regolith regions (Figure 2.5.1).

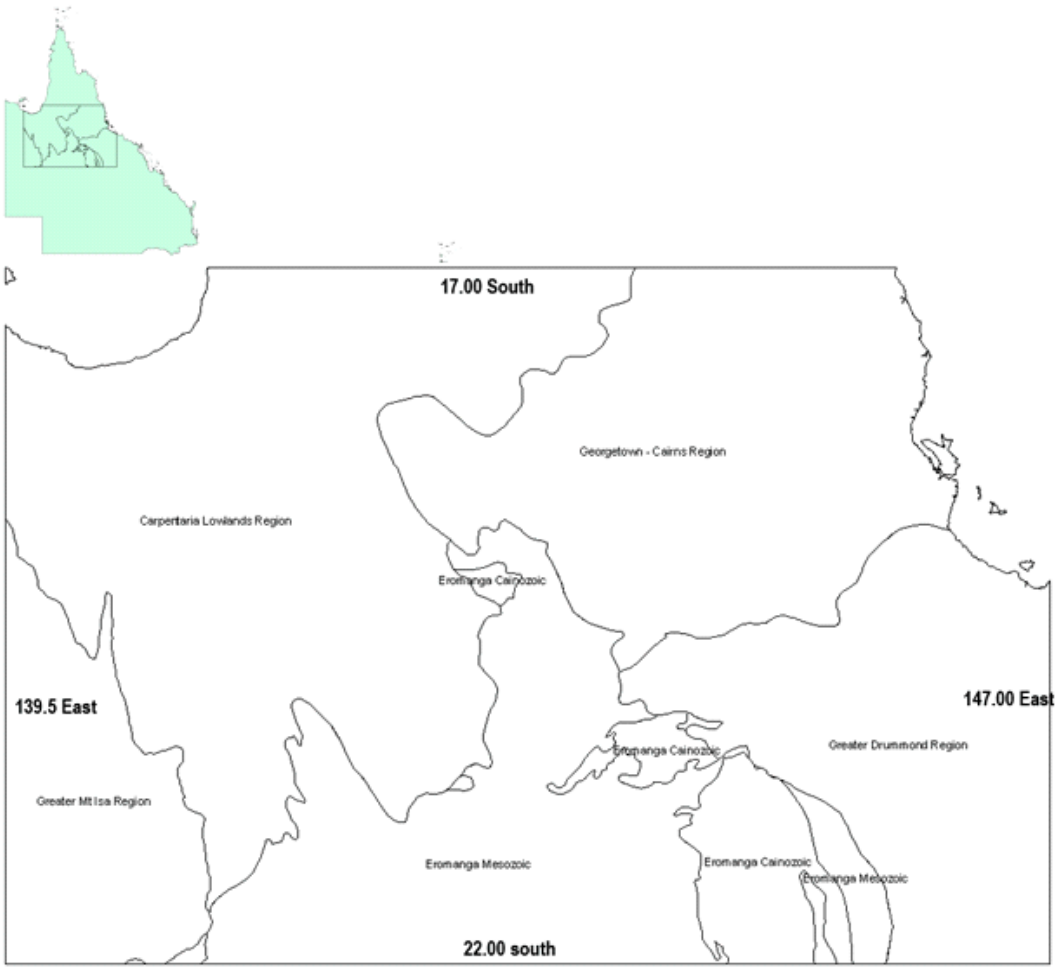

Figure 2.5.1: *Surface geological regions in the North Queensland 3D map area.*

Regolith landform units in the North Queensland region

Figure 2.5.2 shows the broad distribution of regolith-landform units extracted from the 1:2 500 000 scale Regolith-Landform map (Craig et al., 2008). Figure 2.5.3 shows the broad distribution of regolith-landform units extracted from the 1:250 000 scale Regolith-Landform map (Craig et al., 2008). Map symbols in Figure 2.5.3 are after Pain et al. (2007).

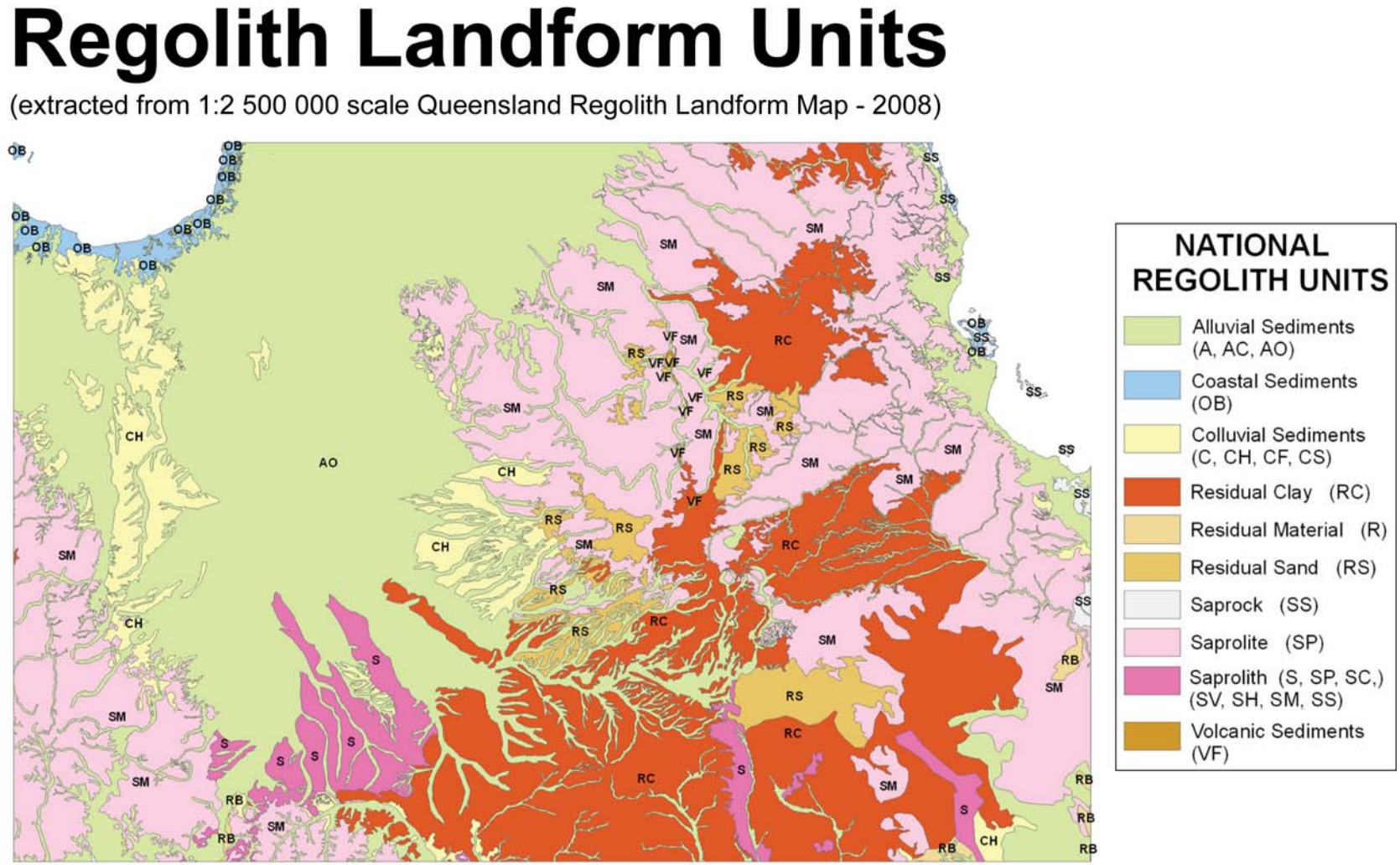

Figure 2.5.2: *Regolith landform units in the North Queensland 3D map area, extracted from the Queensland 1:2 500 000 regolith-landform map (Craig et al., 2008).*

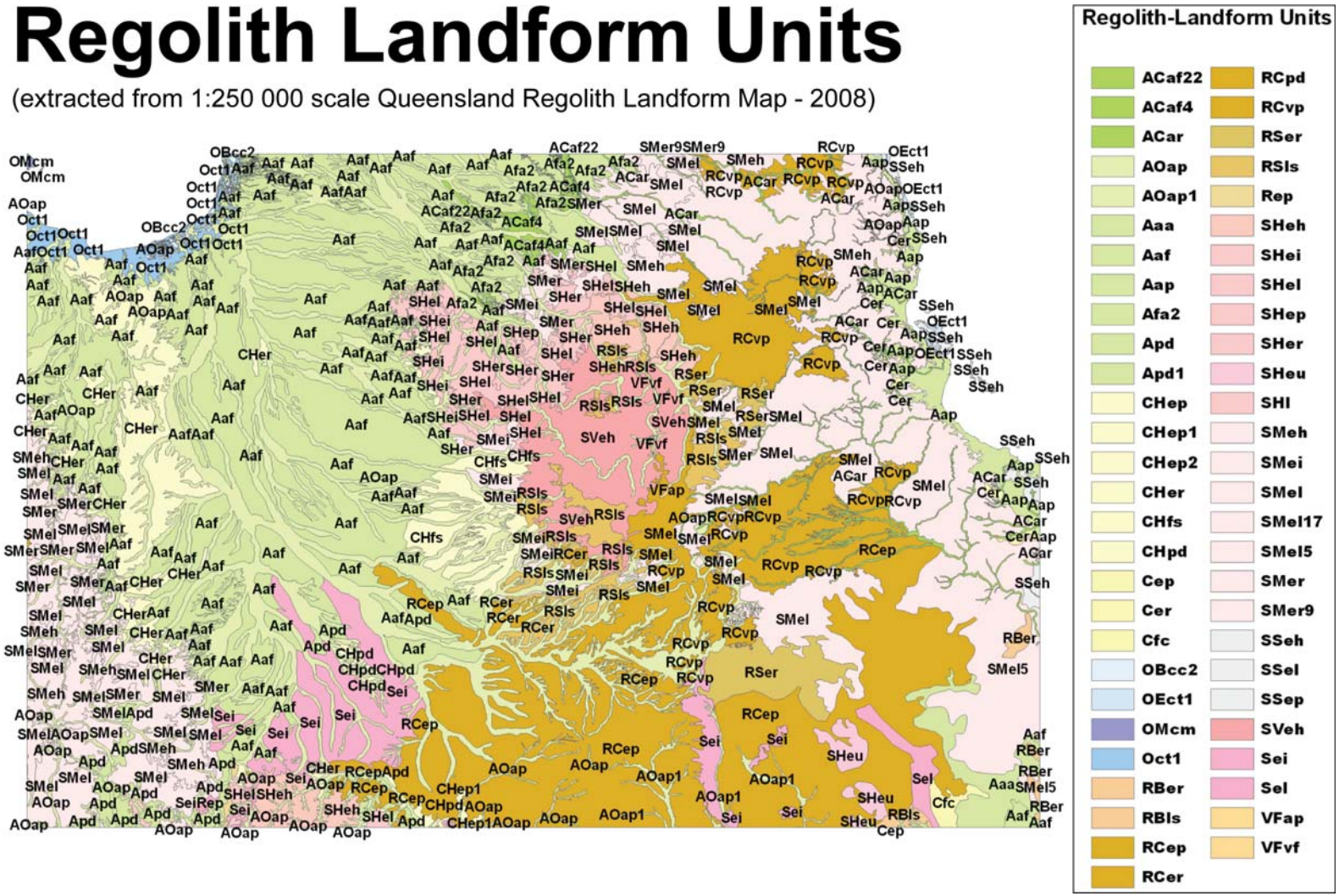

Figure 2.5.3: *Regolith landform units in the North Queensland 3D map area, extracted from the Queensland 1:2 500 000 regolith-landform map (Craig et al., 2008). Map units are labelled as per Pain et al. (2007).*

Characteristics of regolith in the North Queensland region

Ten regolith landform units occur throughout the North Queensland area. They are defined in the Queensland 1:2 500 000 scale regolith-landform map (Figure 2.5.2). Considerably more detail in the abundance of regolith units is apparent in the 1:250 000 regolith landform map (Figure 2.5.3); nevertheless, the 1:2 500 000 scale regolith landform map provides a broad overview of the distribution of regolith units in the North Queensland region.

It is apparent from the 1:2 500 000 scale regolith-landform map (Figure 2.5.2) that *in situ* regolith is dominant in the region. In total, only 39% of the region is transported material whereas *in situ* material cover approximately 61%. Of the *in situ* regolith material, there is an approximate 50-50 split between pedolith (that is, residual materials) and saprolith (that is, saprolite and saprock). Figure 2.5.4 shows more clearly the relationships between these various regolith material and the terms used to describe the regolith components.

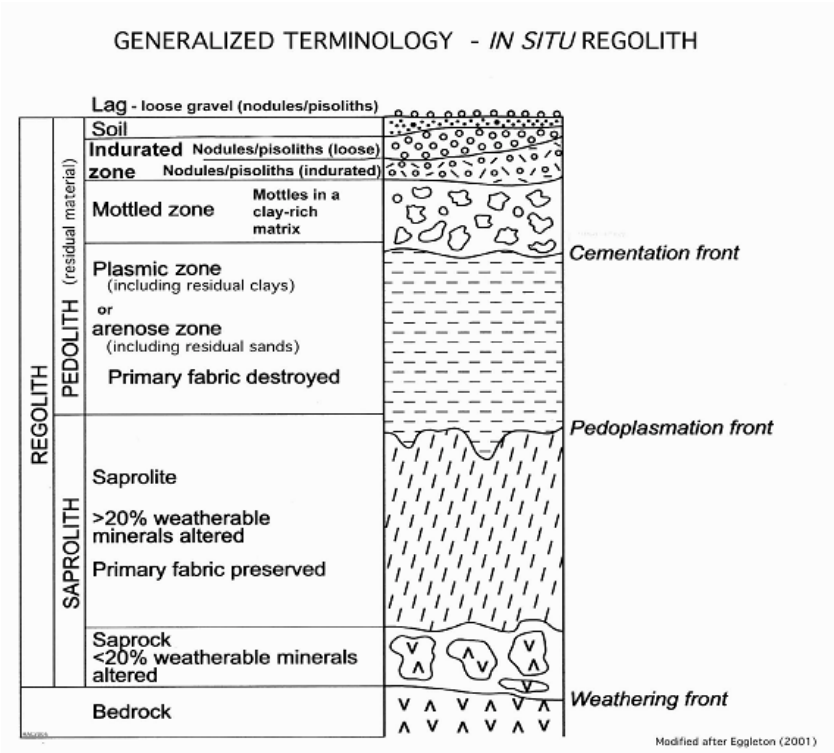

Figure 2.5.4: *Generalised regolith profile terminology.*

Of the transported regolith material in the North Queensland region, the majority (around 31% of the area) is alluvial material. Most of the rest of the transported material are colluvial sediments (7% of the area) and coastal sediments (1.3% of the area), with only very minor volcanic sediments in the North Queensland area.

Implications of the nature of regolith in the North Queensland region

Regolith tends to obscure the nature of fresh rock outcrops. The extent to which regolith material obscures the fresh rock outcrop can be measured by determining the overall proportion of transported regolith, plus the proportion of pedolith (see definition in Figure 2.5.4) in the remaining *in situ* regolith. Pedolith is often an obscuring component and should be included in such assessments for the North Queensland area, given the extensive nature of it in this area.

On this basis, regolith covers approximately 70% of the landscape, thus obscuring bedrock exposure. Of the bedrock that is in some way visible at the surface (30% of the area), very little is unweathered. Only about 12% of the total area is unweathered. Here, unweathered means bedrock that ranges from slightly weathered to relatively fresh. Most of the *in situ* regolith exposures (nominally bedrock) in the region are quite weathered.

The nature of weathering in the North Queensland region

Weathering is extensive across the region. In some parts, it is more obvious because of the landscapes that have resulted from these processes. Escarpments and isolated tablelands or hills (Figure 2.5.5) are the more distinctive features that are the most easily seen.

There are, however, more subtle, often pervasive effects visible in the *in situ* regolith across the region. In particular, the effects of weathering are especially visible in the *in situ* components of regolith within the Eromanga Mesozoic geological region (see Figure 2.5.1). Across this region of the North Queensland 3D map area, *in situ* regolith includes very highly weathered components of the relatively flat-lying Cretaceous bedrock. Very little, if any, of these Cretaceous sediments remain unweathered. Mostly, they are characterised by extensive meso- to mega-mottling caused, mainly, by the redistribution of iron oxides, which are widely interpreted to be the result of weathering. The visible result is blotchy red and white patterns in the bedrock, which have been likened to the patterns visible of a giraffe's neck. Figures 2.5.6 and 2.5.7 show very good examples of the appearance of these weathering patterns in Cretaceous sediments from within North Queensland region.

Figure 2.5.5: *An isolated hill, an example of a butte-like feature, with a distinctive, progressively retreating, caprock forming due to erosion a local, roughly circular, bounding escarpment.*

Figure 2.5.6: *Mottling in Cretaceous sediments and showing residual regolith (iron nodules) within an indurated zone (the pedolith) forming the upper most surface in the region.*

Figure 2.5.7: *Examples of meso- and mega-mottles interpreted to be caused by iron redistribution because of weathering. They occur in a road cutting through very highly weathered Cretaceous "bedrock" sediments (*in situ *regolith) and form part of the loca saprolith in the North Queensland region.*

Summary

Ferruginous regolith is extensive across the North Queensland 3D map area, and is distinctive. In some parts, it is thought to have resulted from the weathering of the Cretaceous sediments across Queensland. Those linked to Cretaceous weathering are particularly highly visible within the North Queensland region. Estimates of the age of weathering of Cretaceous and other weathered bedrock across Queensland generally, and in the North Queensland area in particular, give ages within the range of latest Cretaceous to early Tertiary (75-55 Ma) and some within the range of late Tertiary (20-0 Ma.). These estimates are based on the results of studies using palaeomagnetism, and apply more generally to eastern and southeastern Australia (Craig et al., 2008).

Knowledge of the varied nature and distribution of regolith materials can assist in mineral exploration by highlighting the potential geochemical sampling media likely to be of greatest value for geochemical exploration programs. Mapping the regolith is the simplest way to achieve this quickly. This important early step of assembling data to help address major exploration decisions provides a valuable regolith and landscape context in which to plan exploration programs or to view their results. Links between regolith and the associated landscape may help explain the nature and location of identified anomalies. Sampling media can include, for example, weathered bedrock ferruginous duricrusts, nodules, or some combination of these materials. It is especially important to know if sampled regolith materials are transported or *in situ* to help establish if there is any likely link to an identified anomaly and its mineralisation source. For example, if the regolith is transported, any links may prove to be weak or unlikely, whereas if the regolith is *in situ* the case for a more direct link with the anomaly and the source of mineralisation may be much stronger. A landscape context also becomes important in helping confirm such decisions.

References

Craig, M.A., 2008. *Regolith-Landform Map of Queensland and GIS.* Cooperative Research Centre for Landscape Environments and Mineral Exploration, Perth, Australia.

Craig, M.A., Robertson, I.D.M., Thomas, M., Chamberlain, T. Jones, M.R. and Pillans, B.J., 2008 *Atlas of Regolith Materials of Queensland companion to the 1:2 500 000 Regolith-Landform map and GIS*. Open File Report 242, Cooperative Research Centre for Landscape Environments and Mineral Exploration, Perth, Australia, 357p.

Eggleton, R.A., 2001. *The Regolith Glossary.* Cooperative Research Centre for Landscape Enviroments and Mineral Exploration, Perth, Australia, 144p.

Pain, C., Chan, R., Craig, M., Gibson, D., Kilgour, P. & Wilford J., 2007. *RTMAP Regolith Database Field book and users guide (Edition 2).* Cooperative Research Centre for Landscape Environments and Mineral Exploration, Perth, Australia, Open File Report 321, 92p.

2.6 ROCK PROPERTIES

A.J. Meixner and R. Chopping

Physical properties are an important input to forward modelling studies of gravity and magnetic data (Section 3.2) and to inverse modelling of geophysical data (Section 3.4).

A compilation of rock property data, consisting of approximately 450 samples from the Mount Isa Region, is available (Meixner, 2009). These data were compiled from the following sources:

- Approximately 200 samples collected and measured by the Economic Geology Research Unit, School of Earth and Environmental Sciences, James Cook University and the Queensland Department of Mines and Energy, Geological Survey of Queensland (Blenkinsop et al., in prep). The samples, which included 11 samples from cores at Century mine and 10 samples from cores at Osborne mine, were collected along the deep seismic lines (06GA-M1, 06GA-M2, 06GA-M3 and 06GA-M6) in the Mount Isa-Cloncurry area during the period July-August 2007;
- Approximately 180 samples consisting of density and magnetic susceptibility measurements from Hone et al. (1987);
- Approximately 20 samples consisting of density measurements and magnetic susceptibility measurements from Sampath and Ogilvy (1974); and
- Approximately 50 samples consisting of density and magnetic susceptibility measurements from Mutton and Almond (1979).

In contrast to the comprehensive rock property data available in the Mount Isa region, rock property values for the Georgetown region of the 3D map area have been derived from literature values for standard rocks (for example, Telford et al., 1990). Literature values were used in this region as the other available rock property information included significant proportions of weathered or chemically altered materials.

References

Blenkinsop, T., Hutton, L., Bressan, G., Brown, A., Shah, A., and Josey, J., in prep. *Collection of rock properties along the Mount Isa seismic transects.* James Cook University.

Hone, I.G., Carberry, V.P., and Reith, H.G. 1987. *Physical property measurements on rock samples from the Mount Isa Inlier, northwest Queensland.* Bureau of Mineral Resources, Geology and Geophysics, Canberra, Report 265, 30p.

Meixner, A.J., 2009. *Rock property data (densities and magnetic susceptibilities) of the Mount Isa region.* Geoscience Australia, Canberra, Geocat #: 66166. https://www.ga.gov.au/products/servlet/controller?event=FILE_SELECTION&catno=66166.

Mutton, A.J., and Almond, R.A., 1979. *Geophysical mapping of buried Precambrian rocks in the Cloncurry area, northwest Queensland.* Bureau of Mineral Resources, Canberra, Australia, Record 1972/110.

Sampath, N., and Ogilvy, R.D., 1974. *Cloncurry area geophysical survey, Queensland, 1972.* Bureau of Mineral Resources, Canberra, Australia, Record 1974/135, 17p.

Telford, W.M., Geldart, L.P. and Sheriff, R.E., 1990. *Applied Geophysics (Second Edition).* Cambridge University Press, Cambridge, 790p.

3. Geophysical studies

3.1 DEPTH TO BASEMENT OF THE MOUNT ISA AND GEORGETOWN REGION

A.J. Meixner

Introduction

A depth to basement map (Figure 3.1.1) has been generated of the Mount Isa and Georgetown regions (Meixner, 2009). The map shows the depth of burial of basement geology, such as the Mount Isa province, beneath younger flat-lying cover material, such as the Eromanga Basin. The map was generated from point located depth values, in meters below the topography, sourced from drill hole data, depth to magnetic source estimates and seismic refraction data. The depth to magnetic source estimates incorporates data from previous studies as well as new depth estimates generated as part of this study. The point depths were gridded using the minimum curvature technique (Briggs, 1974) with a cell size of 1000 m.

A companion map Basement Geology of North Queensland (Liu, 2009) shows the interpretation of basement geology for which this is the depth to basement surface.

Data compilation

Drill hole data were compiled from a number of sources and include only holes that entered basement. Drill hole data consist of:

- Mineral, Stratigraphic and Coal drill holes sourced from the Queensland Department of Mines and Energy's Interactive Resource and Tenure Maps system (http://www.dme.qld.gov.au/mines/tenure_maps.cfm);
- Drill holes included with a GIS of the North Queensland Gold and Base Metals Study (Georgetown) sourced from the Queensland Department of Mines and Energy web site (http://www.dme.qld.gov.au/mines/seqgis.cfm#Georgetown); and
- Drill holes from the North-West Queensland Mineral Province Report (Queensland Department of Mines and Energy et al., 2000).

The seismic refraction depth estimates were generated from refracted first break seismic data for the North Queensland seismic lines 06GA-M4, 06GA-M5 and 07GA-IG1 (Jones et al., 2009).

Depth to magnetic source estimates were obtained from the following datasets:

- Magnetic depth determinations from the North-West Queensland Mineral Province Report (Queensland Department of Mines and Energy et al., 2000);
- Estimated depths to magnetic basement of the Springvale and Boulia 1:250 000 sheet areas (Meixner, 1997a, b);
- Depth to magnetic source estimates from airborne magnetic profile data using the Naudy method, generated as part of this study; and
- Depth estimates from manual 2D forward modelling, generated as part of this study.

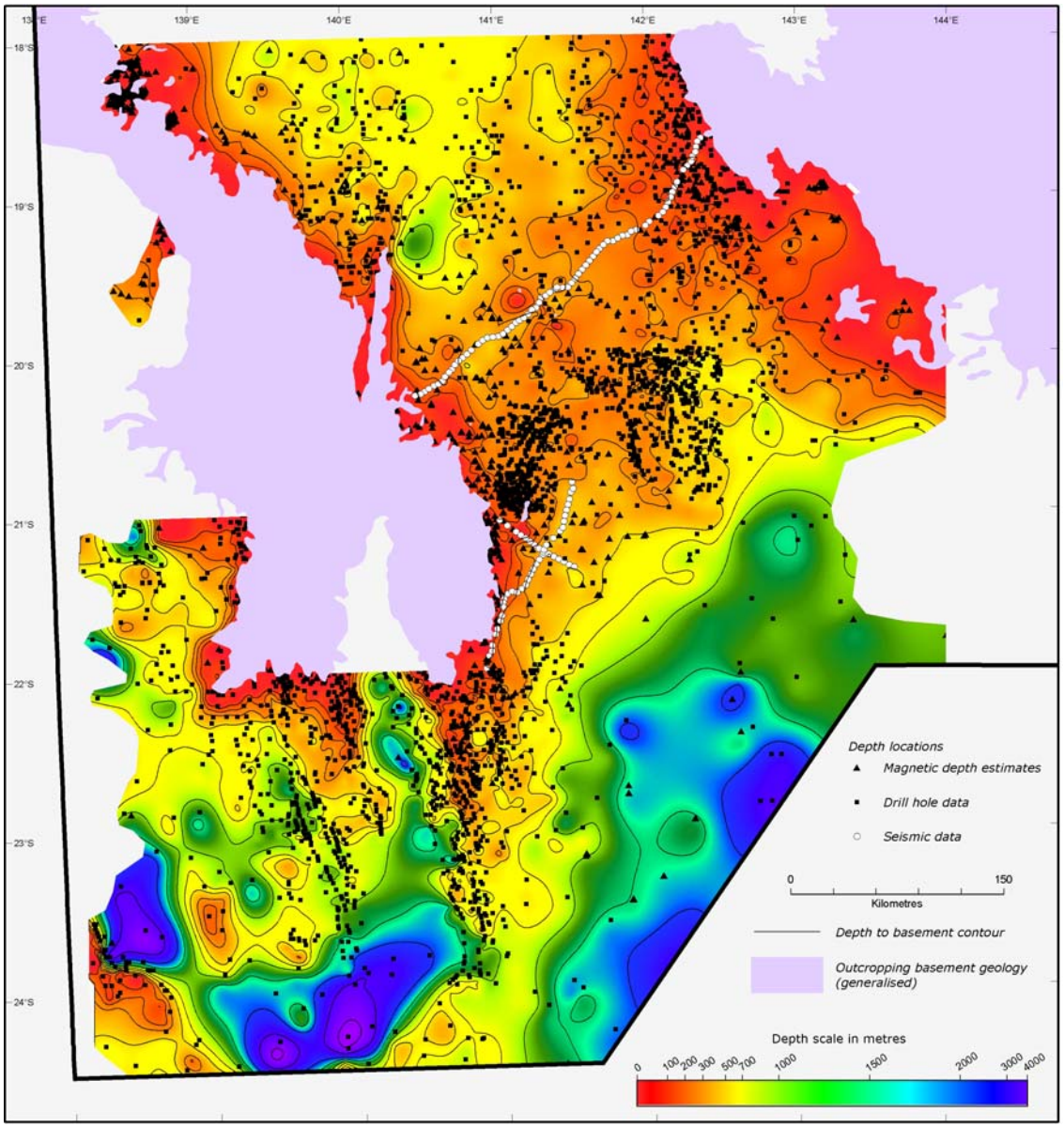

Figure 3.1.1: *Depth to basement map of the Mount Isa and Georgetown region.*

Naudy magnetic depth estimates

Estimates of depth to magnetic sources were generated using the Naudy Automatic Model tool from Intrepid™. This tool is based on the Naudy (1971) method and generates depth to the top of magnetic source bodies from magnetic profile data. The Naudy method identifies the position of individual anomalies along survey lines and compares the anomalous field of a theoretical body, such as a dyke, step or flat prism to the observed magnetic field. A similarity coefficient trace is generated along the survey line using different sample windows, the larger the sample window, the deeper the source body. A good correlation between the magnetic response of the theoretical body and the observed magnetic field results in a minima in the similarity coefficient.

A body solution is then generated at the minima consisting of estimates of the position, dip angle and depth to the top of the model. The tool estimates the quality of the solution based on the value of the similarity coefficient allowing for filtering of the solutions based on the solution quality. A physical model of the body may be generated from the body solution and the calculated response of that body

compared with the observed magnetic field, allowing a visual verification of the validity of the solution (Figure 3.1.2).

The ability to visually verify a solution allows for increased confidence of the validity of the solution, as well as allowing for the manual removal of solutions that are not considered a good fit. All of the depth estimates for this study were generated using a dipping dyke-like body.

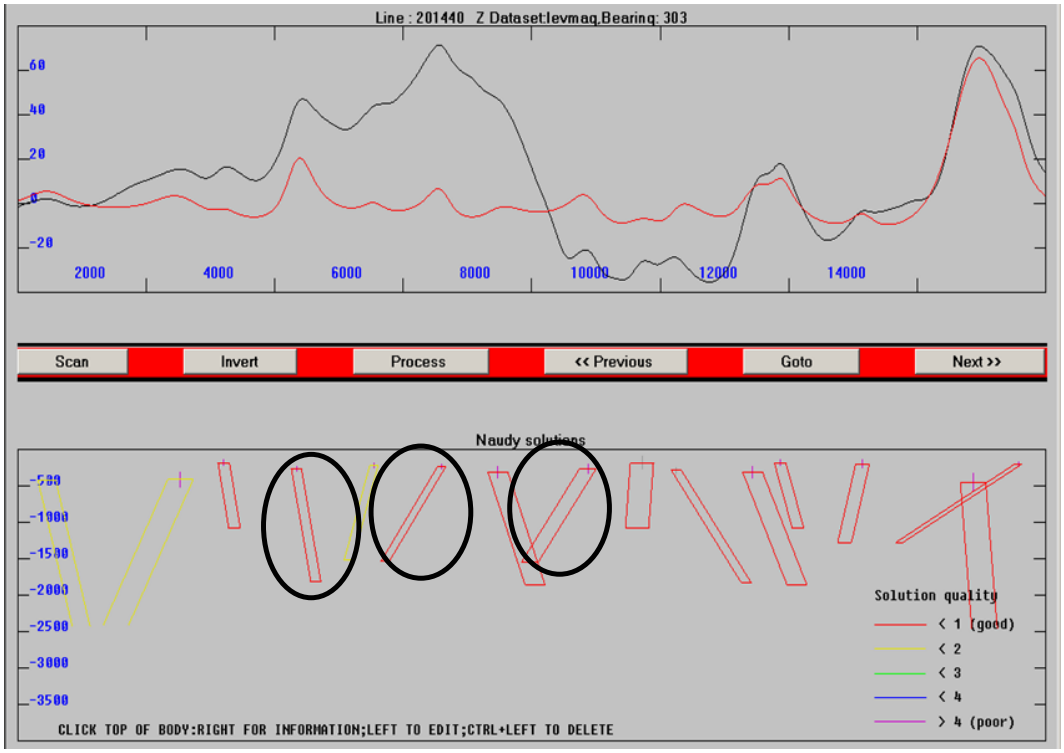

Figure 3.1.2: *An example of dyke bodies generated by the Naudy Automatic Model tool from an airborne survey profile. The upper panel shows the observed magnetic field (black) and the calculated body response (red) after the Naudy solutions have been converted into dipping dyke like bodies. In this example, only those body solutions corresponding to a solution quality (calculated by the Naudy Automatic Model tool) of ≤ 2 were converted to dipping dyke-like bodies (lower panel). After inspection of the observed and forward modelled profiles, only the three bodies (circled in black) were considered to have produced a sufficient match between observed and calculated body response, ignoring the offset of the observed field due to source bodies that have not been modelled, to be included in the depth to basement map.*

The method assumes that the strike length of any elongated body is infinite and oriented orthogonal to the magnetic profile. The Naudy Automatic Model tool has the ability to apply a strike correction for source bodies that are not orthogonal. This is achieved by applying a trend spline gridding routine to the line data in order to determine the existence of any anomaly correlation between adjacent lines, as well as determining the strike direction if correlations exist. The source body depth estimates were strike corrected using this method (Figure 3.1.3). The resulting strike-corrected depth estimates were further filtered to remove solutions generated near the ends of elongate anomalies which do not satisfy the assumption of an infinite strike length.

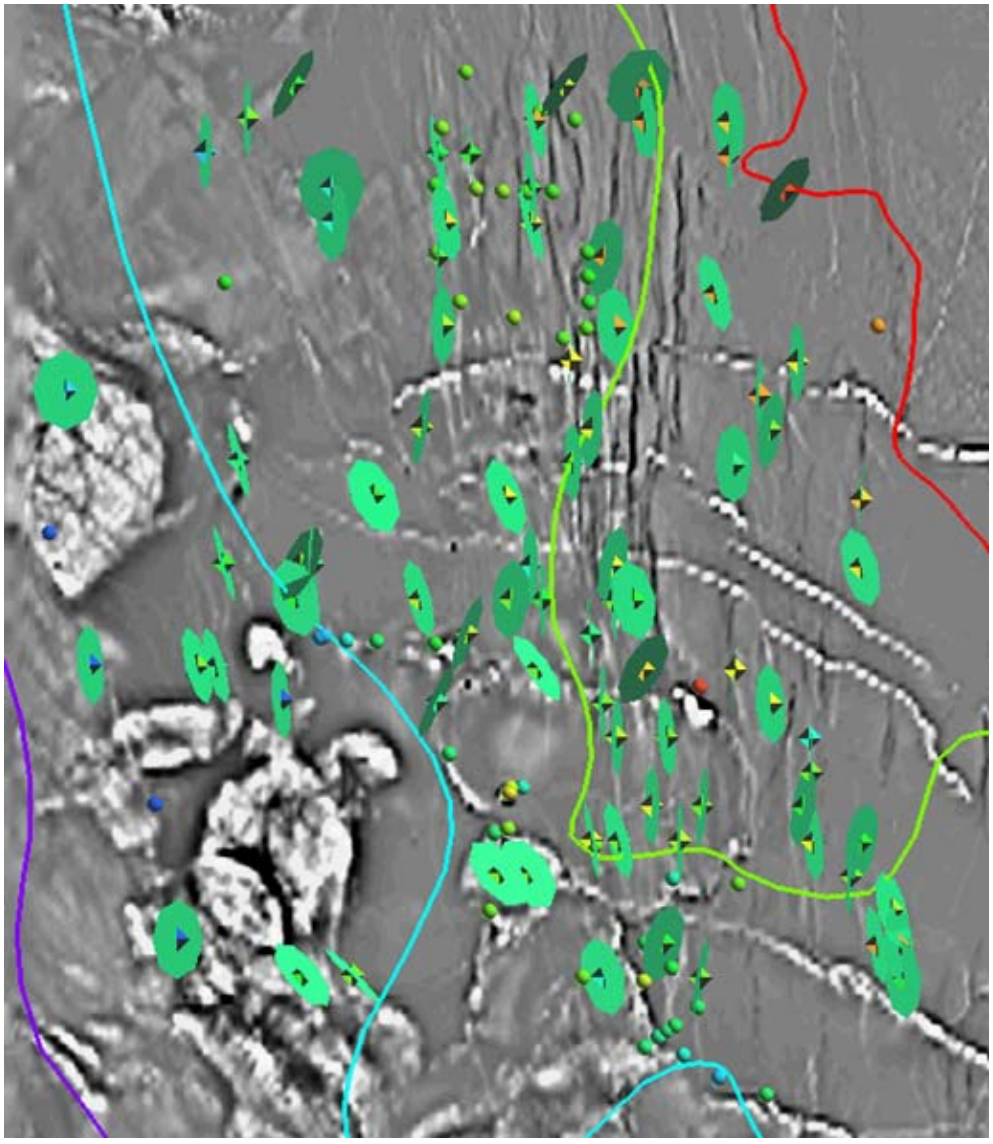

Figure 3.1.3: *Strike-corrected body solutions (points) overlying an image of the first vertical derivative of the total magnetic intensity in a small region of the study area. The green disks indicate the strike direction and dip of the dipping dyke-like solutions. The solutions were filtered to remove those where the strike direction was not aligned with an elongate magnetic anomaly.*

Forward modelled depth estimates

Manual forward modelling was carried out, as part of this study, on elongated anomalies where no valid solutions were generated by the Naudy Automatic Model tool. In these instances it was considered valid and subsequent forward modelling showed that accurate depth solutions, when compared with drill hole data, could be generated by 2D modelling using the dipping dyke-like model as the source body were chosen. Only discrete anomalies that were interpreted as sourced from a dipping dyke-like body. Manual forward modelling was necessary in regions of greater depth of burial where the magnetic anomalies exhibit larger wavelengths. The modelling was carried out on profiles extracted from a total magnetic intensity grid, perpendicular to the elongated anomaly. Only depth estimates displaying a good fit between the modelled and the observed magnetic field (Figure 3.1.4), were incorporated into the depth to basement map.

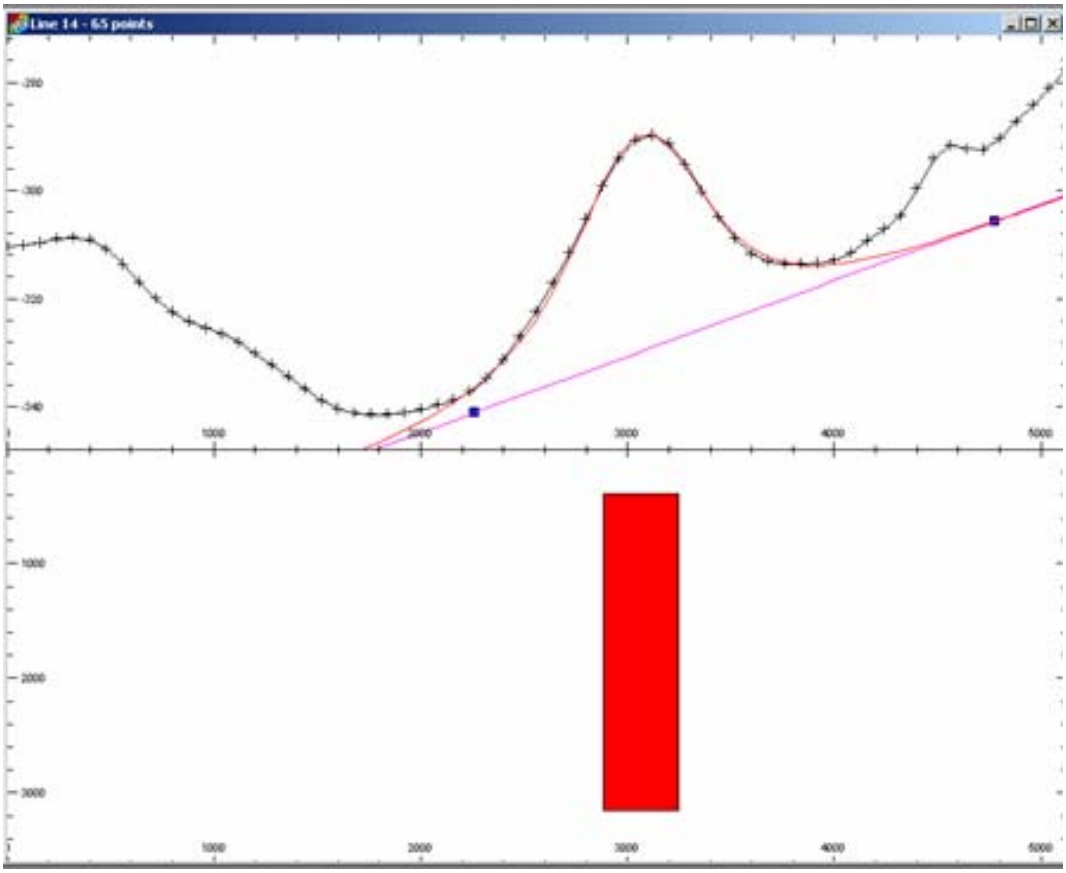

Figure 3.1.4: *An example of a 2D forward model of a dipping dyke-like body. The upper panel shows the observed magnetic profile (blue) and the calculated body response (red). A degree one polynomial has been incorporated to account for the regional field (purple).*

The depth to magnetic source estimates generated by the Naudy and 2D forward modelling methods may contain errors for the following reasons:

- The top of the source body is situated below the upper surface of the basement, or is due to a magnetic source within the cover. These errors are mitigated by visual inspection of the anomaly. Often the interpreter can judge, due to the character and wavelength of the anomaly of interest, that it is sourced either significantly deeper or shallower when compared to surrounding anomalies. Drill hole data, if they exist, can also be used to give the interpreter an idea of the expected depth to basement. Only depth estimates from sources considered to occur at the top of the basement surface were included in the depth to basement map.
- Weathering of the basement prior to the deposition of cover material will result in the oxidation of magnetite, a highly magnetic mineral, to hematite, a significantly less magnetic mineral. This will produce demagnetisation of the source body in the weathered zone, resulting in an over estimation of the depth to the top of the body. Weathering profiles vary depending on the age, morphology and composition of the basement surface but are considered to be less than approximately 50 m.
- A source body that is not a 2D dipping dyke-like body will produce inaccurate depth estimates. Only depth estimates from elongate anomalies which are considered to be sourced from a dipping dyke-like body and where the length of the anomaly is at least five times the width were included in the depth to basement map.

Summary

The depth to basement map highlights the differences, approximately a 4 km depth range, in the topography of the top of basement in the Mount Isa and Georgetown regions. The majority of the top of basement topography to the south of the Mount Isa Province, and the central and northern portions of the study area, are under less than 500 m of cover. The use of a wide variety of data sources, as well as the new interpretations of magnetic data in the region presented above, ensures a high degree of certainty in the depth to basement map. The disparate data used for this study provide measures of depth to basement that are consistent with each other, as is depicted by the relatively regular topography of the top of basement.

References

Briggs, I.C., 1974. Machine contouring using minimum curvature. *Geophysics*, **39**(1), pp. 39-48.

Jones, L.E.A., Maher, J.L., Costelloe, R.D., Holzschuh, J., Nakamura, A. and Saygin, E., 2009. 2007 Isa-Georgetown-Charters Towers Seismic Survey – Acquisition and processing. *Northern Queensland Exploration & Mining 2009 Symposium & North Queensland Seismic and MT Workshop – Extended Abstracts*, Australian Institute of Geoscientists Bulletin No. 49, pp. 149-152.

Liu, S.F., 2009. Basement Geology of Northern Queensland (First Edition), 1:1 000 000 scale. Geoscience Australia, Canberra, GeoCat #: 68592. https://www.ga.gov.au/products/servlet/controller?event=GEOCAT_DETAILS&catno=68592.

Meixner, A.J., 2009. *Depth to Basement of Northern Queensland (First Edition), 1:1 000 000 scale*. Geoscience Australia, Canberra, GeoCat #: 69234. https://www.ga.gov.au/products/servlet/controller?event=GEOCAT_DETAILS&catno=69234

Meixner, A.J., 1997a. *Estimated depths to magnetic basement of Boulia, Qld, scale 1:250 000.* Australian Geological Survey Organisation, Canberra.

Meixner, A.J., 1997b. *Estimated depths to magnetic basement of Springvale, Qld, scale 1:250 000.* Australian Geological Survey Organisation, Canberra.

Naudy, H., 1971. Automatic determination of depth on aeromagnetic profiles. *Geophysics*, **36**(4), pp. 717-722.

Queensland Department of Mines and Energy, Taylor Wall & Associates, SRK Consulting Pty Ltd and ESRI Australia, 2000. *North-West Queensland Mineral Province Report.* Queensland Department of Mines and Energy, Brisbane.

3.2 VALIDATING NORTH QUEENSLAND SEISMIC INTERPRETATIONS THROUGH GRAVITY FORWARD MODELLING

A.J. Meixner and R. Chopping

Introduction

Although seismic data provide a powerful and, in many ways, a unique view of subsurface geology, it is important to validate any interpretation of these data. The wide availability of high-quality and relatively high-resolution gravity data (Section 2.2) provides a mechanism to test seismic interpretations. Gravity data are preferable to magnetic data for the validation of interpretations of crustal-scale seismic reflection data, as it is more sensitive to deeper features (response decreases with increase depth slower) and density is a property of bulk mineralogy of a lithology whereas magnetic response can depend only very small quantities of a few magnetic minerals such as magnetite. Gravity data have the potential to add to the seismic interpretation: dense features may not be reflective, or they may have geometries, such as very steeply dipping contacts, which are not adequately resolved by reflection seismic techniques.

Forward modelling, the subject of this section, is a technique whereby a geological model is used to produce a model of physical properties, such as a model of densities; this model is then used to calculate a geophysical response, such as a gravity response. This geophysical response is compared to the observed geophysical data, and revised by the geophysicist as appropriate.

A crucial step in forward modelling is the conversion from a geological model to a rock property model, which is made through an understanding of rock properties in a region. For the Mount Isa region, these rock properties are compiled from existing literature values, as well as a recent study (Section 2.5); in other regions in the study area, properties were derived from literature values only.

Forward modelling cannot verify a proposed geological interpretation: it can only disprove a proposed interpretation. An infinite number of physical property models account for observed geophysical data. A geophysical response calculated from an incorrect geological model will not match the observed geophysics to within estimated errors. Due to the non-uniqueness of forward-modelling, any areas of mismatch need to be explained with physical properties which also make geological sense; for example, it may be highly misleading to attribute a region of significantly higher observed gravity to a zone of ultramafic rocks in a purely sedimentary environment.

The following results for the forward modelling of the North Queensland seismic interpretations (Section 2.2) illustrate the procedure. The line 07GA-IG2 is examined first, as it provides an excellent example of forward modelling, and then 07GA-IG1, 07GA-GC1 and 07GA-A1 are examined in turn. For the locations of these lines refer to Figure 2.1.1 and for their location relative to available gravity and magnetic data refer to Figures 2.2.2 and 2.2.3.

Results

07GA-IG2

The interpretation of the 07GA-IG2 line does not produce an adequate match between observed and calculated gravity (Figure 3.2.1). The calculated gravity response does not reproduce three high amplitude gravity anomalies. Two of these anomalies have relatively short spatial wavelengths indicating shallow and dyke-like causative bodies; the third (western) anomaly has a longer wavelength, suggesting a deeper and more tabular body.

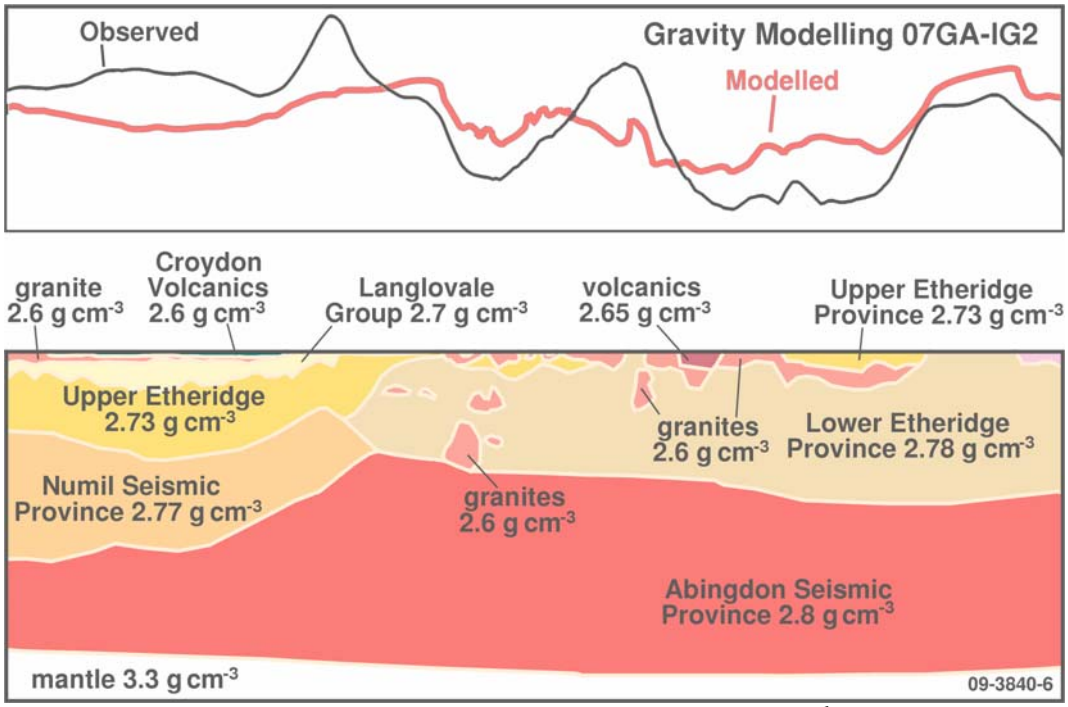

Figure 3.2.1: *Observed gravity profile, extracted from national gravity data[1], compared to the calculated gravity response due to the property model derived from the 07GA-IG2 interpretation. Significant mismatch is apparent between the observed and calculated gravity profiles. An interpretation of the seismic section is shown below the physical property model.*

Mafic components of the Etheridge Province are known to exist, and although the Numil seismic province is not exposed at the surface and thus its composition is unknown, it may also contain mafic components. Mafic rocks are, in general, denser than average crust and will produce high-amplitude gravity anomalies.

The addition of some bodies to account for these anomalies significantly improves the fit between the observed and calculated gravity responses (Figure 3.2.2).

These three bodies may have been partially imaged by the seismic data. The westernmost body, which has a tabular shape and is interpreted to be a mafic component of the Lower Etheridge Province, appears to be marked by the truncation of some seismic reflections (Figure 3.2.3). Furthermore, this body is approximately at the depth of a high-velocity (and, thus, a high-density) layer with similar geometry observed in the Mount Isa region (Drummond et al., 1998). Note that no reflectivity is observed in the core of this lozenge-shaped body (Figure 3.2.3). High amplitude reflectivity is associated with both of the other mafic bodies (e.g. Figure 3.2.4).

[1] Although gravity data are acquired along the seismic lines, these data are located on the station line, that is, along the line that the seismic data are acquired. Processing and subsequent interpretations of non-straight 2D seismic lines generally are performed along a common depth point (CDP) line. The station and CDP lines are not necessarily colocated; for the purposes of forward modelling the gravity data should be located directly on the CDP line and not the station line.

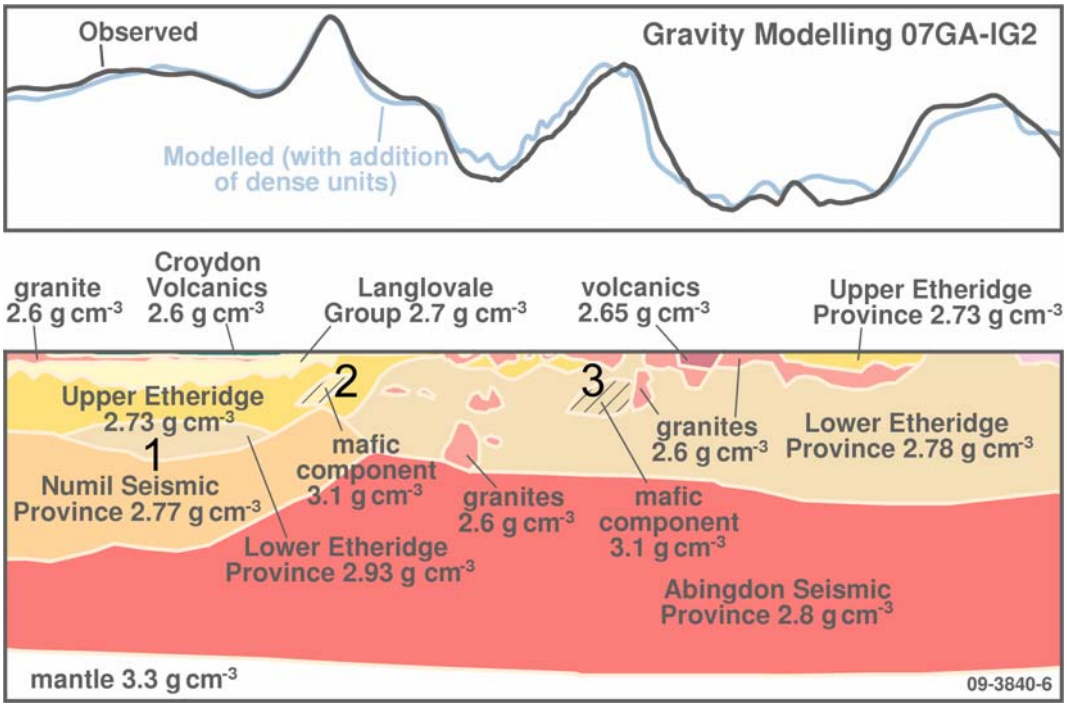

Figure 3.2.2: *Observed gravity profile, extracted from national gravity data, compared to the calculated gravity response due to the property model derived from the 07GA-IG2 interpretation with three bodies added (labelled 1 through 3).*

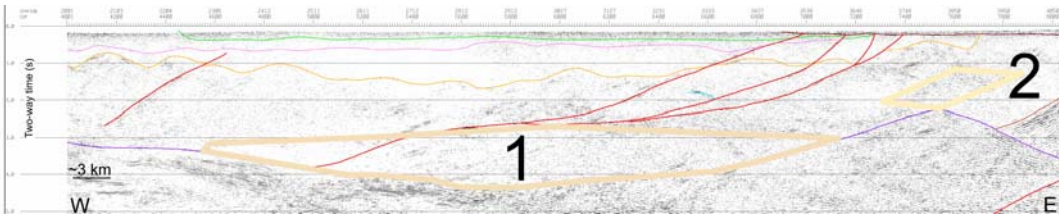

Figure 3.2.3: *Seismic reflections proximal to the tabular westernmost mafic body (buff coloured lines - 1) and the central mafic body (light yellow coloured lines - 2). Faint indications of the westernmost body are apparent in the seismic data; the central mafic body appears to have some higher amplitude reflectivity proximal to its top and western boundaries.*

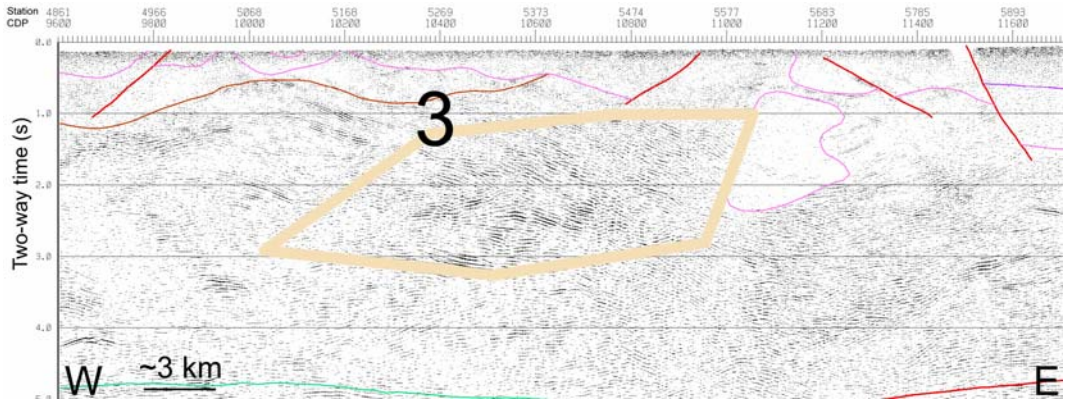

Figure 3.2.4: *Seismic reflections associated with the third mafic body (dark buff to yellow coloured lines - 3) interpreted from gravity forward modelling.*

The integration of the seismic data and its interpretation, and the gravity forward modelling, produces an improved geological model. Importantly, some of the dense units are associated with increased seismic reflectivity not interpreted as separate bodies in the initial seismic interpretations.

07GA-IG1

In general, the fit to the observed gravity for line 07GA-IG1 is excellent, but some mafic components to the Kowanyama Province and the Etheridge Province (denoted as Lower Etheridge) were required to improve the fit to the observed gravity (Figure 3.2.5).

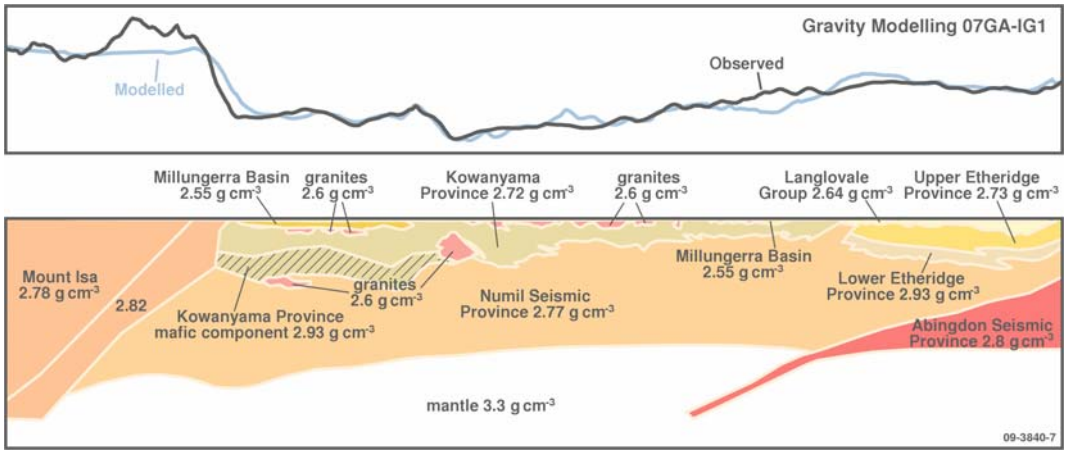

Figure 3.2.5: *Forward modelling of the seismic line 07GA-IG1. Mafic components to the Kowanyama Province and the Etheridge Province (denoted as Lower Etheridge) were added to the initial seismic interpretation. The Lower Etheridge Province approximately correlates to the westernmost mafic body interpreted on line 07GA-IG2.*

07GA-GC1

The seismic interpretation for 07GA-GC1 generally reproduced the broad-scale features in the observed gravity data (Figure 3.2.6). Some mafic components were required to be added to reproduce some higher-amplitude anomalies.

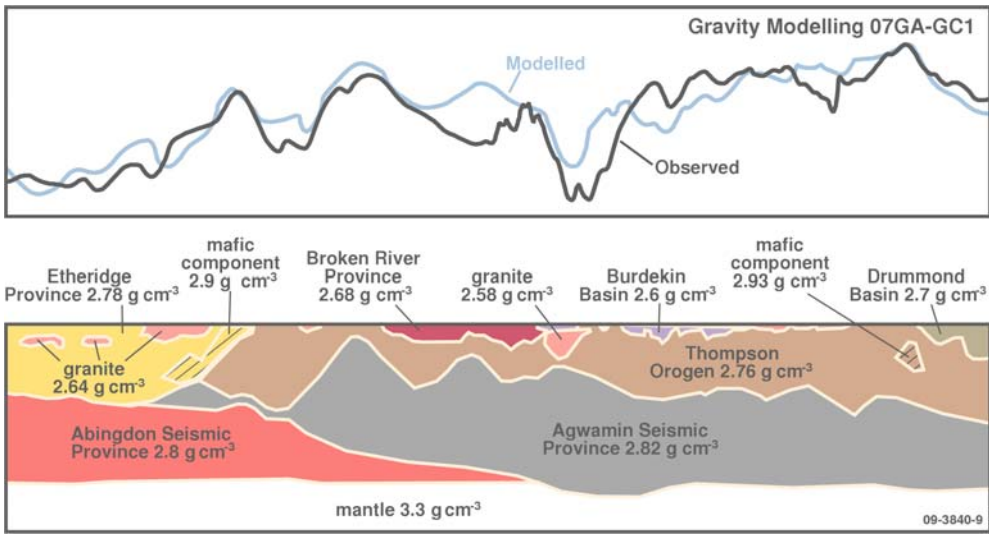

Figure 3.2.6: *Forward modelling of the seismic line 07GA-GC1.*

07GA-A1

As for the other seismic lines acquired in 2007, the interpretation for line 07GA-A1 was generally acceptable and reproduced the broadest wavelength (deepest) features (Figure 3.2.7). Line 07GA-A1 required some off-line dense bodies, accounting for dense units at the eastern end of line 07GA-IG2 (Figure 3.2.2).

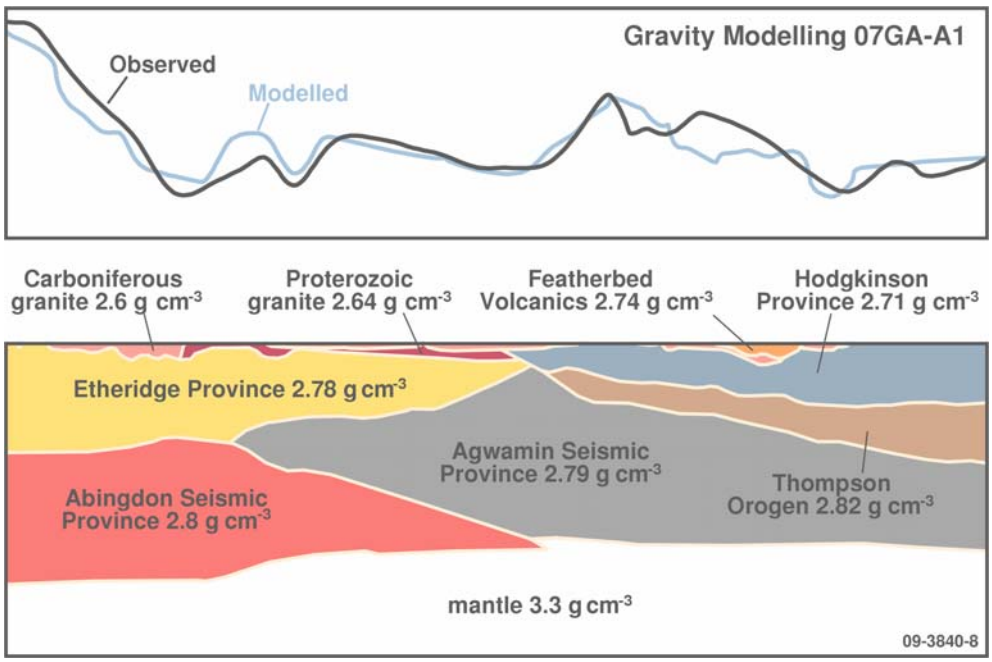

Figure 3.2.7: *Forward modelling of the seismic line 07GA-A1.*

Summary

In general, the forward modelling of the seismic interpretations produced close matches to the observed gravity data in the region. Mismatch between the observed and calculated forward models was in the vicinity of gravity anomalies that were high-amplitude and short wavelength, indicating shallow and dense bodies. These bodies, which had densities similar to those expected for mafic bodies (Telford et al, 1990), are geologically plausible, as mafic units are known in the Etheridge Province and are possible (although unknown as they do not crop out) in the Numil and Kowanyama Seismic Provinces.

References

Drummond, B.J, Goleby, B.R., Goncharov, A.G., Wyborn, L.A.I., Collins, C.D.N. and MacCready, T., 1998. Crustal-scale structures in the Proterozoic Mount Isa Inlier of north Australia: their seismic response and influence on mineralisation. *Tectonophysics*, **288**(1-4), pp. 43-56.

Telford, W.M., Geldart, L.P. and Sheriff, R.E., 1990. *Applied Geophysics (Second Edition).* Cambridge University Press, Cambridge, 790p.

3.3 WORMS AND THEIR INTERPRETATIONS

P.A. Henson and P.R. Milligan

Introduction

A technique has been developed by Murphy et al. (2006) to analyse fault length, in relation to potential sites of mineralisation, using derivatives of potential field data. The technique was first applied in the western Victoria to target gold mineralisation. Following the same methodology, a similar process has been used to analyse the North Queensland region. The process is based on the analysis of gradients of magnetic and gravity data, with emphasis on using an automated edge detection technique called multiscale wavelet edges ('worms'), initially developed by CSIRO and Fractal Graphics (Hornby et al. 1999).

The basis of this technique is to determine the relative potential for mineralisation associated with increased permeability proximal to large faults. It is well documented that there is a general relationship between maximum displacement and fault length at a range of scales (Kim & Sanderson, 2005). These observations have been determined through field observations of faults and analysis of faults using 3D seismic reflection data. This assumption therefore can be used as evidence to support a potential field interpretation of fault length in the North Queensland region.

Multiscale edges

Following the method of Hornby et al. (1999), multiscale edges were generated using Intrepid™ software for both the magnetic and gravity data of the North Queensland region. The total magnetic intensity (TMI) data were reduced to the pole before edge generation. The edges are initially represented by a series of points located at positions of maximum gradients for a series of upward continuations of the data. Upward continued potential field data reduces the power of the shorter wavelengths, the greater the upward continued distance, the more the reduction in power. Continuous sets of the gradient points are combined into lines. Both points and lines are attributed with the scaled value of the maximum horizontal gradient, and the lines are also attributed with length, thus enabling selection based on this criterion.

A further refinement for the display of such fault-length data is to combine the data for both gravity and magnetic edges for lines longer than a minimum length. These combined data can then be gridded using length as an attribute. Images of such grids, representing fault lengths under the assumption that gradient maxima positions represent faults, may then be displayed and further analysed with other data such as mineral locations. The main assumptions in the process are explained below in more detail.

Interpretation hypotheses

Multiscale wavelet edges ('worms') are produced at positions of maximum gradient in the potential field data. Gradients occur where there is a contrast in the physical property of density (gravity) or susceptibility (magnetic) of the Earth. In some instances, there may be significant geological features, including faults, but they will only produce a gradient in either magnetic or gravity data if a property contrast occurs. Cover also has a significant influence by masking the high amplitude gradients of underlying material, either by its thickness, or due to property variations in the cover.

Gradients in potential field data occur:

- On intrusive boundaries where the density or magnetic susceptibility of the intrusive body varies from the country rock, and will be depicted as:
  - linear bodies, or
  - circular bodies.

- At basin margins,
  - delineated by basin bounding faults, or
  - where onlap occurs.
- At dipping lithological contacts with significant density contrasts, or
- Where faults offset units of different density.

Manual interpretation

A manual process used a subset of the worms at different levels of upward continuation (Table 3.3.1) that were plotted on A0 paper and overlay used to delineate the most laterally continuous and deepest worm strings.

Table 3.3.1: Levels of upward continuation for magnetic and gravity data.

LEVELS OF UPWARD CONTINUATION FOR MAGNETIC DATA (METRES)	LEVELS OF UPWARD CONTINUATION FOR GRAVITY DATA (METERS)
616, 1207, 1690, 2366, 3312, 4637, 6492, 9089, 12725, 17815, 24941, 34917, 48884, 68438	1120, 1568, 2195, 3073, 4302, 6023, 8432, 11805, 16527, 23138, 32393, 45350, 63490

There was a deliberate attempt to honour the data to ensure consistency in interpretation. It must be noted that this is a subjective process, although it did enable the integration of geological concepts into the interpretation. The manual interpretation was then digitised and the worm fault length images were generated.

Results and interpretation

Figures 3.3.1 through Figures 3.3.4 highlight the results of the worm characterisation of the potential field data. The worms are first displayed on the total magnetic intensity image (reduced to the pole – Figure 3.3.1) and the gravity image (Figure 3.3.2) for the region. From these, a worm length map was derived (Figure 3.3.3), based on joint interpretation of both the gravity and magnetic worms. Comparison of the worm fault length image to the known mineralisation in the North Queensland region indicates that the majority of known mineralisation in the region corresponds to longer fault lengths (Figure 3.3.4). Some of the mineralisation, especially the heavily mineralised Mount Isa Province (southwest corner of the map) appears to be hosted in relatively long faults which are secondary to the longest faults in the region. The length of interpreted worms may therefore represent a new method of targeting based on geophysics and careful interpretation.

Summary of results

This technique provides a medium to combine both magnetic and gravity worms and analyse the relationship between worm lengths. The output has provided a method spatially compare the relationship between worm length and existing mineralisation. It also provided insights into possible mineralisation in regions of no known mineralisation.

References

Hornby, P., Boschetti, F. and Horowitz, F., 1999. Analysis of potential field data in the wavelet domain. *Geophysical Journal International*, **137**(1), pp. 175-196.

Murphy, F.C., Rawling, T.J., Wilson, C.J.L., Dugdale, L.J. and Miller, J.M., 2006. 3D structural modelling and implications for targeting gold mineralisation in western Victoria. *Australian Journal of Earth Sciences*, **53**(5), pp. 875–889.

Kim, Y. & Sanderson, D.J., 2005. The relationship between displacement and length of faults: a review. *Earth Science Reviews*, **68**(3-4), pp. 317-334.

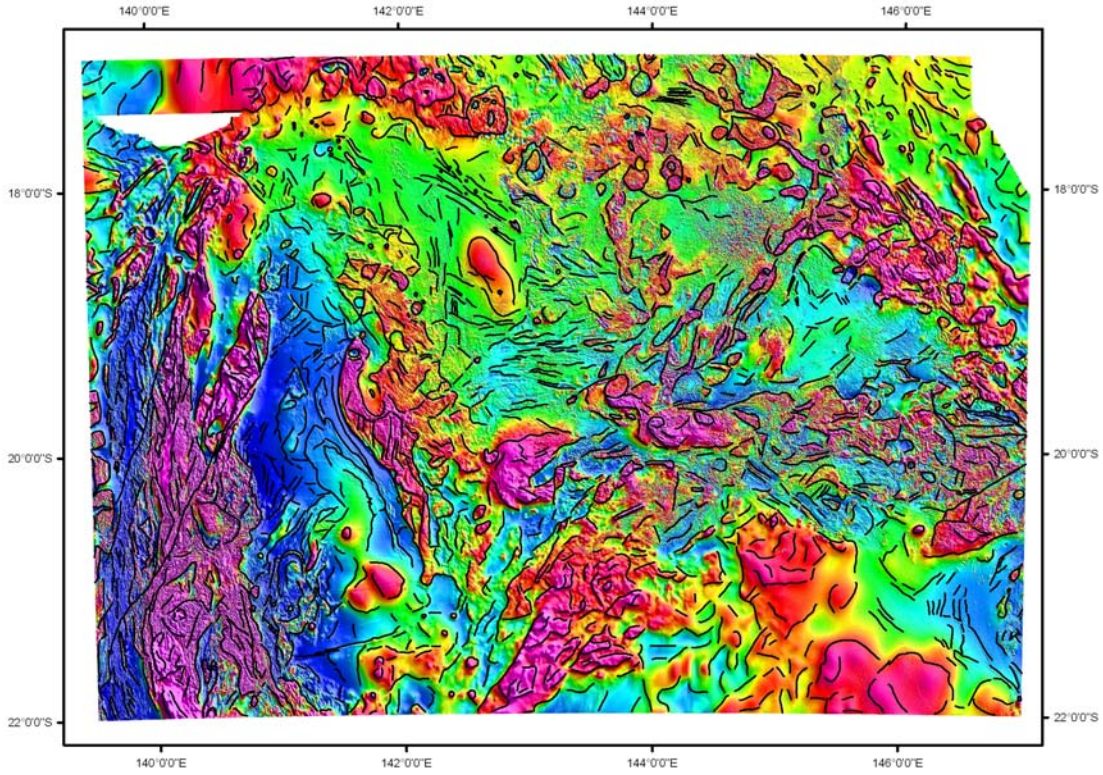

Figure 3.3.1: *Image of the TMI, reduced to the pole, overlain with the "worm" interpretation derived from the TMI data, as described in the text.*

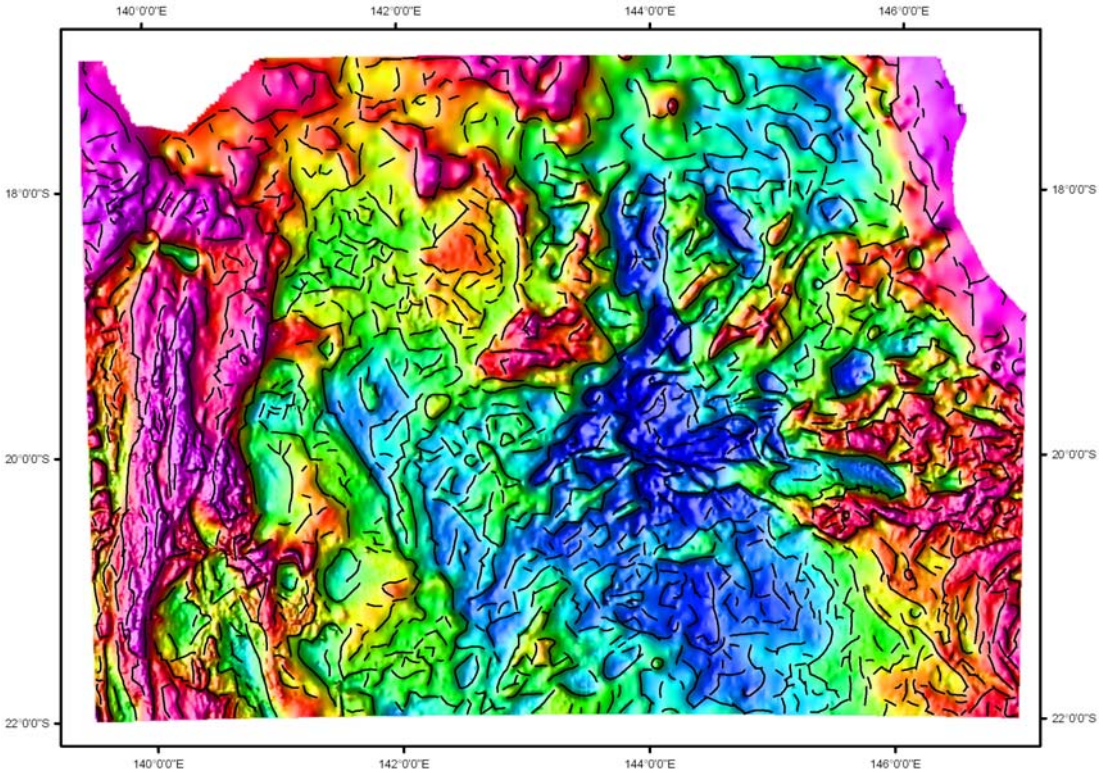

Figure 3.3.2: *Image of the gravity, overlain with the "worm" interpretation derived from the gravity data, as described in the text.*

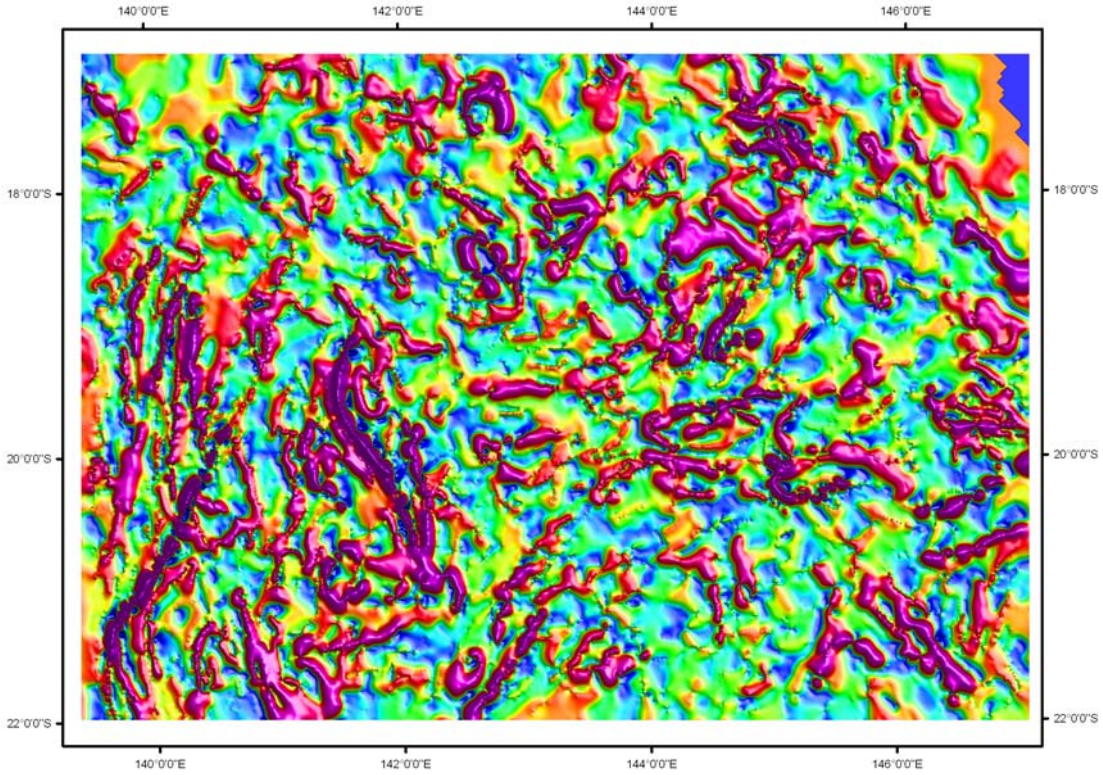

Figure 3.3.3: *Fault-length image, derived from a combination of gravity and magnetic manually-interpreted worms and gridded with the attribute of length of fault.*

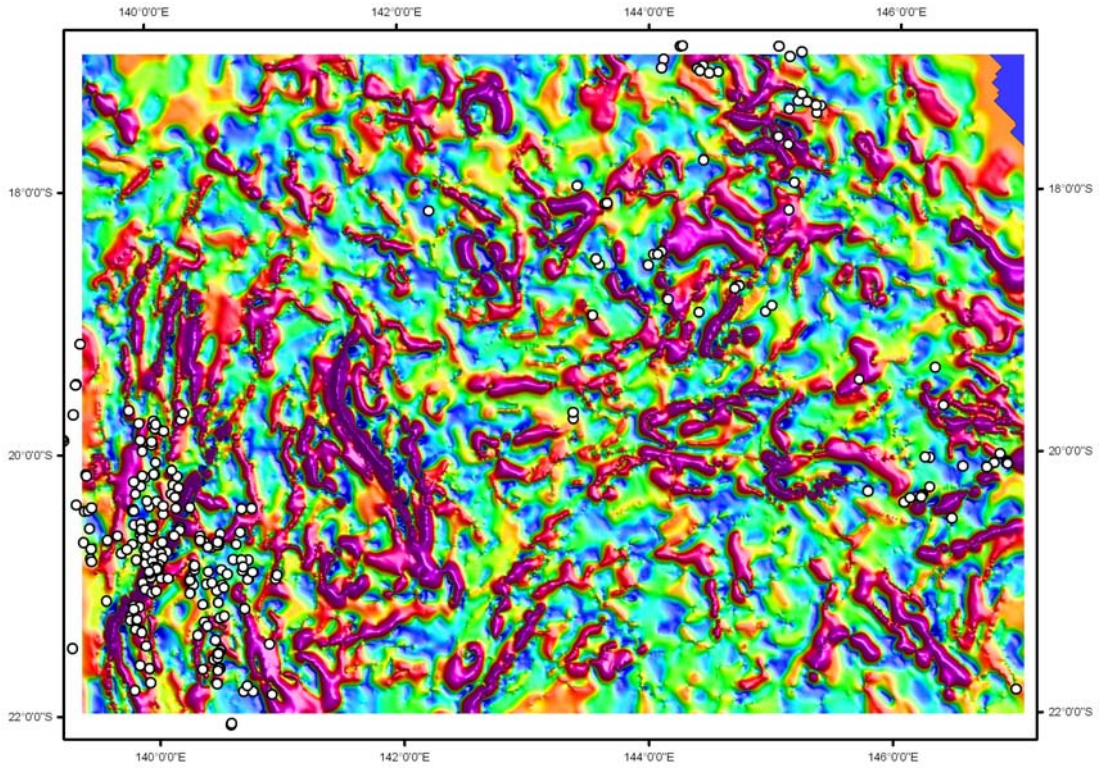

Figure 3.3.4: *Fault-length image as per Figure 3.3.3 overlain with major mineral deposits.*

3.4 INVERSE MODELLING OF POTENTIAL FIELD DATA

N.C. Williams, I.G. Roy and R. Chopping

Introduction

Inverse modelling is a technique where a computer algorithm calculates a suitable physical property (such as density) distribution which reproduces the observed geophysical data (such as gravity). Inversions are a powerful tool for understanding subsurface geology. Although inversion results are non-unique, they provide a quantitative estimate of the physical properties beneath a study area. Modern computing power, and refined algorithms, allows these inversions to be conducted at high resolution in 3D.

For this study, there are three main aims for the inverse results. The inverse results should provide a basic model of the gross geometries and property variations in the subsurface, which are a useful guide for geological predictions. The inversion results also allow the seismic reflection interpretations to be extended beyond the seismic lines, assuming suitable constraints derived from the seismic data are included in the inversions. Finally, the quantitative estimate of physical properties allows the prediction of subsurface chemical alteration (see Section 4.2), or the prediction of the possible nature of buried granites (see Section 4.3).

Two areas were selected for inverse modelling (Figure 3.4.1). The first is an area which covers the entire 3D map region. The second area is a region encompassing approximately the width of the southern Mount Isa Province and continuing south of Cloncurry to ~24.5° S. The second region (S. Cloncurry inversion in Figure 3.4.1) was selected to examine if the inversions could be used to successfully trace the highly mineralised Mount Isa Province to the south, where it is covered by relatively shallow younger sediments (see Section 3.1 for depth to basement interpretation of this region). To enable regional gravity and magnetic trends to be removed uniformly for both of these inversions, a regional inversion was conducted that encompassed both inversion areas (regional inversion in Figure 3.4.1) and was padded appropriately (see Method section, below).

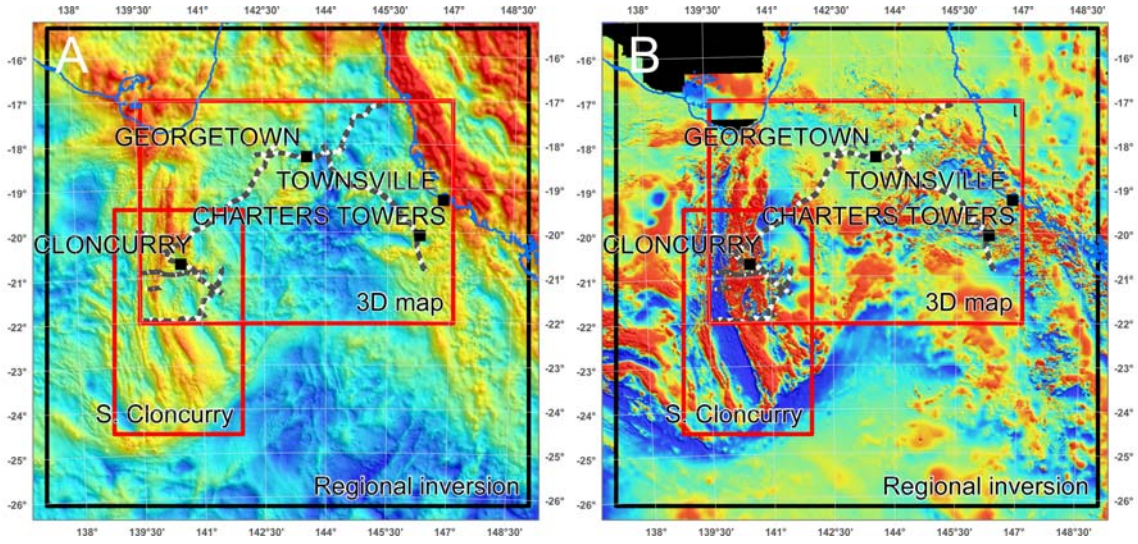

Figure 3.4.1: *Outline of the two areas for inverse modelling (red rectangles) and the regional inversion (black rectangle), overlain on (A) the national gravity data (Bacchin et al., 2008) and (B) the national magnetic intensity data (Milligan and Franklin, 2004). Coastline (blue line), seismic lines (dashed grey-white lines) and major towns are also shown.*

This study used the UBC-GIF inversion utilities GRAV3D and MAG3D (Li and Oldenburg, 1996, 1998a). The deterministic property inversion approach implemented in these algorithms seeks an optimal physical property model that explains the observed geophysical data while also satisfying any prior geological knowledge, in the form of constraints on the recovered physical properties. These geological constraints can be as simple as a uniform starting model, i.e. no prior knowledge of the expected geology and hence property model. Recovered physical property models will generally appear smooth, and will only recover detailed subsurface property distributions where mandated by either the geophysical data or the prior geological knowledge. UBC-GIF recovered models provide a best estimate of the physical properties associated with broad-scale features in the subsurface given the available geophysical data and geological constraints.

There are two important limitations to the North Queensland density and magnetic susceptibility models developed here. The first is the wide spacing of gravity stations across much of the region (Figure 3.4.2). Although data from a number of small detailed surveys are included, the average regional data spacing ranges from 2 km in the Mount Isa area to ~12 km between stations in the southeast, with a median data spacing of around 4 km. To incorporate the maximum resolution gravity data of 2 km, cells in the inversions are 2 km in horizontal resolution. Because of the smoothness requirement of the inversions, the smallest features recoverable by either the gravity or magnetic inversions will be > 4-6 km across (2-3 cells). District and regional-scale features, therefore, are the focus of the models rather than deposit-scale anomalies.

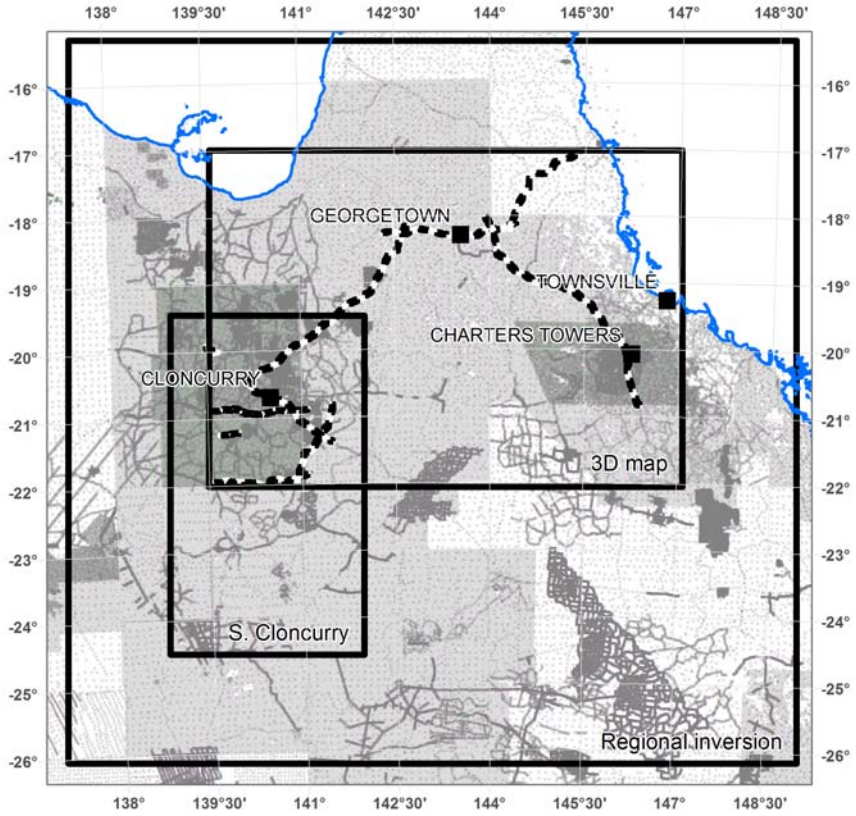

***Figure 3.4.2**: Gravity coverage for the inversion regions. Note that this map is presented in the TM144 projection used for the majority of this study. This is a transverse mercator projection, datum GDA94, central meridian 144°E.*

Magnetic data coverage is generally more closely spaced. The majority of the data are ≤ 500 m flight-line spaced data (Figure 3.4.3). Due to the limitations of the gravity data, a horizontal cell size of 2 km was also used for the magnetic inversions. The extra resolution contained in the more closely spaced magnetic data is therefore not used. Some regions, however, have much worse coverage in the 2004 national compilation data used here. Regions noted in the blue colours in Figure 3.4.3 are > 1500 m flight-line spaced data, with regions up to ~3200 m flight-line spacing.

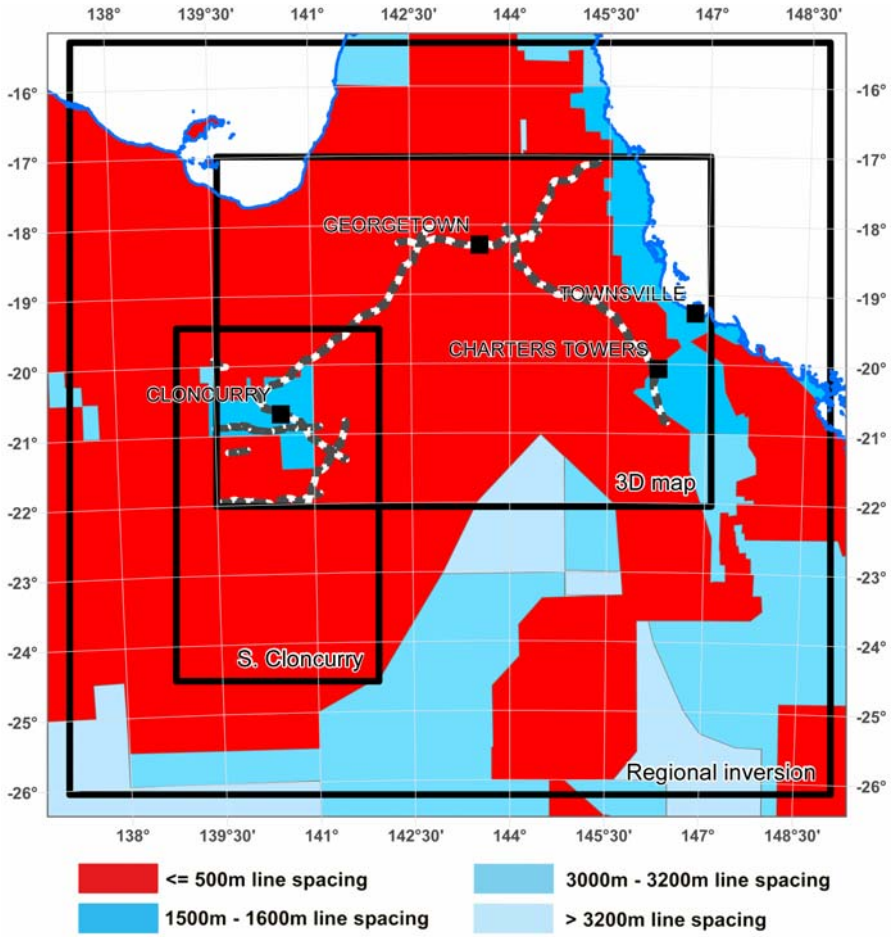

Figure 3.4.3: *Magnetic survey coverage for the inversion regions. Note that this map is presented in the TM144 projection used for the majority of this study. This is a transverse mercator projection, datum GDA94, central meridian 144°E.*

The second major limitation is the lack of prior geological knowledge regarding the subsurface, in particular, the scarcity of physical property measurements. The models presented, therefore, are mostly unconstrained by geological knowledge and so represent only one possible outcome that is consistent with the geophysical observations. Property constraints are applied to the inversions over the 3D map area based on the 3D province model (Section 4.1) and 2D profile forward modelling of gravity data (Section 3.2). In general, however, each province does not have significant property contrast to another so the constrains can be viewed as relatively loose or weak constraints on the inversions. In addition, a geometrical constraint is imposed on all inversions to indicate that source bodies are expected to be several times wider than they are tall, based on the geometries observed in the reflection seismic data (for example, Korsch et al., 2009). Finally, since the 3D map area extends over the Coral Sea and the Gulf of Carpentaria, a set of constraints was developed to account for the presence of the ocean.

Data sources

Gravity and magnetic data were derived from the national-scale potential field compilations (Section 2.2). Topographic data was extracted from DEM-9S (Geoscience Australia, 1998), and bathymetry data for modelling the oceanic areas was extracted from national 250 m grid cell bathymetry-topography data (Geoscience Australia, 2005).

Method

The inversions were prepared following the standard GRAV3D and MAG3D inversion workflow described by Williams et al. (2008). This workflow explains how the geophysical data should be prepared, how the various inversion parameters should be tuned, and how geological information can be incorporated into the inversions. The key points as applied to the North Queensland model areas are summarised below.

Data preparation

A key assumption implicit in any geophysical modelling procedure is that all of the observed data response can be explained by the model being developed. Where source features lie outside the model, beyond the region of interest, their contributions must be removed. Although many far-field influences are removed during standard gravity data processing, such as the removal of the reference ellipsoid, gravity and magnetic sources just outside the model area can be more difficult to account for. Various regional-residual separation techniques exist to remove the influence of these external bodies. The approach used here follows that of Li and Oldenburg (1998b) by nesting a detailed local inversion model within a coarse larger regional inversion model. The regional inversion model effectively models the source features outside the region of interest, and then their contribution to the data over the local inversion model can be calculated and removed. The calculated regional contributions for the gravity and magnetic data over the 3D map area and the Cloncurry area are shown in Figures 3.4.4-3.4.7.

Both the regional and the local inversions for the 3D map area and the area to the south of Cloncurry were prepared using the same general procedure. First the core volume of interest was defined. For the regional inversions, the depth extent was defined as 40 km, the approximate depth to the Moho based on seismic reflection data. For the local inversions the depth was specified as 25 km, based on the average inferred depth to the top of the lower crust. The core volumes and discretisation applied are indicated for each area in Table 3.4.1. The procedure outlined by Williams et al. (2008) uses standard anomaly half-width depth estimates (Telford et al., 1990), and the lateral size and depth of the core volume of interest, to define the larger extent of geophysical data required to avoid edge effects, and the extent of model padding cells required to effectively model that data area. These padding zones ensure that anomalies near the edge of the data are treated appropriately. As a result, the size of the inverted model is considerably larger than the core volume of interest. A similar approach is used to define the size of the regional inversion volume required to adequately model all sources that could contribute to the observed local data.

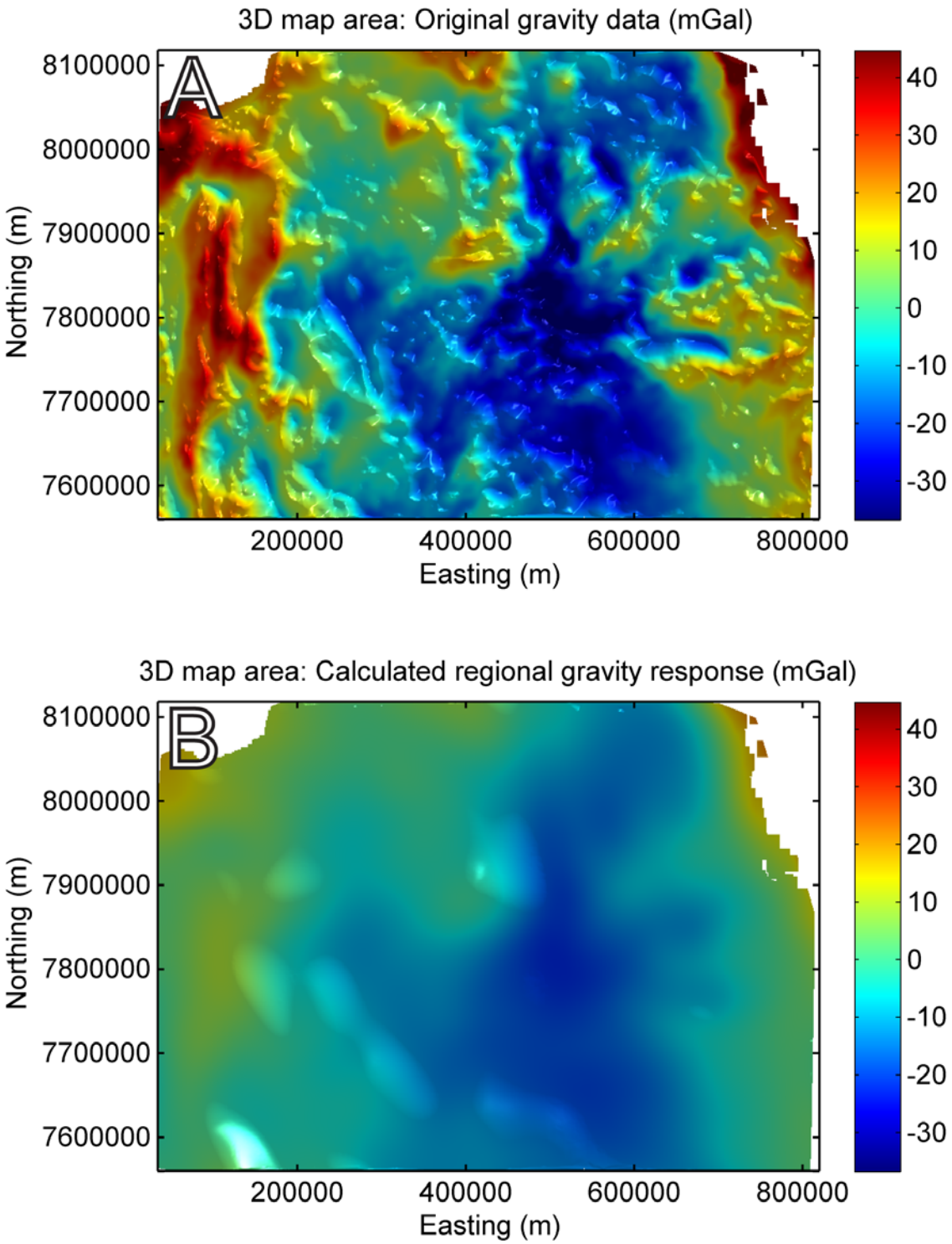

Figure 3.4.4: *(A) Observed Bouguer gravity data over the 3D map local inversion area and (B) the regional gravity response calculated from a larger regional inversion volume, as per Li and Oldenburg (1998b).*

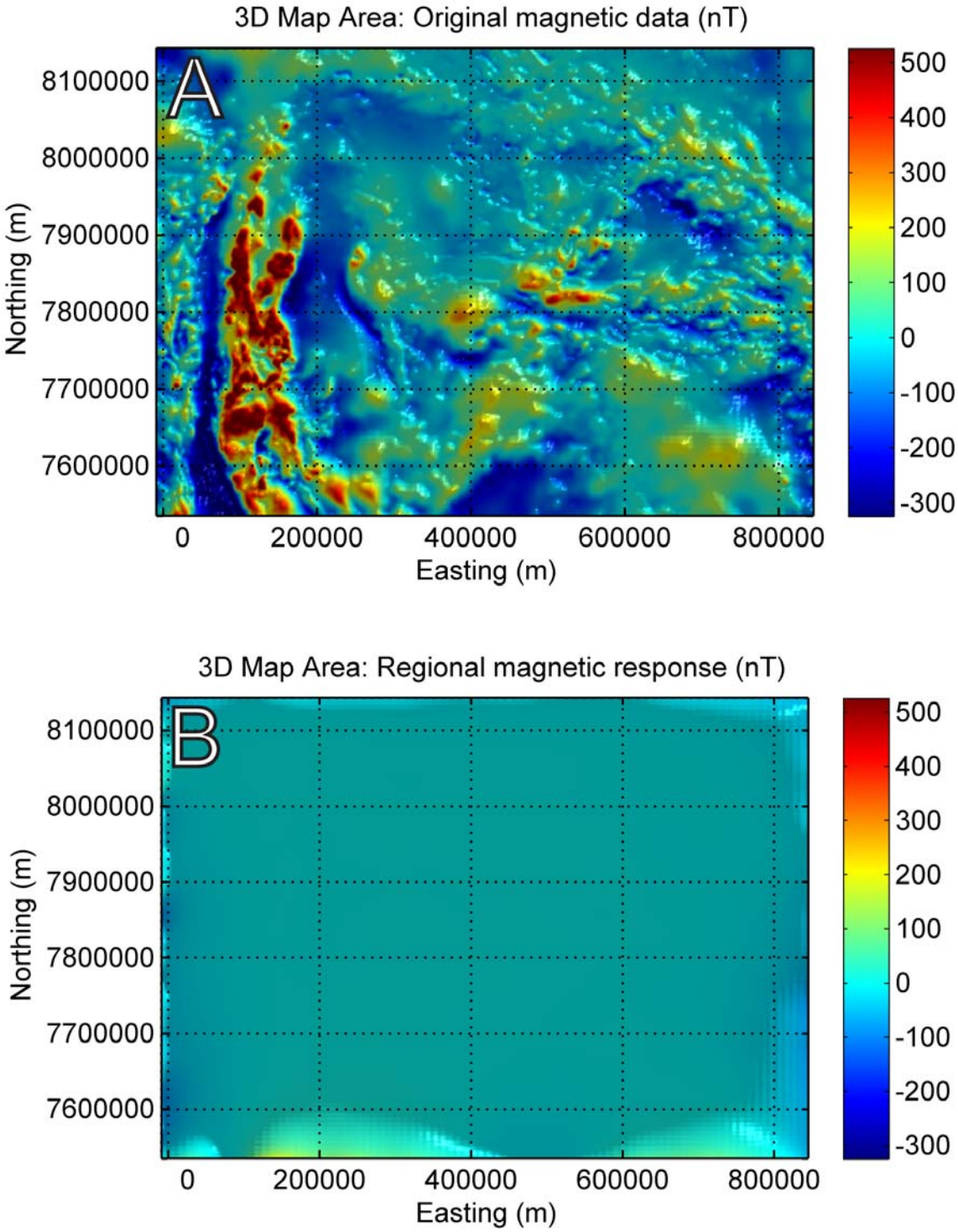

Figure 3.4.5: *(A) Observed total magnetic intensity data over the 3D map local inversion area and (B) the regional magnetic response calculated from a larger regional inversion volume, as per Li and Oldenburg (1998b). Note that the local inversion volume extends to 25 km and the regional inversion volume extends to 40 km below surface, below the inferred depth to magnetic basement, so the regional magnetic response is controlled by sources adjacent to the local volume, rather than below it.*

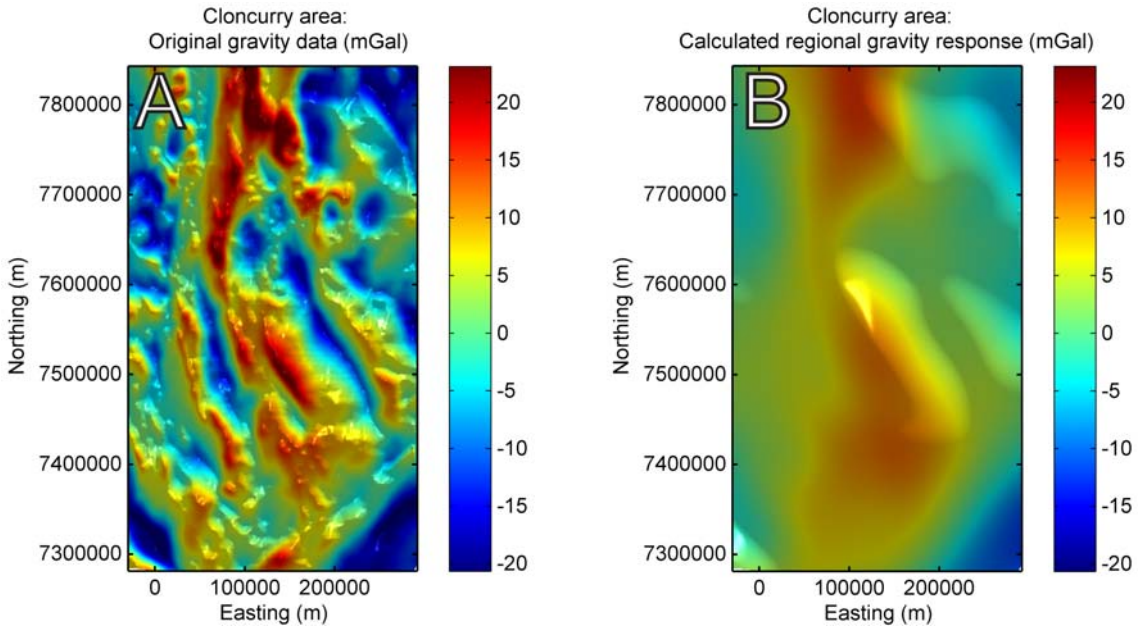

Figure 3.4.6: *(A) Observed Bouguer gravity data over the 3D map local inversion area and (B) the regional gravity response calculated from a larger regional inversion volume, as per Li and Oldenburg (1998b).*

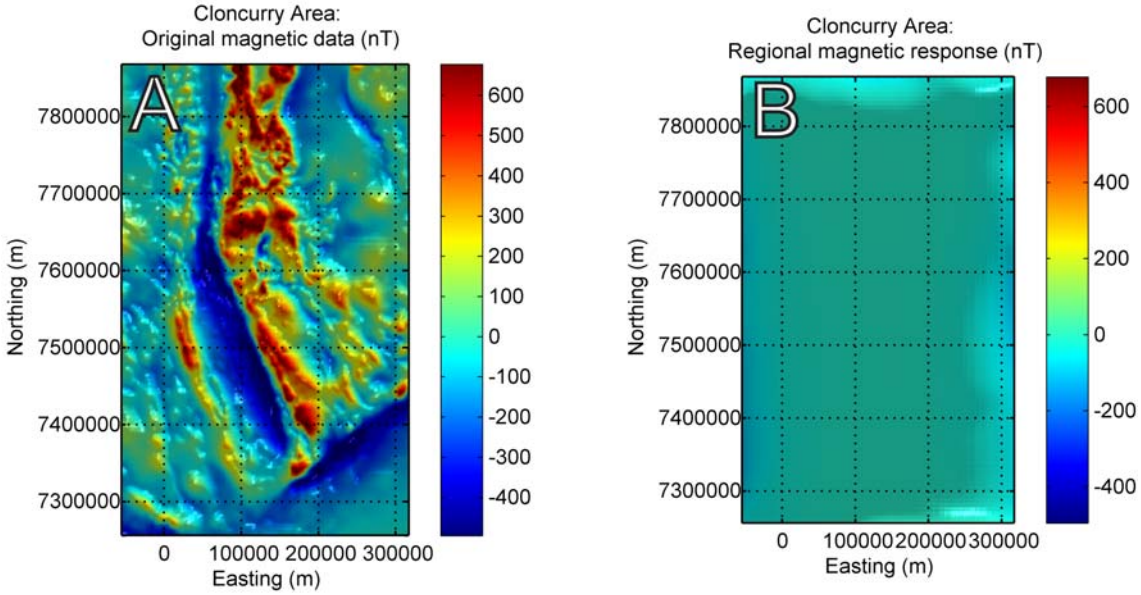

Figure 3.4.7: *(A) Observed total magnetic intensity data over the Cloncurry local inversion area and (B) the regional magnetic response calculated from a larger regional inversion volume, as per Li and Oldenburg (1998b). Note that the local inversion volume extends to 25 km and the regional inversion volume extends to 40 km below surface, below the inferred depth to magnetic basement, so the regional magnetic response is controlled by sources adjacent to the local volume, rather than below it.*

Table 3.4.1: Details of the core, data, and padding regions for each of the inversion models. The core contains the main volume of interest. The data area and padding zones are designed to allow for sources and data near the edge of the core volume. Coordinates are listed in UTM Map Grid of Australia Zone 54.5 K, relative to a central meridian of 144.0º E.

	3D MAP AREA	SOUTH CLONCURRY AREA
CORE VOLUME		
Size (east x north)	786 km × 558 km	298 km × 562 km
Maximum depth below surface	25 km	25 km
Most common cell size (east x north x vertical)	2000 m × 2000 m ×1000 m	2000 m × 2000 m × 1000 m
Number of cells	2.74 million	1.13 million
Southwest corner	34 000 mE, 7 560 000 mN	-30 000 mE, 7 281 000 mN
Northeast corner	820 000 mE, 8 118 000 mN	292 000 mE, 7 843 000 mN
DATA AREA		
Size (east x north)	836 × 608 km	372 km × 612 km
Median data spacing	Gravity: 2260 m Magnetic: 2000 m (gridded)	Gravity: 2300 m Magnetic: 400 m (gridded)
Elevation of data (above ground, including upward continuation)	Gravity: 2000 m Magnetic: 2000 m	Gravity: 2000 m Magnetic: 2000 m
Number of data	Gravity: 50 441 Magnetic: 130 057	Gravity: 31 661 Magnetic: 57 409
Southwest corner	9 000 mE, 7 535 000 mN	-55 000 mE, 7 256 000 mN
Northeast corner	845 000 mE, 8 143 000 mN	317 000 mE, 7 868 000 mN
PADDING VOLUME		
Size (east x north)	886 km × 658 km	422 km × 622 km
Total number of cells	3.64 million	1.75 million
Southwest corner	-16 000 mE, 7 510 000 mN	-80 000 mE, 7 231 000 mN
Northeast corner	870 000 mE, 8 168 000 mN	342 000 mE, 7 893 000 mN

The geophysical data were extracted as grids from the relevant national data (Section 2.2), cropped to the required areal extent, and upward continued to a height equal to the inversion model cell width to remove any high frequency signal that cannot be accommodated by such large model cells. It is usually more desirable to use non-gridded geophysical data in inversions, since gridding algorithms introduce interpolated data points where no original observations exist, and these additional points may bias the inversion results. This is especially problematic for ground-based gravity data which locally can contain large gaps between observation stations. Since upward continuation is performed in the frequency domain on regularly-spaced data grids, a compromise can be achieved by upward continuing gridded data, and then removing any introduced grid stations that are not close to original observations. The approach applied here is to remove all but the single closest grid point to each original observation location.

A procedure for defining the appropriate zero level for the supplied gravity or magnetic data is outlined by Williams et al. (2008). The zero level depends primarily on the data processing applied and the contributions of deep, long-wavelength sources outside the volume of interest, and not the actual geology. If these contributions are present in a dataset, the inversion will introduce excessively large physical property contrasts, source volumes, and/or property gradients to compensate. A first pass estimate of the appropriate zero level is usually provided by the mean data value. Further refinement can be achieved by running a suite of inversions adding small (~5%) constant shifts to the data and identifying which data shift minimises the introduction of excessive

property contrasts, source volumes and property gradients in the recovered models. For magnetic inversions in this study, the appropriate zero level was generally found by subtracting the mean value and adding ~25 nT. For gravity inversions, the mean gravity value provided an effective zero level.

The final data preparation step is to assign an estimate of the uncertainty and noise contained in the data to each data point. Typically, values of ~2.5 mGal for gravity data and 3 nT + 3 % of the magnetic anomaly for magnetic data were appropriate.

Inversion parameters

Due to the fundamental non-uniqueness of inversion, the results are intrinsically controlled by the choices of inversion parameters that are assigned. The workflow described by Williams et al. (2008) includes advice on how to efficiently identify appropriate values for each parameter depending on the problem to be addressed.

To avoid the Green's equivalent layer solution in which all gravity or magnetic sources are clustered in a thin surface layer (Blakely, 1996), the inversions must employ a potential field weighting function that compensates for the decay of potential fields with distance from the source (as described by Li and Oldenburg, 1996). All inversions were performed using a distance-based potential field weighting function that balances the r^2 and r^3 potential field decay shown by gravity and magnetic data respectively.

The other critical inversion parameters are the smoothness weights that control the relative importance of smallness versus smoothness along each orthogonal axis of the model (east, north, and vertical). The balance of smoothness versus smallness is usually specified using length scales based on the width of the mesh cells. The length scales should initially be assigned values equal to two times the dominant cell width in each direction, but these initial values can be further modified based on knowledge of the broad scale geometry of rocks in the model volume. Williams et al. (2008) describe a method whereby the cell-width-based length scales are multiplied by the expected aspect ratio of packages of rocks in each direction. Based on the geometries observed in the reflection seismic data, rock units are expected to be at least five times wider than they are thick, and this inference was used to assign length scales in both the regional and local inversions. Based on the typical cell size of 2000 m east-west by 2000 m north-south by 1000 m tall for the local inversion models, the corresponding length scales in each direction were defined as 20 000 m (= 2000 m × 2 × 5), 20 000 m (= 2000 m × 2 × 5), and 2 000 m (= 1000 m × 2 × 1). The same approach and aspect ratios were also used in the regional-removal inversions.

Geological constraints

The remaining parameters defined in the inversions relate to the inclusion of prior geological knowledge. This knowledge is supplied using:

- A reference model of best estimate physical properties in each model cell,
- A model of unitless smallness weights that indicate the user's relative confidence in the reference model properties for each cell, and
- A bounds model indicating the maximum possible range of properties allowed within each cell.

In both the regional-removal and local inversions we include an estimate of the depth to non-magnetic basement. Magnetite, the primary magnetic mineral in the crust, becomes paramagnetic above its Curie temperature of 580 ºC, and most other magnetic minerals, such as ilmenite, pyrrhotite, and hematite, are also paramagnetic at these temperatures (Hunt et al, 1995). Under a typical linear geothermal gradient of 30 ºC/km this corresponds to a depth of 18.5 km. Based on this

inference, we use bounds to impose a conservative constraint that only paramagnetic susceptibilities $< 1 \times 10^{-3}$ SI are expected below 20 km depth.

The inversions over the 3D map area must also allow for the influence of the Gulf of Carpentaria and the Coral Sea in the northwest and northeast corners. Because the height of the cells used in the models are taller than the water depth in most areas, we use a proportional representation of the height and density of the water versus the height and estimated density of underlying rock within each cell:

$$\tilde{\rho} = \left(\frac{h_{water}}{h_{cell}} \right) \cdot \rho_w + \left(\frac{h_{rock}}{h_{cell}} \right) \cdot \rho_{rock}, \quad h_{cell} = h_{water} + h_{rock} \qquad \text{(Eq. 3.4.1)}$$

where $\tilde{\rho}$ is the estimated cell density, h_{water}, h_{rock}, and h_{cell} are the median heights of the water, rock and cell respectively, and ρ_w and ρ_{rock} are the expected densities of seawater (1.03 g.cm^{-3}) and rock (2.78 g.cm^{-3}). Because the estimated density of seawater is significantly more reliable than the estimated density of the underlying rock, the smallness weights, which indicate the confidence in the reference model property, are scaled accordingly, from a maximum of 10 for a pure water cell to a default value of 1 for all pure rock cells. A similar approach is used to define property bounds that limit the range of possible property recovered in each cell according to estimates of the minimum and maximum properties of pure water and rock cells, and the minimum and maximum sea floor depth within each cell.

For the 3D map inversion volume additional constraints are available from the 3D province model (Section 4.1). Within each interpreted domain, best estimate reference and properties were assigned based on 2D potential field modelling (Section 3.2) and the results of preliminary gravity and magnetic inversions prior to the addition of geological constraints. The properties assigned within each domain are listed in Table 3.4.2. All cells contained within a defined domain were assigned a smallness weight of 2 to indicate that the assigned reference model was more reliable in those cells than in the padding cells where no prior geological knowledge was supplied. Since the gravity inversions operate on density contrasts, density contrasts were prepared by subtracting the inferred mean density of 2.78 g.cm^{-3} within the 3D map volume. Density contrasts recovered from the inversions are converted to densities by adding the same 2.78 g.cm^{-3} background value.

Inversion calculation

Due to the large size of the inversion volumes, the inversion calculations could not be performed on a single 32-bit PC due to memory and speed limitations. Instead, an automated tiling approach developed by R. Lane (written communication, 2009) was used to break a single inversion into multiple smaller inversion jobs. This method divides the supplied inversion input files and creates appropriate padding zones around each inversion sub-volume. The 3D map volume was divided into 24 separate inversion tiles; the Cloncurry models were divided into 12 tiles. These smaller inversion problems were then submitted to multiple PCs on a distributed computing cluster using the Condor High Throughput Computing software developed by the University of Wisconsin Computer Science Department (Litzkow et al., 1988). The results for each individual tile are then stitched together using sine-based weighting functions to create a seamless model of the whole volume (R. Lane, written communication, 2009).

Table 3.4.2: Estimated physical properties for each geological domain in the 3D map area based on potential field profile forward modelling (Section 3.2) and preliminary inversion results.

		DENSITY (G/CM^3)			MAGNETIC SUSCEPTIBILITY (SI)		
PROVINCE OR DOMAIN	UNIT ID	LOWER BOUND	REFER-ENCE	UPPER BOUND	LOWER BOUND	REFER-ENCE	UPPER BOUND
Abingdon	1	2.20 2.80		3.50 1	× 10^{-6}	1.5 × 10^{-2}	3 × 10^{-2}
Etheridge (main)	2	2.20	2.75	3.50	1 × 10^{-6}	2 × 10^{-2}	1 × 10^{-1}
Etheridge (sliver)	3	2.20 2.75		3.50 1	× 10^{-6}	3 × 10^{-2}	6 × 10^{-2}
Hodgkinson (includes ocean)	4	2.00 2.71		3.50 1	× 10^{-6}	1 × 10^{-2}	5 × 10^{-2}
Isa	5	2.20 2.80		4.00 1	× 10^{-6}	3 × 10^{-2}	1 × 10^{-1}
Millungera	6	2.20 2.55		3.20 1	× 10^{-6}	5 × 10^{-3}	2 × 10^{-2}
Numil	7	2.20 2.77		3.50 1	× 10^{-6}	2 × 10^{-2}	1 × 10^{-1}
Thomson (lower)	8	2.20 2.80		3.50 1	× 10^{-6}	1 × 10^{-2}	6 × 10^{-2}
Thomson (upper)	9	2.20 2.80		3.50 1	× 10^{-6}	1 × 10^{-2}	7 × 10^{-2}
Agwamin and unknown	10	2.20 2.82		3.50 1	× 10^{-6}	2 × 10^{-2}	6 × 10^{-2}

The tiling approach not only makes inversions of this size tractable, but provides the additional benefit that parameters for individual tiles can be customised if needed. In this study, the only customisation that was applied to individual tiles was that the ambient magnetic field used in each magnetic inversion was defined for the centre of each individual tile, rather than applying a single field direction for the whole model based on the centre of the entire data area. This allows for variations in the magnetic field strength and direction across the large model area. For the 3D map area, the magnetic field varies over a range of 5.9º in inclination, 2.1º in declination, and 3160 nT in intensity (Lewis, 2005).

Results and interpretation

3D map inversion

The inversion for the 3D map volume predicts a number of density and magnetic susceptibility features. A perspective view of these inversion volumes highlights these features (Figure 3.4.8, gravity inversion results and Figure 3.4.9, magnetic inversion results).

A striking feature in the results of the gravity inversion is the sublinear belt of high-density material extending from the north of the model, passing just to the east of Mt Watson and Mt Cuthbert, then heading south-southeast and passing just to the west of Duchess (Figure 3.4.8). This trend may represent a major corridor in the Mount Isa province. The entire Mount Isa Province itself is characterised by high magnetic susceptibility; the inversion results may provide a more detailed constraint on the 3D geometry of this province. Note that these results required an initial 3D geological model to constrain the inversions; these results indicate that the inversions could be used in an iterative process whereby a 3D map is constructed, inversions are constrained by this map, and then the map is updated according to the inversion results.

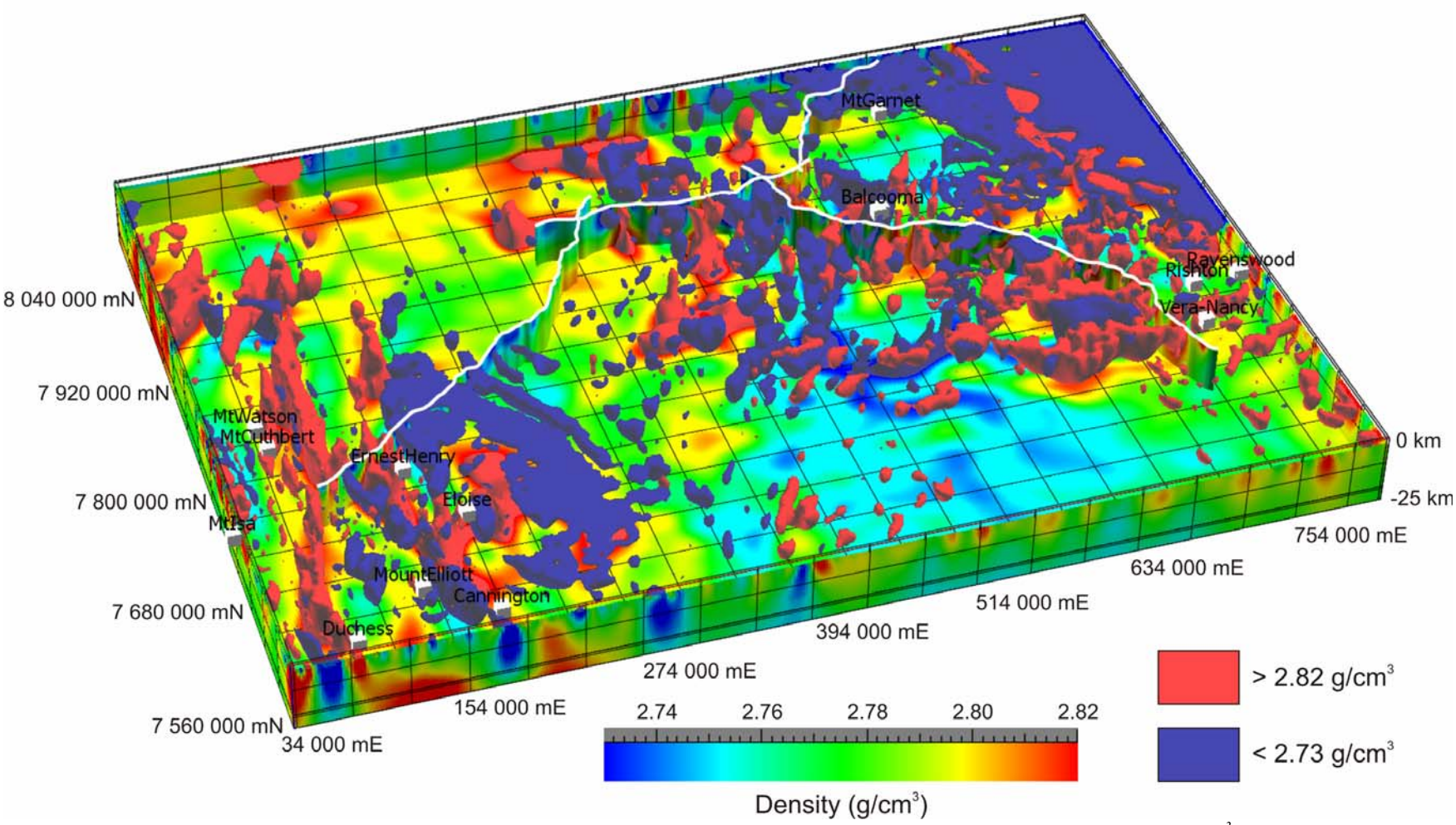

Figure 3.4.8: *Recovered density model, 3D perspective view from the SW corner of the model. Isosurfaces (3D contours) for > 2.82 g/cm^3 (red – high density) and < 2.73 g/cm^3 (blue – low density) are also noted. Background depicts slice through base of model, and properties painted on the 2007 seismic lines are also shown.*

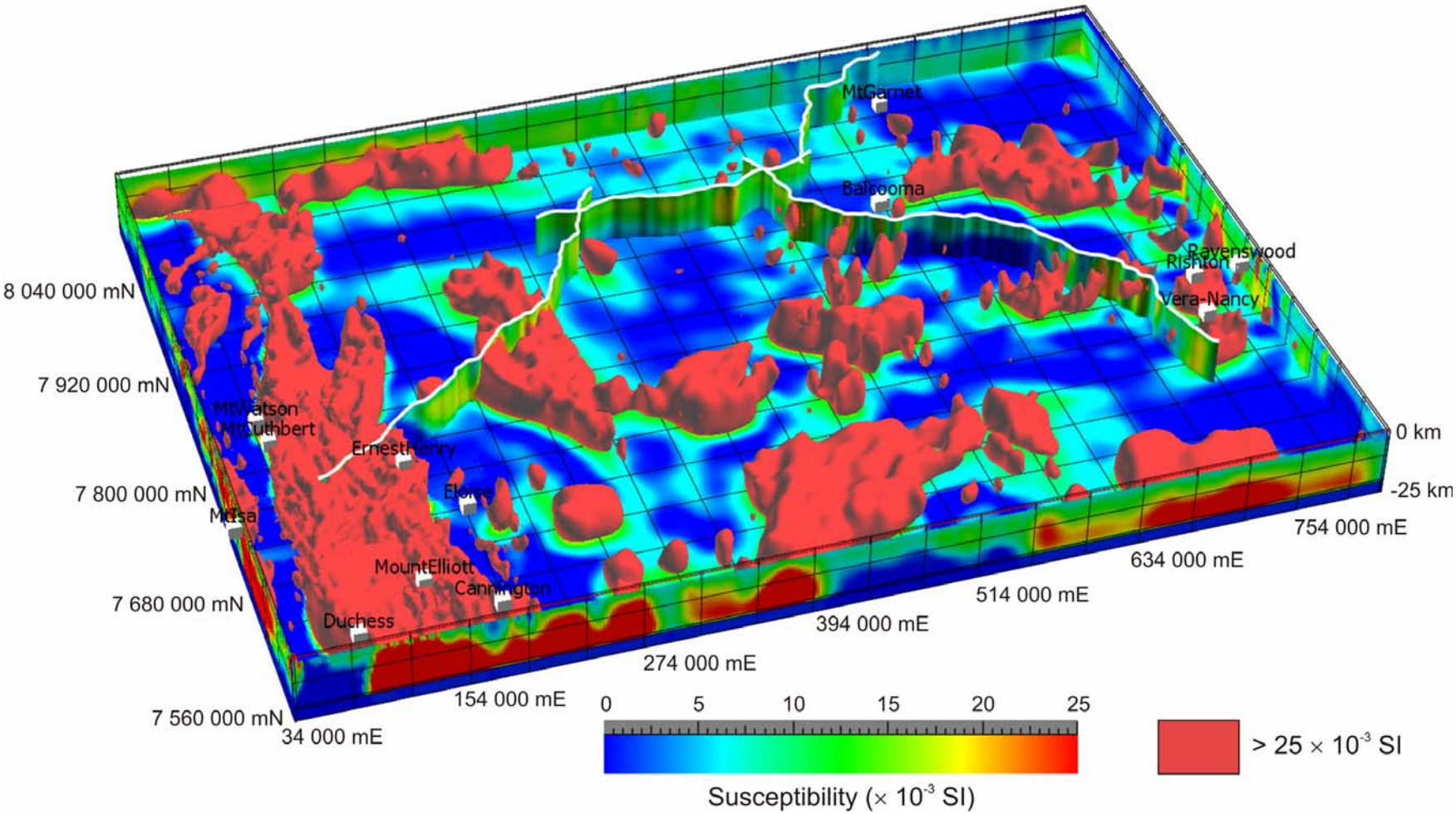

Figure 3.4.9: *Recovered magnetic susceptibility model, 3D perspective view from the SW corner of the model. Isosurfaces (3D contours) of high magnetic susceptibilities (> 25 x 10^{-3} SI) are shown in red. Background depicts slice through base of model, and properties painted on the 2007 seismic lines are also shown.*

The geometry of the Millungera Basin is recovered in the gravity inversion (Figure 3.4.10). This is despite the fact that there was no significant reference density difference between the Millungera Basin and the rocks that surround it, that is, the reference model did not force the geometry of the basin into the inversion results.

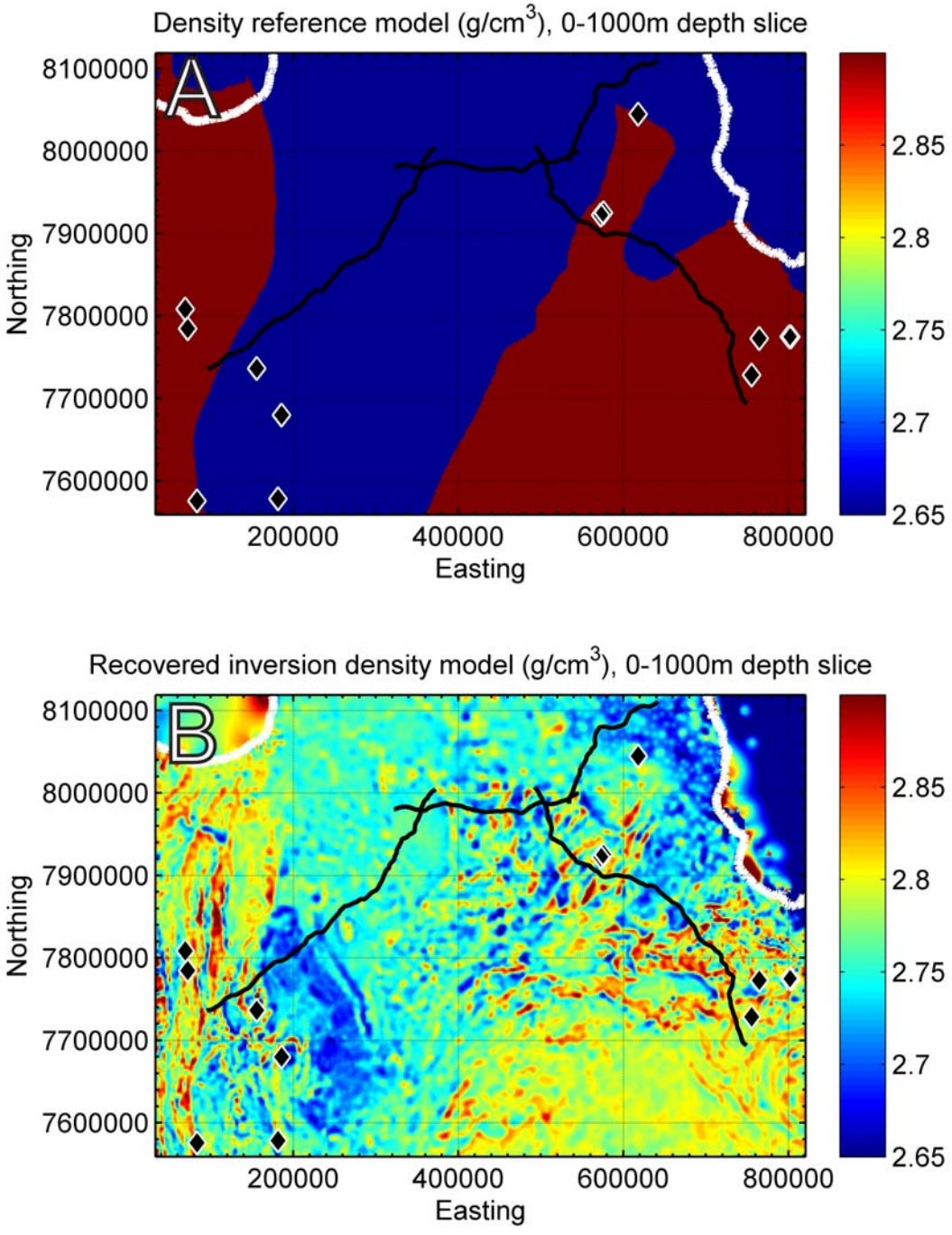

Figure 3.4.10: *0 to 1 km depth slice through the gravity inversion reference density and inverted density volumes. Note that the geometry of the Millungera Basin is recovered as a generally low-density feature, even though it was assigned a reference density the same as the rocks which surround it. Diamonds are the locations of significant mineral deposits in the region.*

The eastern boundary of the Mount Isa Province, imaged on the 07GA-IG1 seismic line as a dipping series of reflections, is imaged by the gravity and magnetic inversions (Figure 3.4.11). The recovered densities do not fully image the dip of the boundary, however, the boundary is apparent as a change from higher densities in the Mount Isa Province to lower densities east of the boundary. The geometry of the boundary is resolved more adequately by the magnetic inversions where a dipping boundary is recovered between a more magnetic region, representing the Mount Isa Province, and the less magnetic provinces to the east.

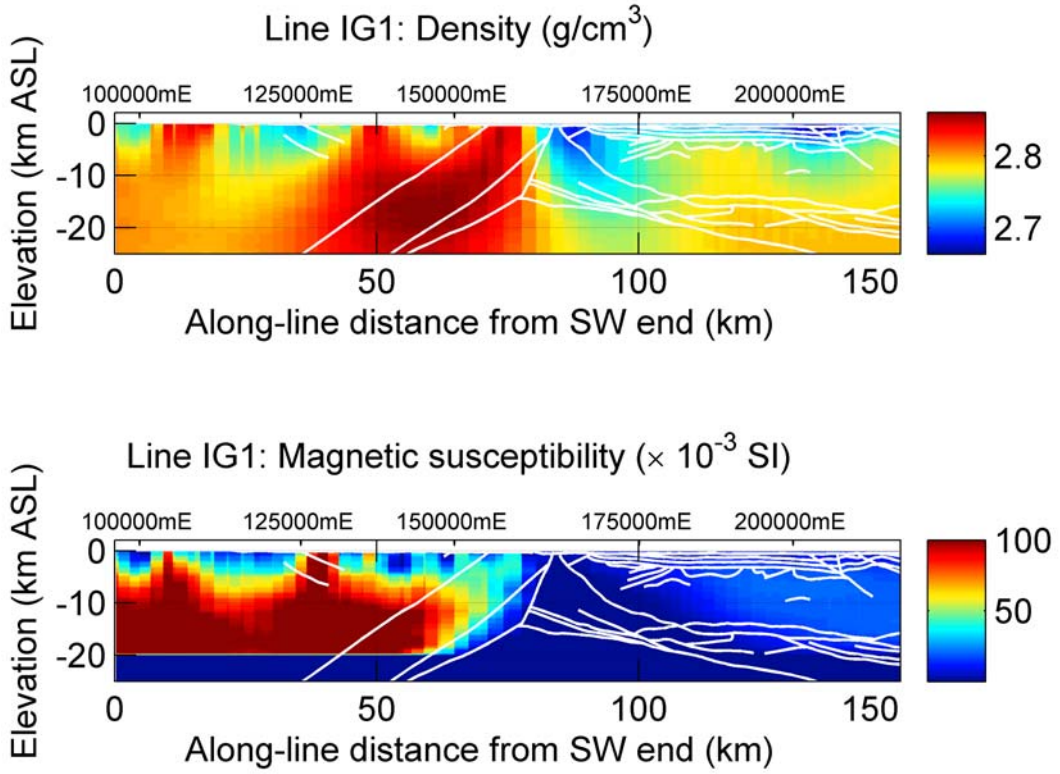

Figure 3.4.11: *Densities and magnetic susceptibilities along the 07GA-IG1 seismic line, as recovered by the gravity and magnetic inversions. The eastern boundary of the Mount Isa Province is recovered by the inversions, although the dip is better resolved by the magnetic inversion.*

South Cloncurry inversion

The South Cloncurry inversion predicts the location of extensions of the Mount Isa Province (relatively high density and magnetic material) under increasing cover, which occurs to the south of the exposed Mount Isa Province (Figures 3.4.12 and 3.4.13). The distribution of high density units are relatively patchy due to the difficulty of recovering their geometries under the increasing cover. The magnetic results, however, show two belts of relatively continuous magnetic material trending southeast.

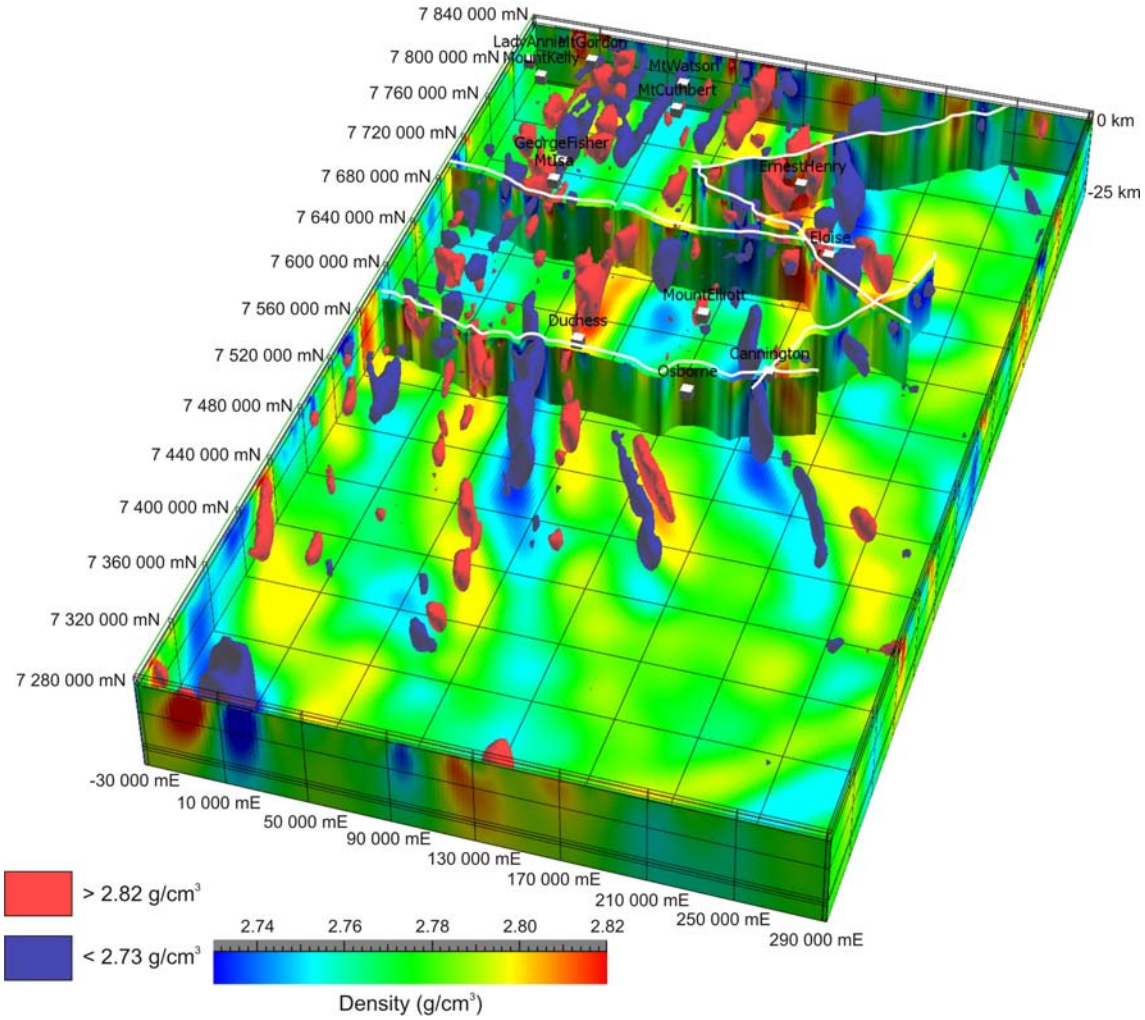

Figure 3.4.12: *Recovered density model for the south Cloncurry inversion. Isosurfaces of high (red) and low (blue) densities are shown, along with densities along the sides of the model and a depth slice at 18 km depth. Properties are also depicted on seismic lines. Patchy sublinear trends of high density to the south of the exposed Mount Isa Province show the undercover extensions of some units of this province. For inversion location refer to Figure 3.4.2.*

Summary

The inversions performed in the North Queensland region allow us to extend our knowledge of the potential field data into the third dimension. The use of the 3D provinces (Section 4.1) to constrain the inversion in the area of the 3D map increases the property contrast and thus the ability to resolve subsurface changes using the inversions. The south Cloncurry inversions also provide an estimate of the extension of the Mount Isa Province under cover to the south of the exposed Mount Isa Province.

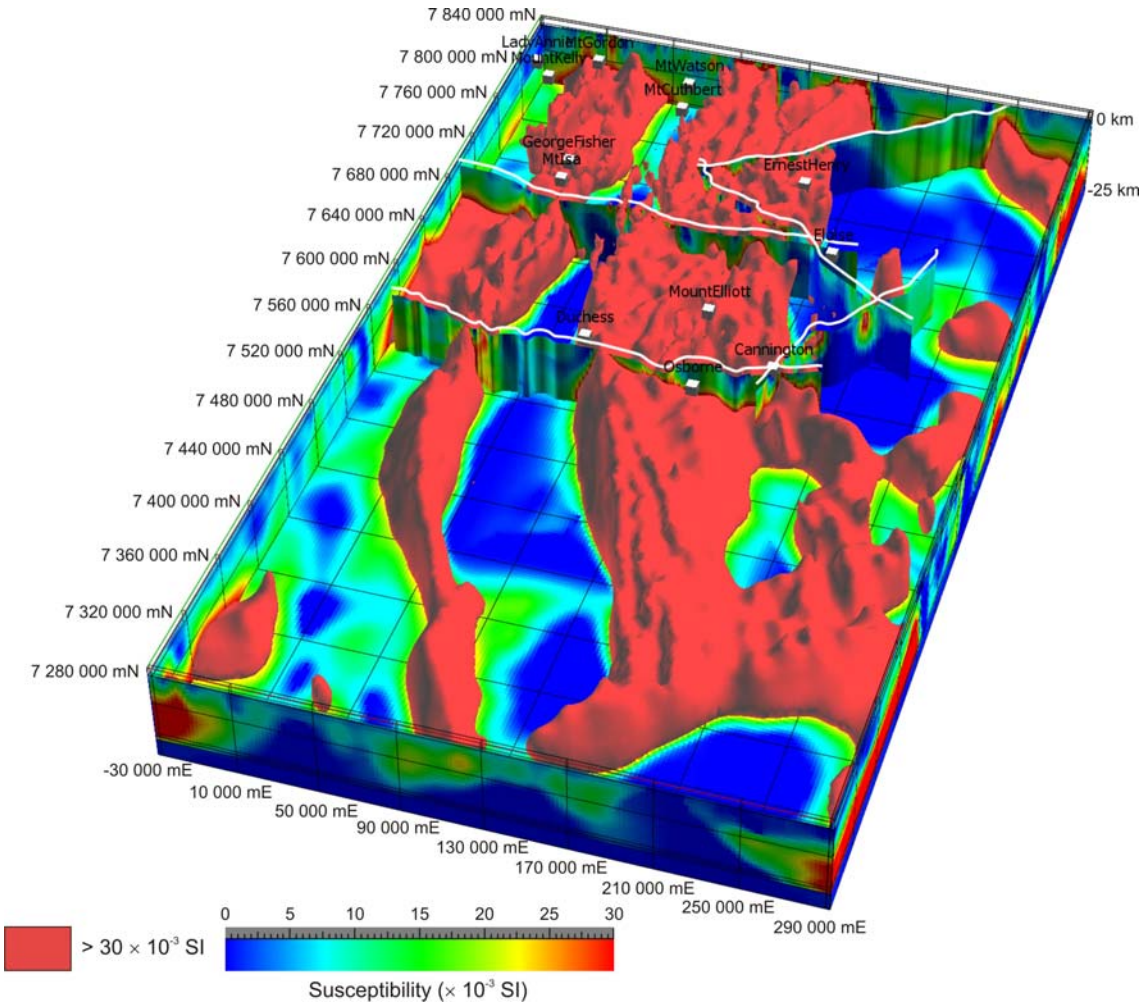

Figure 3.4.13: *Recovered magnetic susceptibility model for the south Cloncurry inversion. Isosurfaces of high (red) magnetic susceptibilities are shown, along with magnetic susceptibilities along the sides of the model and a depth slice at 18 km depth. Properties are also depicted on seismic lines. Sublinear trends of high magnetic susceptibility material to the south of the exposed Mount Isa Province show the undercover extensions of some units of this province. For location map refer to Figure 3.4.3.*

References

Bacchin M., Milligan, P.R., Wynne, P. and Tracey, R., 2008. *Gravity anomaly map of the Australian region (Third Edition)*. Geoscience Australia, Canberra.

Blakely, R.J., 1996. *Potential theory in gravity and magnetic applications*. Cambridge University Press, 464p.

Geoscience Australia, 1998. *GEODATA 9 Second Digital Elevation Model (DEM-9S) Version 2*. http://www.ga.gov.au/meta/ANZCW0703005624.html. Geoscience Australia, Canberra.

Geoscience Australia, 2005. *Australian bathymetry and topography grid, June 2005*. http://www.ga.gov.au/meta/ANZCW0703008022.html. Geoscience Australia, Canberra.

Hunt, C. P., Moskowitz, B. M. and Banerjee, S. K., 1995. Magnetic Properties of Rocks and Minerals. In: Ahrens, T. J. (Ed.). *Rock Physics & Phase Relations: A Handbook of Physical Constants*. American Geophysical Union, Reference Shelf 3, pp. 189-204.

Korsch, R.J., Withnall, I.W., Hutton, L.J., Henson, P.A., Blewett, R.S., Huston, D.L., Champion, D.C., Meixner, A.J., Nicoll, M.G., and Nakamura, A., 2009. Geological interpretation of deep seismic reflection line 07GA-IG1: The Cloncurry to Croydon transect. In: Camuti, K., and Young, D. (Eds.). *Northern Queensland Exploration and Mining 2009 and North Queensland Seismic and MT Workshop*. Australian Institute of Geoscientists Bulletin 49, pp. 153-157.

Lewis, A.M., 2005. *The Australian Geomagnetic Reference Field – Epoch 2005 (model)*. Geoscience Australia, Canberra. http://www.ga.gov.au/oracle/geomag/agrfform.jsp#agrfmodel.

Li, Y. and Oldenburg, D. W., 1996. 3-D inversion of magnetic data. *Geophysics*, **61**(2), pp. 394-408.

Li, Y. and Oldenburg, D. W., 1998a. 3-D inversion of gravity data. *Geophysics*, **63**(1), pp. 109-119.

Li, Y. and Oldenburg, D. W., 1998b. Separation of regional and residual magnetic field data. *Geophysics*, **63**(2), pp. 431-439.

Litzkow, M. J., Livny, M. and Mutka, M. W., 1988. Condor – A Hunter of Idle Workstations. *Proceedings of the 8th International Conference of Distributed Computing Systems*, pp. 104-111.

Milligan, P.R. and Franklin, R., 2004. *Magnetic Anomaly Map of Australia (Fourth Edition)*. Geoscience Australia, Canberra.

Telford, W.M., Geldart, L.P. and Sheriff, R.E., 1990. *Applied Geophysics (Second Edition)*. Cambridge University Press, Cambridge, 790p.

Williams, N. C., Lane, R., Oldenburg, D. W., Lelievre, P., Phillips, N. and Jones, F., 2008. A workflow for preparing and applying UBC–GIF gravity and magnetic inversions. In: Williams, N. C. *Geologically-constrained UBC–GIF gravity and magnetic inversions with examples from the Agnew-Wiluna greenstone belt, Western Australia*. Ph.D. thesis, University of British Columbia, 478p. http://hdl.handle.net/2429/2744.

4. 3D map and interpretations

4.1 3D MAP

P.A. Henson

Introduction

The main aims of this project were to compile and import all the available data into 3D space, and using these data, produce a series of volumetric regions that represented the 3D architecture of different provinces. These were constrained at the surface, where possible, by the new solid geology map, whereas their subsurface geometries were primarily constrained by the new seismic reflection data. Interpretation of the seismic data followed an iterative process, whereby the surface geology, geophysics, metamorphic, geochemical and age constraints were used to guide the interpretations on paper copies (Henderson et al., 2009; Hutton et al., 2009a; Hutton et al., 2009b; Korsch et al., 2009; Withnall et al., 2009a). Although these interpretations were valid on the individual seismic lines, it was difficult to link all the geometries and timing constraints between the array of seismic lines. In order to provide a series of internally consistent interpretations, the seismic lines were imported into GOCAD™ and the interpretations were modified to suit. This provided an essential component of the process and also allowed the data to be viewed in its true georeferenced coordinates, highlighting any bends in the trace of the seismic lines that can alter the true architecture or dip of reflections.

Building the 3D architecture

The goal of this study was to build a 3D architecture of the North Queensland region. A variety of data are available to interpret the geological components of the region, although there are only some datasets that provide constraints on the deep crustal architecture. The data used in this study to constrain the architecture have significantly different coverages. Seismic reflection data provided one of the most significant understandings of the crustal architecture, although it only constrains the subsurface geometries vertically beneath the line. Magnetotelluric data is equally restricted to the subsurface vertically beneath the acquisition stations. Gravity and magnetic data have good regional coverage in the study area and were used extensively, in conjunction with surface constraints, to extrapolate out from the interpretations made on the seismic reflection lines. An additional dataset used in this study to constrain the architecture was Sm-Nd isotopic data. These data provide some insights into the different model ages of crustal source regions. Consequently, these data provided important spatial constraints to the 3D and 4D interpretations of the region.

Constraining the crustal components using Sm-Nd isotopes

The age variations noted in the Sm-Nd data for the region (Figure 4.1.1) are interpreted to reflect the model dependant ‘estimate’ of the bulk age of the source rock (assumed to be dominantly middle to lower crustal), based on the Sm-Nd isotope systematics (see Champion & Cassidy, 2008). A broad younging trend to the east is evident in the data, with a gradient occurring within the Eastern Fold Belt of the Mount Isa Province and a major gradient occurring to the east of Georgetown. Sm-Nd data were compared spatially against the seismic reflection and magnetotelluric data in order to derive an understanding of the different crustal components and relative ages of the middle to lower crust where these melts would have been derived. In parallel, the inherited zircon ages were compared against the Sm-Nd model ages and showed very similar trends.

Constraining the province geometries with seismic and magnetotelluric data

The seismic and magnetotelluric data (Section 2.2) provide fundamental constraints on the 3D geometries of the provinces, including the previously unknown seismic provinces such as the Numil,

Abingdon and Agwamin Seismic provinces (see Henderson et al., 2009; Hutton et al., 2009a; Hutton et al., 2009b; Korsch et al., 2009; Withnall et al., 2009a).

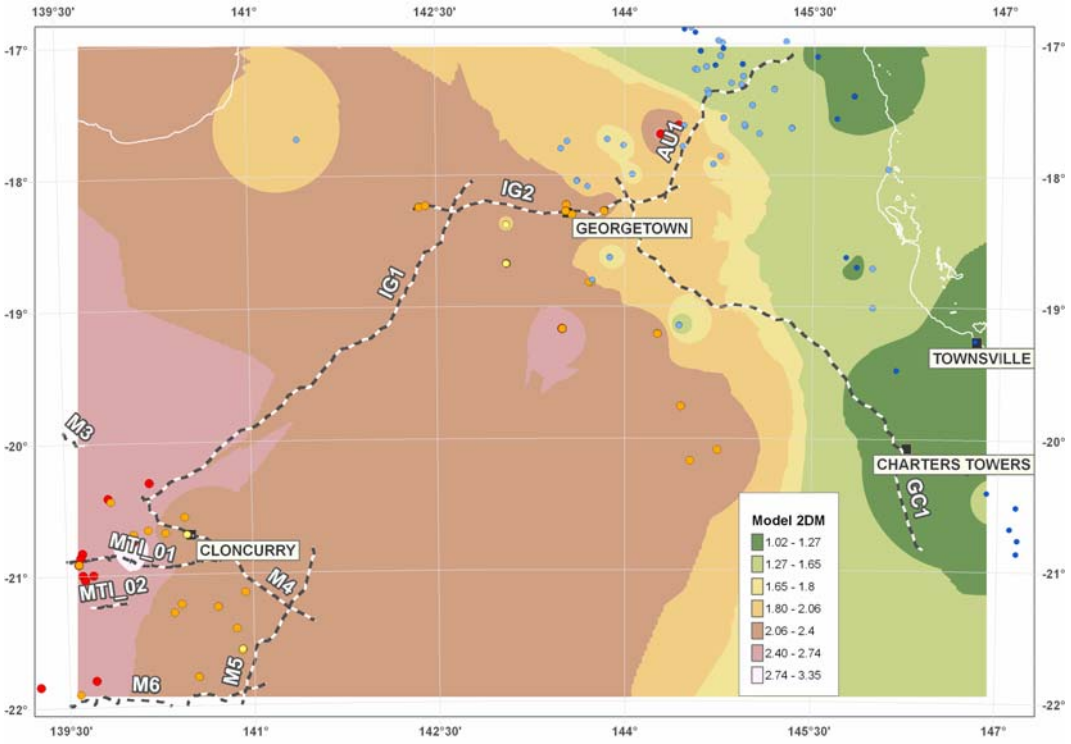

Figure 4.1.1: *Gridded image of Sm-Nd isotopic data showing the model crustal ages in the Mount Isa, Georgetown and Charters Towers region. Coloured dots indicate sample locations (dots young from red, to orange, to light blue to dark blue). Abbreviated and full seismic line names are as follows: M3 = 06GA-M3, M 4= 06GA-M4, M5 = 06GA-M5, M6 = 06GA-M6, MTI_01 = 94MTI-01, MTI_02 = 94MTI-02, IG1 = 07GA-IG1, IG2 = 07GA-IG2, GC1 = 07GA-GC1 and AU1 = 07GA-A1.*

4D geodynamics

In order to construct the 3D architecture of the North Queensland region, a diagrammatic interpretation of the 4D evolution of the region was produced. This provided a framework that enabled both the geometries of the new seismic reflection and the spatial distribution of different lithologies, and the paleogeographic environments in which they formed, to be addressed. The schematic drawings are in the form of a series of east-west sections covering the area from the Mount Isa Province to Charters Towers. This process was integrated with the seismic interpretation, and used all the available data to constrain the spatial distribution of different provinces and their 4D evolution. It must be noted that this is only one possible interpretation of the evolution of the North Queensland region and there may be alternative interpretations that also honour the available data.

Eleven individual cross sections have been constructed to explain the interpreted paleogeographic environments that existed at different time periods (Figure 4.1.2). These interpretations attempt to deconstruct the present architecture and province distribution visible in the new seismic reflection data. The timing and architectural interpretations draw heavily on published data including: Henderson (1987); Fergusson et al. (2007); Henderson et al. (2009); Hutton et al. (2009a); Hutton et al. (2009b); Kositcin et al. (2009); Korsch et al. (2009); Withnall et al. (2009a); Withnall et al. (2009b).

The following descriptions will outline the significance of each individual section and its associated crustal evolution and architectural development at that time.

>1860 Ma and ~1860 Ma

The Mount Isa Province is interpreted to have a west-dipping, convergent plate margin with the Numil- Abingdon Seismic Province to the east. Supporting this hypothesis is the occurrence rocks with arc-like affinities in the Kalkadoon-Leichhardt Belt which may be related to subduction processes. If this assumption is correct, docking of these provinces could have occurred at ~1860, and explains the significant change in reflectivity observed between the Mount Isa Province and the Numil-Abingdon Seismic Province in the current seismic reflection data on 07GA-IG1 line (Korsch et al., 2009).

>1860 Ma-1710 Ma

Docking of the Numil-Abingdon Seismic Province with the Mount Isa Province lead to the possible initiation of a west-dipping subduction zone on the eastern margin of the Numil-Abingdon Seismic Province. Subduction on this margin initiated a potential arc and back-arc geometry. Continued subduction and probable roll-back, attenuated the crust to produce probable oceanic crust, which separated the Numil Seismic Province from the Abingdon Seismic Province by an undetermined distance. Alternatively, the separation and docking of the Numil and Abingdon Seismic Provinces may have occurred prior to them docking with the Mount Isa Province at >1860 Ma.

>1710 Ma and ~1710 Ma

The timing of the docking between the Numil Seismic Province and the Abingdon Seismic Province is determined to be greater than 1710 Ma. In this representation, it is interpreted as occurring post the docking of the Numil-Abingdon Seismic Province with the Mount Isa Province, although docking of these provinces before this time can not be ruled out. Docking at ~1710 Ma is consistent with the maximum age of Etheridge Group and also the Bigie Unconformity in the Mount Isa Western Succession. The docking event produced an abrupt step in the Moho at the boundary between the Numil Seismic Province and Abingdon Seismic Province, and a relict west-dipping subduction zone is interpreted in the 07GA-IG1 seismic line (Korsch et al., 2009). An alternative hypothesis is that the Numil and Abingdon provinces never separated and that the step in the Moho is formed during a whole of crust thrust fault.

~1710–1590 Ma

Following the docking of the Numil and Abingdon Seismic provinces it is interpreted that approximately west-dipping subduction initiated to the east of the Abingdon Seismic Province. Arc, backarc and rollback produced different paleogeographic environments across the Etheridge Province. To the west, the Kowanyama Province and Mount Isa Province were being extended, and there was attenuation of the continental crust. This initiated significant deposition of sedimentary successions in the Kowanyama and Mount Isa Provinces that are temporal equivalents of units in the Etheridge Province. At ~1640 Ma, a north-south contractional event produced approximately east west folds and shortening that cannot be represented in these east-west oriented sections.

~1590 Ma

At 1590 Ma, a major ~east-west contractional event produced significant shortening in the Mount Isa and Kowanyama provinces, with less apparent affect in the Etheridge Province. Inversion occurred on pre-existing extensional faults and new thrusts also developed. Overall thickening of the crust occurred at this time through shortening of all the provinces, which is coincident with the age of peak metamorphism in the Etheridge Province (Cihan et al, 2006; Withnall et al, 2009b), Cape York region (Blewett and Black, 1998) and Mount Isa Province (Betts and Giles, 2006).

~1550–480 Ma (including the breakup of Rodinia)
Extensional tectonic processes affected the Agwamin Seismic Province and the overlying Neoproterozoic Thomson Orogen on the margin of the Etheridge Province and the underlying Abingdon Seismic Province. The breakup of the Rodinian supercontinent produced a passive continental margin with oceanic crust located approximately to the southeast.

490-430 Ma and ~440Ma (Benambran Cycle)
A period of approximately west-dipping subduction developed an accretionary wedge and the Balcooma Windsor arc-backarc system on the eastern margin of the Etheridge Province. At about 440 Ma, an arc collided with the continental margin producing significant shortening of the Agwamin Seismic Province and units in the overlying Thomson Orogen, and overthrusting of the accretionary wedge during the Benambran Orogeny at 440-430 Ma (Kositcin et al., 2009). This event also produced thrusting of the Etheridge Province over units of the Thomson Orogen along the Lynd Mylonite Zone.

~440-360 Ma
Following the arc-continent collision, approximately west-dipping subduction recommenced, generating the arc-forearc units of the Broken River Province and accretionary wedge units of the Hodgkinson Province. Rollback and eastward migration of the subduction zone produced an eastward migration of the arc and forearc units as well as the accretionary wedge.

~380-360 Ma
The east-west contractional event of the Tabberabberan Orogeny shortened the Broken River and Hodgkinson province units. This event is interpreted here to be caused by collision with an arc to the east, thrusting the Hodgkinson Province and parts to the Broken River Province units westward over the and older units to the west. Alternatively, the event may have been driven by shallowing of the subduction zone, putting the upper plate into contraction instead of extension.

Descriptions of 3D provinces

A series of provinces were named in order to define regions of the project area (Figure 4.1.3). These provinces were discrete regions that have a broadly similar seismic character and structural history. The following will describe the present geometries and the constraints that used to construct the 3D provinces. The 3D provinces were constructed to integrate the interpretation of the seismic reflection data and to understand the potential 3D distribution of the provinces.

The provinces to be described are the:
- Mount Isa Province
- Numil Seismic Province
- Abingdon Seismic Province
- Agwamin Seismic Province
- Etheridge Province and Kowanyama Province
- Thomson Orogen
- Broken River Province and Hodgkinson Province

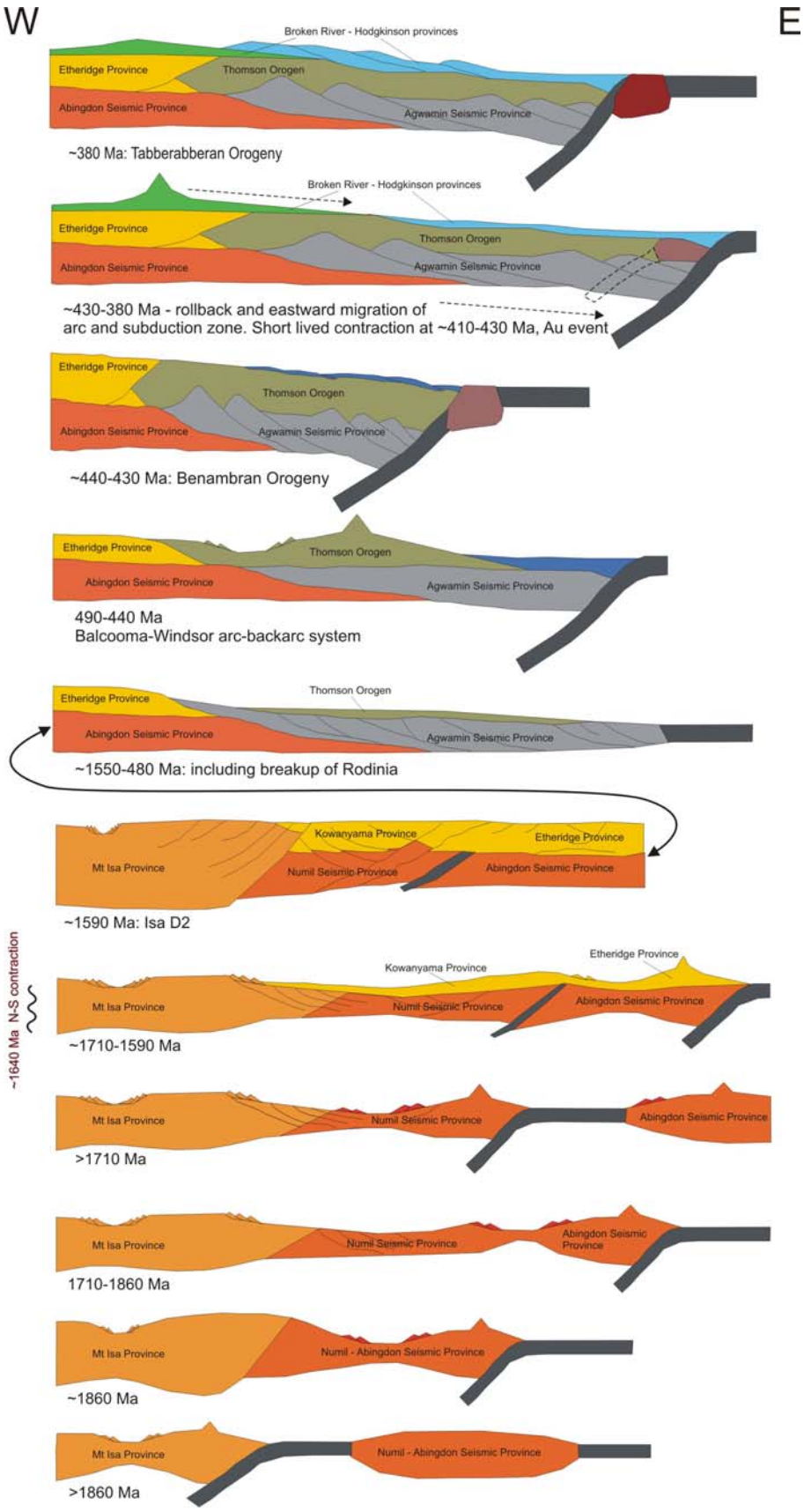

Figure 4.1.2: *Interpretation of the 4D geodynamic evolution of the North Queensland region*

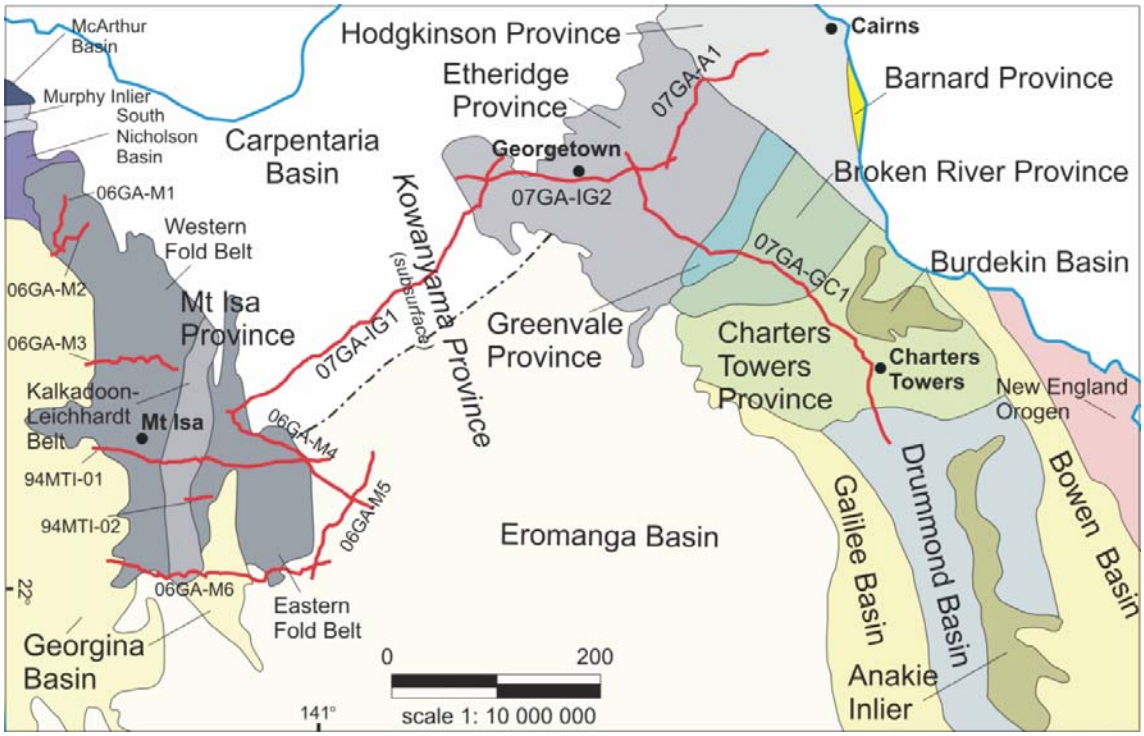

Figure 4.1.3: *Province map of the North Queensland region.*

Mount Isa Province

One aim of this study was to delineate the eastern boundary of the Mount Isa Province (Figure 4.1.4), not to construct the detailed architecture within the province. The eastern boundary of the Mount Isa Province has been defined, in this case, using a number of geophysical and geological constraints. Overall, the Mount Isa Province is defined by a series of linear, approximately north-south trending magnetic and gravity features, although in detail there are significant local variations and truncations to these trends. The eastern boundary of exposed Proterozoic rocks is overlain by sediments of the Carpentaria and Eromanga Basins, making the exact locality of the boundary difficult to define at surface.

Geophysical data were used almost exclusively to define the eastern boundary of the province. This position will be discussed at length below as it is very likely to be a fundamental control on the spatial position of mineralisation. In addition to the seismic constraints, a variety of geological and geophysical interpretations were used.

Eastern boundary of the Mount Isa Province

The link between the Mount Isa Province and the Georgetown Province to its east has been previously unknown. New seismic reflection and magnetotelluric data have been acquired across this boundary, providing an increased understanding of the crustal architecture and geodynamic evolution of this region and the potential ambiguities that arise from these data.

The first insights about the subsurface expression of the eastern boundary of the Mount Isa Province were acquired during the 1994 seismic survey, where the east-west trending 94MTI-01 seismic line crossed the eastern extent of the exposed Paleoproterozoic units just to the south of Cloncurry (Drummond et al 1998). A more extensive survey of six seismic reflection lines were acquired over the Mount Isa Western and Eastern successions during the Mount Isa 2006 Seismic Reflection Survey. Three of the southern lines from this survey (06GA-M4, 06GA-M5 and 06GA-M6) formed an interconnected array across the eastern extent of the exposed Paleoproterozoic units and

connected with the 94MTI-01 seismic at 06GA-M4 (Figure 4.1.1). The latest seismic reflection survey was conducted in 2007 where the 07GA-IG1 seismic line tied to the 06GA-M4 seismic line near its northwestern end and followed a northeast route across the Carpentaria Basin to the Proterozoic units in the Croydon area. It must be noted that the only seismic line that has significant extent to the east of the exposed Mount Isa Province is GA07-IG1.

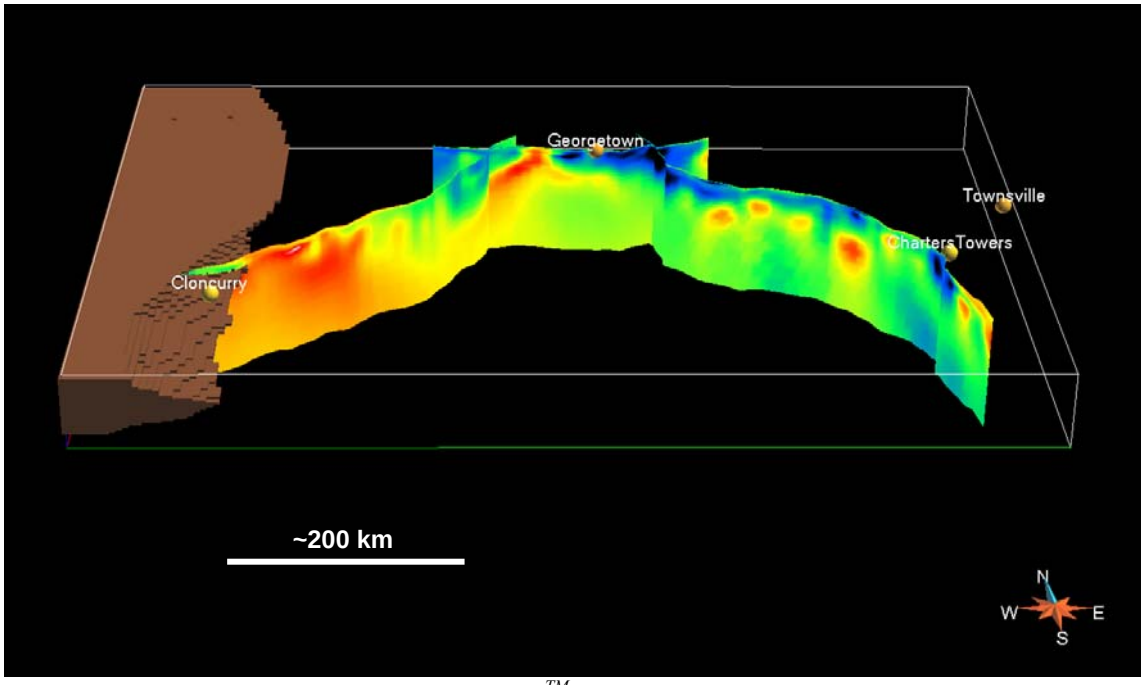

Figure 4.1.4: *3D perspective image from GOCAD™ of the Eastern Mount Isa Province volume and the three magnetotelluric lines.*

The eastern margin of the Mount Isa Province is evident in both magnetic and gravity data. The magnetic data and inversions (Section 3.4) define an abrupt north-northeast to north-south trending boundary to the north of Cloncurry, with high magnetic response in the west and low magnetic response in the east. In contrast, the region around Cloncurry and to the south is less clearly defined. This region displays a broadly north-south trending gradient similar to that north of Cloncurry and is approximately coincident with the Cloncurry Fault. The region to the east of this gradient consists of less magnetic ovoid to linear magnetic responses that display more similarities to the region to the west than in the east. This observation indicates that the upper crustal units at this locality have similar geophysical characteristics, indicating that they are continuous to the east. Overall, the magnetic response is higher in the Mount Isa Province than in the region to the east under the Carpentaria and Eromanga basins.

The gravity data indicate a similar spatial relationship to the magnetic data, with a more clearly defined boundary in the north than the south. One feature of the gravity data is the broadly linear regional north-south linear gravity highs that are dominant in the eastern part of the Mount Isa Province. The eastern-most linear gravity high is coincident with the gradient in the magnetic data to the north of Cloncurry, and although the region to the south is less clearly defined, there are significant divergences of these trends, when compared to the trends in the magnetic data. The southern region does delineate some of the ovoid bodies defined by the magnetics, but the general trend of the regional linear gravity high is north-northwest and to the east of the broadly north-south trend in the magnetic data.

In summary, to the north of Cloncurry there are good spatial correlations between the linear trends in the gravity and magnetic data defining a boundary at the eastern margin of the Mount Isa Province to the north of Cloncurry. To the south of Cloncurry, or at approximately the location where the Fountain Range and Pilgrim Faults intersects this boundary, it becomes difficult to define a sharp boundary using the geophysics and there are significant divergences in the gravity and magnetic trends.

When the potential field relationships are spatially compared with the seismic reflection data, a number of similarities and differences are revealed. The 07GA-IG1 seismic line is the northernmost line and crosses the eastern boundary of the exposed Mount Isa Province at a region that clearly defines broadly coincident abrupt magnetic and gravity gradients. This location is also coincident with a large change in the Moho depth, with the Mount Isa Province being significantly thicker than the region to its east. The Mount Isa Province is seismically non-reflective and is separated from the highly reflective region to the east by a series of moderate west-dipping reflections. The westernmost portion of the line crosses the Fountain Range and Pilgrim Faults and is marked by moderately east-dipping reflections that sole out in the upper crust and appear to truncate the large west-dipping boundary previously mentioned.

The architecture visible on the 07GA-IG1 seismic line across the Mount Isa Province boundary is less clearly defined on the array of seismic lines to the south. A hypothesis is that there should be a similar structural discontinuity visible on one of the southern seismic lines. Both the north-south trend of the magnetics and the more north-northeast trajectory of the gravity were tested. These analyses were conducted in 3D using GOCAD^{TM}, as all of the geophysical and geological data were able to be viewed in their correct spatial coordinates.

Analysis of both trends proved to be difficult as there is not an exact analogue to the 07GA-IG1 seismic line architecture on the southern lines. This is partially due to the limited eastern extent of these lines. There is, however, strong evidence of a west-dipping structure imaged on the 06GA-M6 seismic line that is non-reflective on the western side and reflective on the eastern side. This structure is truncated by an interpreted sole thrust onto which an array of upper crustal reverse faults sole. At this location this fault is interpreted to be the subsurface expression of the Fountain Range and Pilgrim Faults. This relationship is consistent with that on the 07GA-IG1 seismic line and it is this relationship that is interpreted here to be the continuation of the abrupt boundary imaged on 07GA-IG1. Analysis of the spatial location of the gravity trend did not indicate a coincident structure in the seismic reflection data, although this cannot be ruled out as an additional structure on the eastern boundary of the Mount Isa Province.

Numil Seismic Province

The Numil Seismic Province has no surface expression and its existence is interpreted entirely from seismic reflection data. The western boundary of the Numil Seismic Province abuts the Mount Isa Province and was described in the previous section on the Mount Isa Province. It is interpreted to cover a significant area and is constrained by 06GA-M4, 06GA-M5, 06GA-M6, 94MTI-01, 07GA-IG1 and 07GA-IG2 seismic lines (Figure 4.1.5). An additional constraint on the location of the western boundary is the Sm-Nd model ages that indicate a boundary broadly occurs between the older Western Succesion and younger Eastern Succession of the Mount Isa Province, at approximately the location of the Fountain Range and Pilgrim Faults.

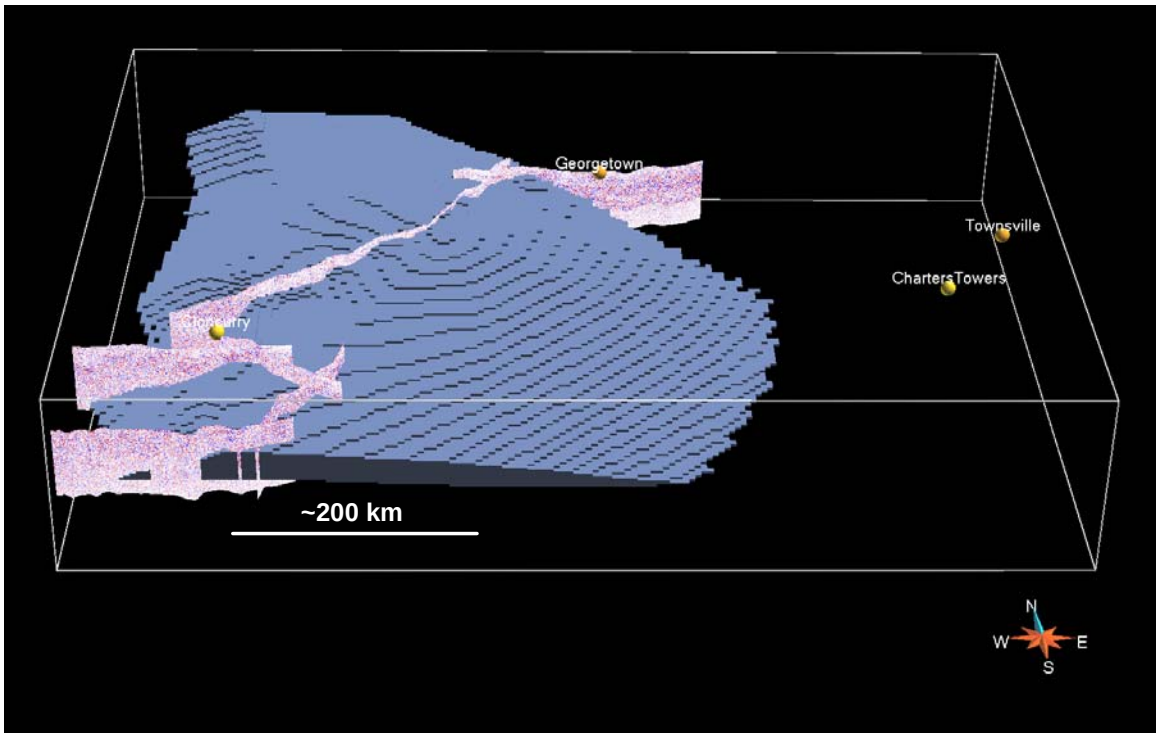

Figure 4.1.5: *3D perspective image from GOCAD™ of the Numil Seismic Province volume and 06GA-M4, 06GA-M5, 06GA-M6, 94MTI-01, 07GA-IG1 and 07GA-IG2 seismic lines.*

The boundary between the Numil Seismic Province and the Abingdon Seismic Province is interpreted from the 07GA-IG1 and 07GA-IG2 seismic lines. This boundary is well defined on the 07GA-IG1 seismic line as a major step (~7 km) in the Moho at an apparent southwest-dipping series of refections, interpreted to be a relict subduction zone that does not extend above the base of the overlying Etheridge Province units (Korsch et al., 2009). The orientation of this boundary is interpreted to be northwest trending, based on the orientation of the interpreted structure on the 07GA-IG1 and 07GA-IG2 seismic lines in 3D. It must be noted that there are no other geophysical datasets that clearly identify this structure. The eastern boundary of the Numil Seismic Province is interpreted to taper to the east against the Moho (Figure 4.1.6).

Abingdon Seismic Province

The Abingdon Seismic Province abuts the Numil Seismic Province to the east, has no surface expression, and is interpreted entirely from seismic reflection data. Its architecture is constrained by the 07GA-IG1, 07GA-IG2, 07GA-GC1 and 07GA-A1 seismic lines (Figure 4.1.6). The eastern boundary tapers to the east against the Moho, which is constrained on the 07GA-GC1 and 07GA-A1 seismic lines. Supporting this interpretation are the Sm-Nd model ages that indicate a transitional zone of model ages younging to the east (Figure 4.1.1). The transitional zone in the Sm-Nd model ages corresponds to where the younger Agwamin Seismic Province onlaps the Abingdon Seismic Province and forms the lower crust (Henderson et al., 2009; Withnall et al., 2009b).

Sm-Nd model ages of granites, gneisses and felsic volcanic units derived from source regions of the Numil and Abingdon provinces indicate that the two provinces have approximately identical model age ranges. This supports the preferred hypothesis that the two provinces evolved as a single entity, which subsequently rifted apart and later collided at the interpreted relict subduction zone.

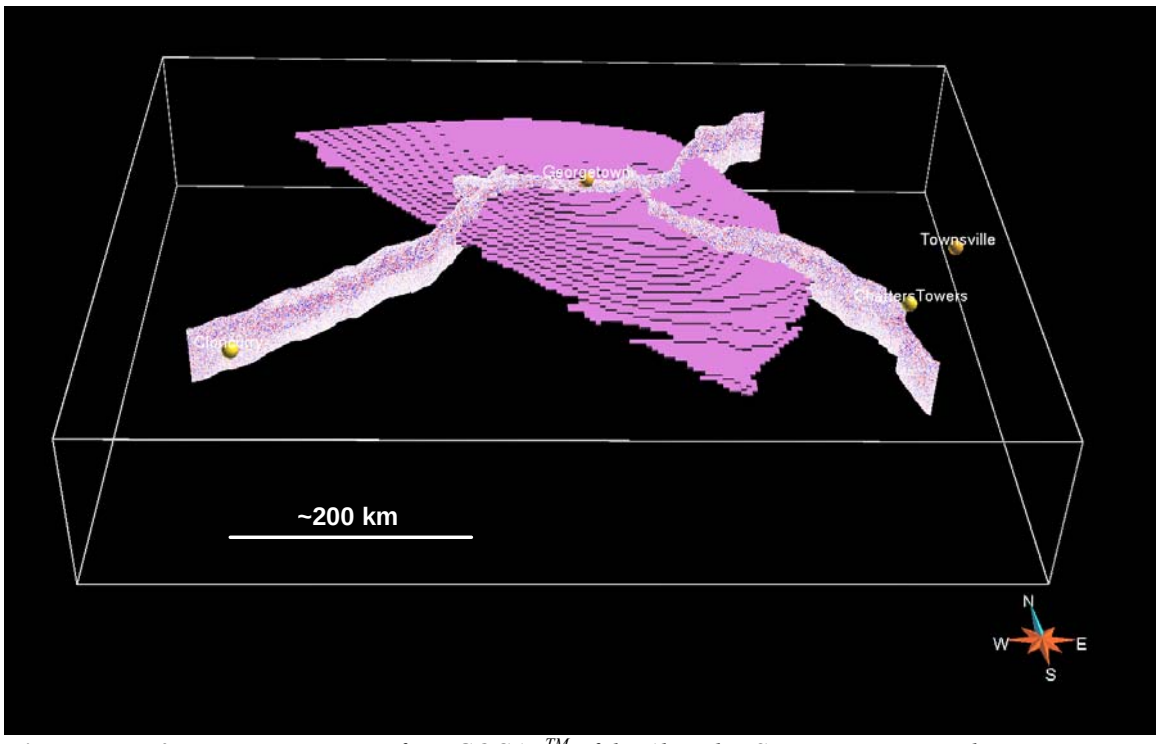

Figure 4.1.6: *3D perspective image from GOCAD™ of the Abingdon Seismic Province volume and the 07GA-IG1, 07GA-IG2, 07GA-GC1 and 07GA-A1 seismic lines.*

Agwamin Seismic Province

The Agwamin Seismic Province abuts the Abingdon Seismic Province to the west. It has no surface expression, and is interpreted entirely from seismic reflection data. Its architecture is constrained by the 07GA-GC1 and 07GA-A1 seismic lines (Figure 4.1.7), and it forms the lower crust beneath the Thomson Orogen. This interpretation is supported by the distribution of Sm-Nd model ages and inherited zircon data, which show that this region displays significantly younger zircon ages than in the Etheridge Province to the west.

The southern and northern extents of this province are currently unknown. This is broadly due to the lack of available seismic reflection data over these areas. There are, however, some generalised trends in the Sm-Nd data that indicate the Agwamin Seismic Province does not extend much further west than the interpreted region in the 3D map (see Figures 4.1.1 and 4.1.7).

Etheridge and Kowanyama provinces

The extent of the Etheridge Province is constrained by the surface outcrop of Paleoproterozoic rocks. These rocks terminate against the Lynd Mylonite Zone, with Thomson Orogen and Broken River Province to the east. To the northeast, units in the Etheridge Province units terminate against the Hodgkinson Province and the Palmerville Fault (Figure 4.1.8). The subsurface architecture of the eastern and northeast boundaries was interpreted using the 07GA-GC1 and 07GA-A1 seismic lines. The 07GA-GC1 seismic line indicates that the eastern termination of the Etheridge Province tapers to the east at depth and overlies the Abingdon Seismic Province (Henderson et al., 2009; Withnall et al., 2009a). This probably reflects the original architecture, whereas the Lynd Mylonite Zone represents a large approximately west-dipping thrust that has juxtaposed the Etheridge Province over the younger units to the east. The subsurface architecture of the northeastern boundary of the Etheridge Province is interpreted on the 07GA-A1 seismic line. At this location, it has the same

architecture as that on the 07GA-GC1 seismic line, but at this location the east-dipping Palmerville Fault thrusts units of the Hodgkinson Province over the northern extension of the Lynd Mylonite Zone. At this location the subsurface Lynd Mylonite Zone has a north-northwest trend.

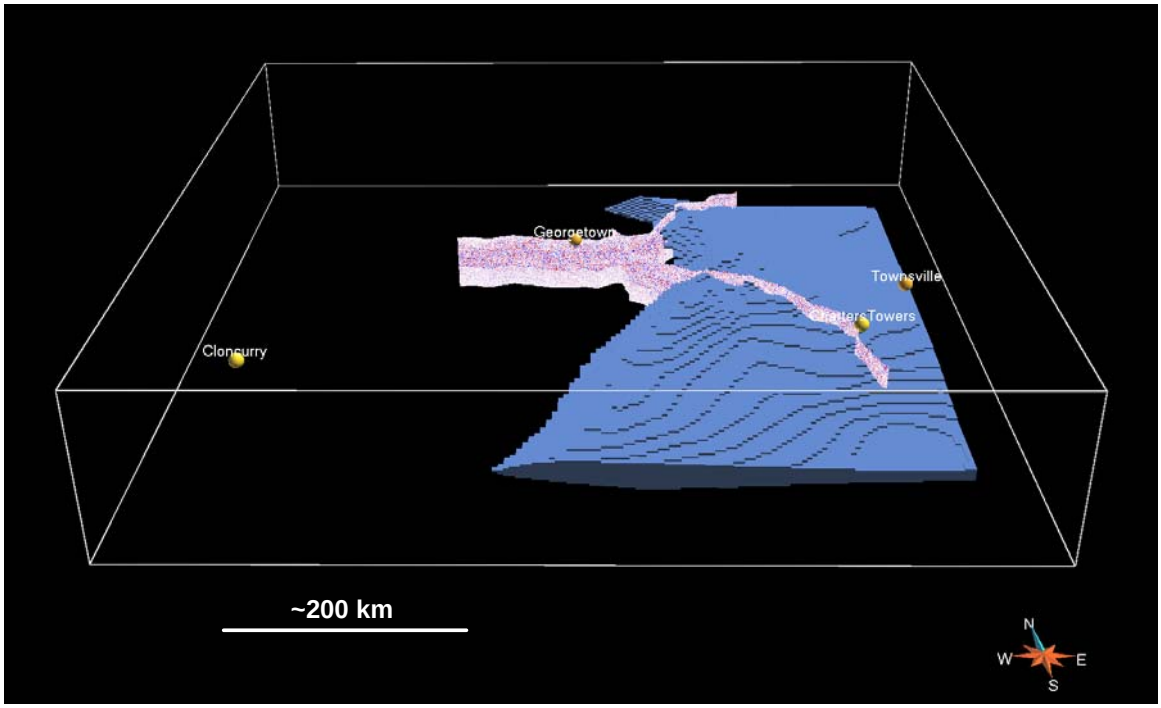

Figure 4.1.7: *3D perspective image from GOCAD™ of the Agwamin Seismic Province volume and the 07GA-IG2, 07GA-GC1 and 07GA-A1 seismic lines.*

Seismically, the Etheridge Province is less reflective than the underlying Abingdon Province, and its base is reasonably well defined on the 07GA-GC1 and 07GA-A1 seismic lines (Henderson et al., 2009; Withnall et al., 2009a). This provided depth constraints at the location of the seismic lines and due to no other regional constraints, these depths and geometries were extrapolated out from the seismic lines in 3D. The western extent of the Etheridge Province is unknown as the younger Carpentaria and Eromanga Basins overlie it. Seismically, the reflectivity of the Etheridge Province is difficult to differentiate from the Kowanyama Province to the west, and there is no clearly defined break between them. In fact, the characteristic reflectivity of the Etheridge Province can be interpreted from the 07GA-IG1 seismic line as continuing through to the Mount Isa Province. Due to the lack of clearly defined differences, it is interpreted here that the Etheridge Province, the Kowanyama and parts of the Mount Isa Province units are lateral equivalents. This is partially supported by the upper Mount Isa Province units being temporal equivalents of the Etheridge Province.

The interpreted eastern boundary of the Etheridge Province (the Lynd Mylonite Zone) is broadly north-northeast trending. Potential field data indicate that this structure may continue to the southwest and truncate the north-northwest trending gravity and magnetic highs of the Mount Isa Province. If this interpretation in correct, then the evolution of the Lynd Mylonite Zone as interpreted on the 07GA-GC1 and 07GA-A1 seismic lines (Henderson et al., 2009; Withnall et al., 2009a) and the geodynamic interpretation (Figure 4.1.2) described previously, can provide insights into the timing of the truncation at the southern end of the Mount Isa Province and the breakup of Rodinia.

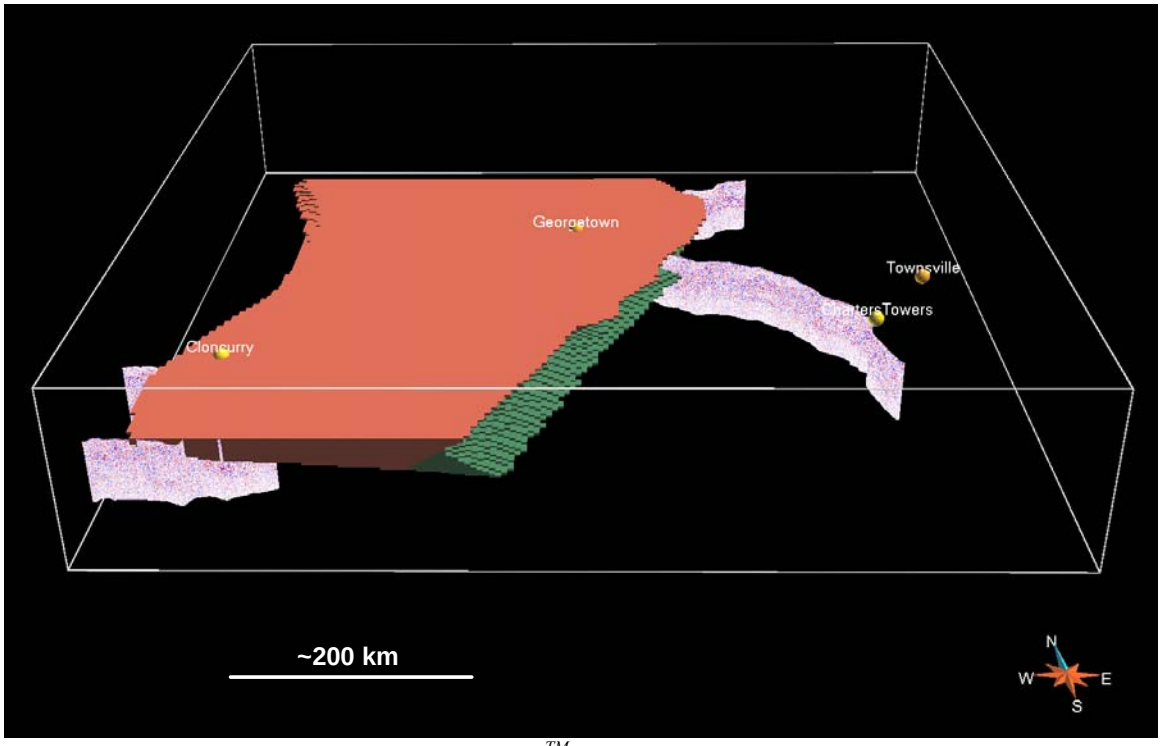

Figure 4.1.8: *3D perspective image from GOCAD™ of the combined Etheridge and Kowanyama province volume. Seismic constraints are 06GA-M4, 06GA-M5, 06GA-M6, 94MTI-01, 07GA-IG1 and 07GA-IG2 seismic lines (not all seismic lines are visible in this in image).*

Thomson Orogen (3D lateral province equivalents)

This province consists of the following lateral province equivalents:

- Anakie Province
- Barnard Province
- Cape River Province
- Greenvale Province
- Charters Towers Province

Analysis of the seismic reflection data has enabled a new understanding of the relationships between provinces that are temporally similar. Interpretation of the seismic reflection lines 07GA-GC01 and 07GA-A1 has shown that that the Cape River Province, Greenvale Province and Charters Towers Province, although spatially separated at surface, can be linked at depth into a single province. Additionally, the temporally-equivalent Anakie Province and Barnard Province, located just to the south and east respectively of the seismic reflection lines could also be lateral equivalents, although this interpretation is not constrained by the seismic data. These combined provinces will be referred to here as the Thomson Orogen due to its similarities to the provinces to the south. The southern end of the 07GA-GC01 seismic line images the northern part of the Drummond Basin. The subsurface geometry of the Thomson Orogen was extrapolated to the west and east at a constant depth due to no other available constraints (Figure 4.1.9).

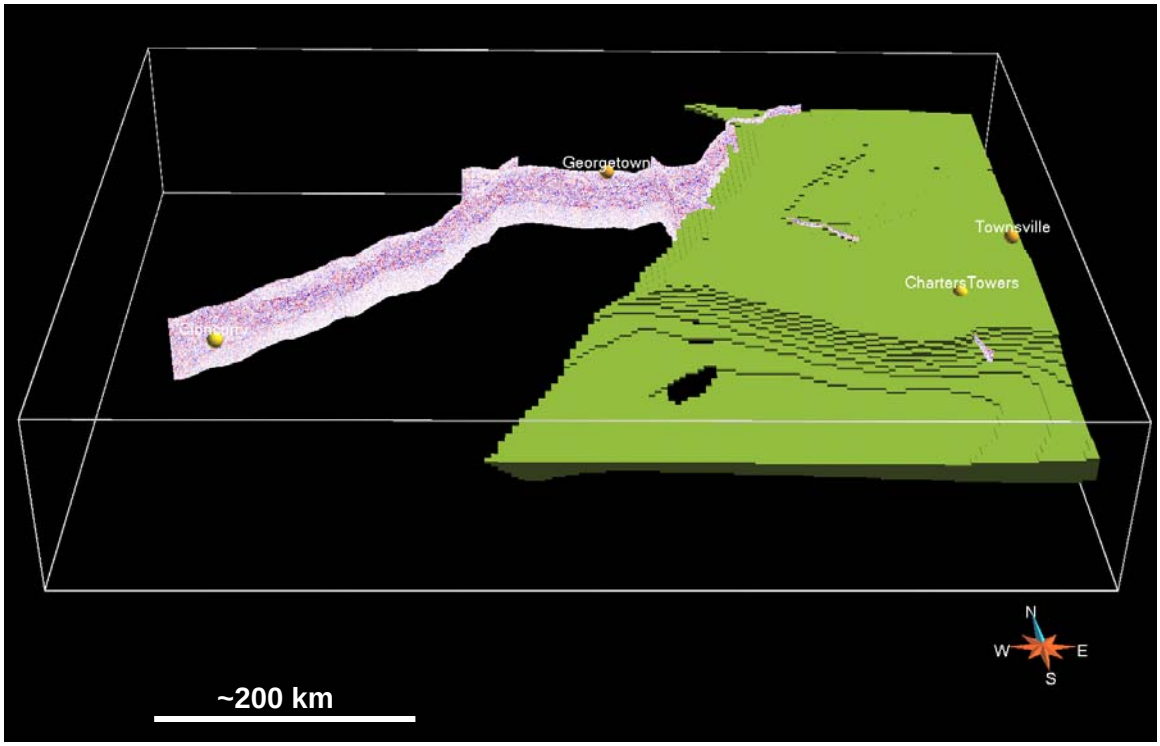

Figure 4.1.9: *3D perspective image from GOCAD™ of the Thomson Orogen volume and the 07GA-IG1, 07GA-IG2, 07GA-GC1 and 07GA-A1 seismic lines (not all seismic lines are visible in this in image).*

Combined Broken River and Hodgkinson provinces

The Broken River and Hodgkinson provinces have been combined in the 3D interpretation due the complexity of their boundaries. A volume was constructed of Broken River and Hodgkinson provinces depicting the component of this combined province that was thrust westwards over the units of the Thomson Orogen. A small component of the Broken River Province bordering the Etheridge Province was not been included in this study. The architecture for this interpretation was constrained by the 07GA-GC01 and 07GA-AU1 seismic lines (Figure 4.1.10).

Concluding remarks

Construction of 3D provinces has enabled a greater understanding of the depth component and relationships between the different geological provinces. The architecture of the different provinces, defined on the seismic reflection lines, has been extrapolated over the region using a variety of different data. These geometries have been constructed to best fit all available data. The current day architectures, combined with structural, geochonological and lithological constraints have enabled a greater understanding of the evolution of the region and helped to unravel a series of geodynamic processes that possibly operated at different time periods. These understandings have implications for targeting both sites of mineralisation and energy potential which are described in detail in Kositcin et al., (2009).

The 3D provinces were used in conjunction with the potential field inversions to constrain the distribution of crustal regions with different physical properties (Section 3.4).

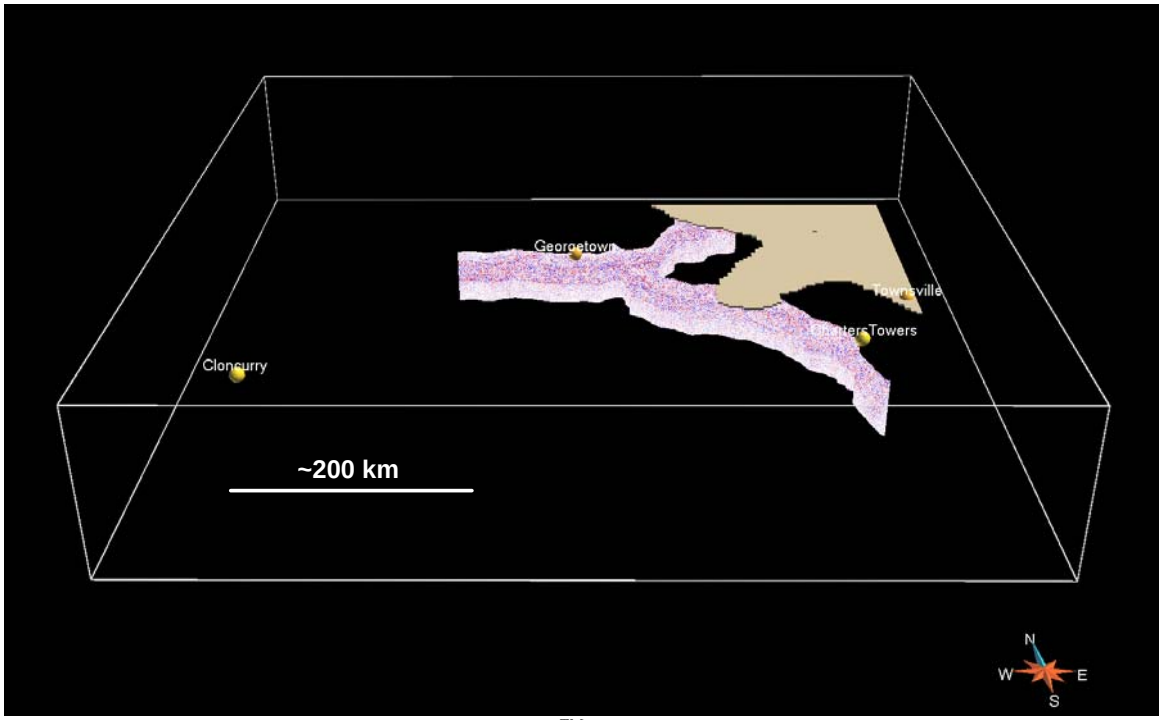

Figure 4.1.10: *3D perspective image from GOCAD™ of the combined Broken River-Hodgkinson province volume and the GA07-IG02, 07GA-GC1 and 07GA-A1 seismic lines.*

References

Betts, P.G. and Giles, D., 2006. The 1800-1100 Ma tectonic evolution of Australia. *Precambrian Research*, **144**(1-2), pp. 92-125.

Blewett, R.S. and Black, L.P., 1998. Structural and temporal framework of the Coen region, north Queensland: implications for major tectonothermal events in east and north Australia. *Australian Journal of Earth Sciences*, **45**(4), pp. 595-609.

Cihan, M., Evins, P., Lisowiec, N and Blake, K., 2006. Time constraints on deformation and metamorphism from EPMA dating of monazite in the Proterzoic Robertson River Metamorphics, NE Australila. *Precambrian Research*, **145**(1-2), pp. 1-23.

Champion, D.C. and Cassidy, K.F., 2008. Geodynamics: Using geochemistry and isotopic signatures of granites to aid mineral systems studies: and example from the Yilgarn Craton. In: Korsch, R.J. and Barnicoat, A.C., (Eds.), 2008, *New Perspectives: the foundations and future of Australian exploration – Abstracts for the June 2008 pmd*CRC Conference*. Geoscience Australia, Canberra, Record 2008/09, pp. 7-16.

Drummond, B.J, Goleby, B.R., Goncharov, A.G., Wyborn, L.A.I., Collins, C.D.N. and MacCready, T., 1998. Crustal-scale structures in the Proterozoic Mount Isa Inlier of north Australia: their seismic response and influence on mineralisation. *Tectonophysics*, **288**(1-4), pp. 43-56.

Fergusson, C.L., Henderson, R.A., Withnall, I.W. and Fanning, C.M., 2007. Structural history of the Gerrnvale Province, north Queensland: Palaeozoic extension and convergence of the Pacific margin of Gondwana. *Australian Journal of Earth Sciences*, **54**(4), pp. 573-595.

Henderson, R.A., 1987. An oblique subduction and transform faulting model for the evolution of the Broken River Province, northern Tasman Orogenic Zone. *Australian Journal of Earth Sciences*, **34**(2), pp. 237-239

Henderson, R.A., Fergusson, C.L., Collins, W.J., Henson, P.A., Korsch, R.J., Blewett, R.S., Withnall, I.W., Hutton, L.J., Costelloe, R.D., Champion, D.C., Blenkinsop, T.G., Wormald, R. and Nicoll, M.G., 2009. Geological interpretation of deep seismic reflection line 07GA-A1: The AuScope Mt Surprise to Mareeba transect. In: Camuti, K., and Young, D. (Eds.). *Northern Queensland Exploration and Mining 2009 and North Queensland Seismic and MT Workshop*. Australian Institute of Geoscientists Bulletin 49, pp. 169-173.

Hutton, L.J, Blewett, R.S., Henson, P.A., Withnall, I.W., Korsch, R.J., Nakamura, A., Collins, W.J., Henderson, R.A., Fergusson, C.L., Huston, D.L., Champion, D.C., Meixner, A.J., Nicoll, M.G., Blenkinsop, T.G. and Wormald, R., 2009a. Geological interpretation of deep seismic reflection line 07GA-IG2: The Croydon to Mt Surprise transect. In: Camuti, K., and Young, D. (Eds.). *Northern Queensland Exploration and Mining 2009 and North Queensland Seismic and MT Workshop*. Australian Institute of Geoscientists Bulletin 49, pp. 159-162.

Hutton, L.J., Gibson, G.M., Korsch, R.J., Withnall, I.W., Henson, P.A., Costelloe, R.D., Holzschuh, J., Huston, D.L., Jones, L.E., Maher, J.L., Nakamura, A., Nicoll, M.G., Roy, I., Saygin, E., Murphy, F.B. and Jupp, B., 2009b. Geological interpretation of the 2006 Mount Isa seismic survey. In: Camuti, K., and Young, D. (Eds.). *Northern Queensland Exploration and Mining 2009 and North Queensland Seismic and MT Workshop*. Australian Institute of Geoscientists Bulletin 49, pp. 137-141.

Korsch, R.J., Withnall, I.W., Hutton, L.J., Henson, P.A., Blewett, R.S., Huston, D.L., Champion, D.C., Meixner, A.J., Nicoll, M.G., and Nakamura, A., 2009. Geological interpretation of deep seismic reflection line 07GA-IG1: The Cloncurry to Croydon transect. In: Camuti, K., and Young, D. (Eds.). *Northern Queensland Exploration and Mining 2009 and North Queensland Seismic and MT Workshop*. Australian Institute of Geoscientists Bulletin 49, pp. 153-157.

Kositcin, N., Champion, D. C. and Huston, D.L., 2009. *Geodynamic Synthesis of the North Queensland Region and Implications for Metallogeny*. Geoscience Australia, Canberra. In prep.

Withnall, I.W., Korsch, R.J., Blewett, R.S., Henson, P.A., Hutton, L.J., Holzschuh, J., Saygin, E., Fergusson, C.L., Collins, W.J., Henderson, R.A., Huston, D.L., Champion, D.C., Nicoll, M.G., Blenkinsop, T.G. and Wormald, R., 2009. Geological interpretation of deep seismic reflection line 07GA-GC1: The Georgetown to Charters Towers transect. In: Camuti, K., and Young, D. (Eds.). *Northern Queensland Exploration and Mining 2009 and North Queensland Seismic and MT Workshop*. Australian Institute of Geoscientists Bulletin 49, pp. 163-167.

Withnall, I.W., Neumann, N.L. and Lambeck, A. 2009. Paleoproterozoic to Mesoproterozoic geology of North Queensland. In: Camuti, K. and Young, D., 2009. In: Camuti, K., and Young, D. (Eds.). *Northern Queensland Exploration and Mining 2009 and North Queensland Seismic and MT Workshop*. Australian Institute of Geoscientists Bulletin 49, pp. 129-134.

4.2 MAPPING ALTERATION IN 3D USING POTENTIAL FIELD DATA

N.C. Williams and R. Chopping

Introduction

The magnetic susceptibility and density of rocks are controlled primarily by mineralogy and porosity. The porosity of crystalline basement rocks is typically < 2 vol. % (e.g. Fowler et al., 2005); hence porosity has minimal influence on density in crystalline rocks, and most variations in density and magnetic susceptibility can be ascribed to variations in mineralogy. Although the mineralogy of a rock may be quite complex, only a relatively small subset of common rock-forming minerals have characteristic extreme properties. Primarily, these will include sulfide and oxide phases. Most silicate and carbonate minerals are paramagnetic, with susceptibilities less than 1×10^{-3} SI and densities approximately similar to the crustal average of 2.67 $g.cm^{-3}$. By assessing departures from this "least-altered" silicate or carbonate host rock, it is possible to predict the likely presence, and possibly approximate abundances of those minerals possessing more extreme properties.

Deterministic property inversions of gravity and magnetic data provide 3D models of estimated densities and susceptibilities capable of explaining the observed geophysical data. The physical properties recovered from the inversions can be interrogated to predict the mineralogy that would be required to explain any departures from the inferred host rock properties.

To predict the presence of, and improve the understanding of, the distribution of large alteration systems in the North Queensland region, this study derives predictions of the mineralogy that adequately could explain the predicted density and magnetic susceptibility models derived using the gravity and magnetic inversions presented in Section 3.4.

Two approaches are employed here, a qualitative approach and a quantitative approach. The qualitative approach identifies whether a specific mineral is likely to be present, or not, based on user-defined physical property thresholds and inferred host rock properties. In the quantitative approach, an optimisation routine is used to extract a numerical estimate of the required abundance of each candidate mineral, relative to a set of mineralogical constraints and an estimate of the host rock properties. The results of the qualitative approach are appropriate for initial target selection, and the quantitative approach can be used to impose specific mineral system models on the solution, and to rank prospective target areas.

The reliability of the 3D mineralogy maps predicted using these approaches is heavily dependent on several key limitations. The biggest limitation comes from ambiguity and nonuniqueness in the possible solutions. Consider minerals A and B in a host rock R. Mineral A has a density less than that of rock R, and mineral B has a density greater than that of rock R. All three have similar magnetic susceptibilities. Given a sample with density and susceptibility measurements equal to that expected for rock R, it is impossible to determine from the physical property measurements alone whether the density indicates that the sample is purely rock R, some mixture of minerals A and B, or some mixture of all three components. One solution is to include a model of the host rock geology in the volume of interest. This is possible where: (1) the geology is well known; (2) the geology is simple, with widespread and homogeneous units; or (3) where the physical property contrasts between the various host rock lithologies are small, and the dominant physical property variations come from alteration (e.g. Chopping and van der Wielen, 2009). None of these scenarios apply in the area covered by the North Queensland model.

The second important limitation comes from the uncertainty in the results from the gravity and magnetic inversions. As discussed in Section 3.4, these are limited by the paucity of gravity stations,

physical property knowledge, and the resolution of the inversion models. With cells 2 km wide, only those features that are larger than 6-7 km across will be resolved. Finally, the quality of physical property estimates for the inferred host rocks, and the uncertainty in those estimates, provides an additional limitation in an area such as this, where the 3D geology is poorly known.

Methods

Qualitative method

The qualitative estimates of a possible alteration assemblage are conducted using the concept of the alteration cone (Chopping and van der Wielen, 2009). Alteration cones are produced by trends away from the extreme properties of unaltered host rocks to alteration mineral(s). The concept of the alteration cone requires interpretation of trends in magnetic susceptibility and density. Alteration to different mineral assemblages produces different trends, when viewed on crossplots of magnetic susceptibility versus density (Figure 4.2.1). To simplify the interpretation, it is generally done using diagnostic end-member minerals. The alteration systems in North Queensland are best characterised by examining trends to magnetite and to hematite or sulfides. In general, magnetite alteration will produce cells which are both significantly denser and more magnetically susceptible than expected for unaltered host rocks; hematite and sulfides (predominantly pyrrhotite and pyrite) will produce predominantly denser results when compared to the properties of unaltered host rocks.

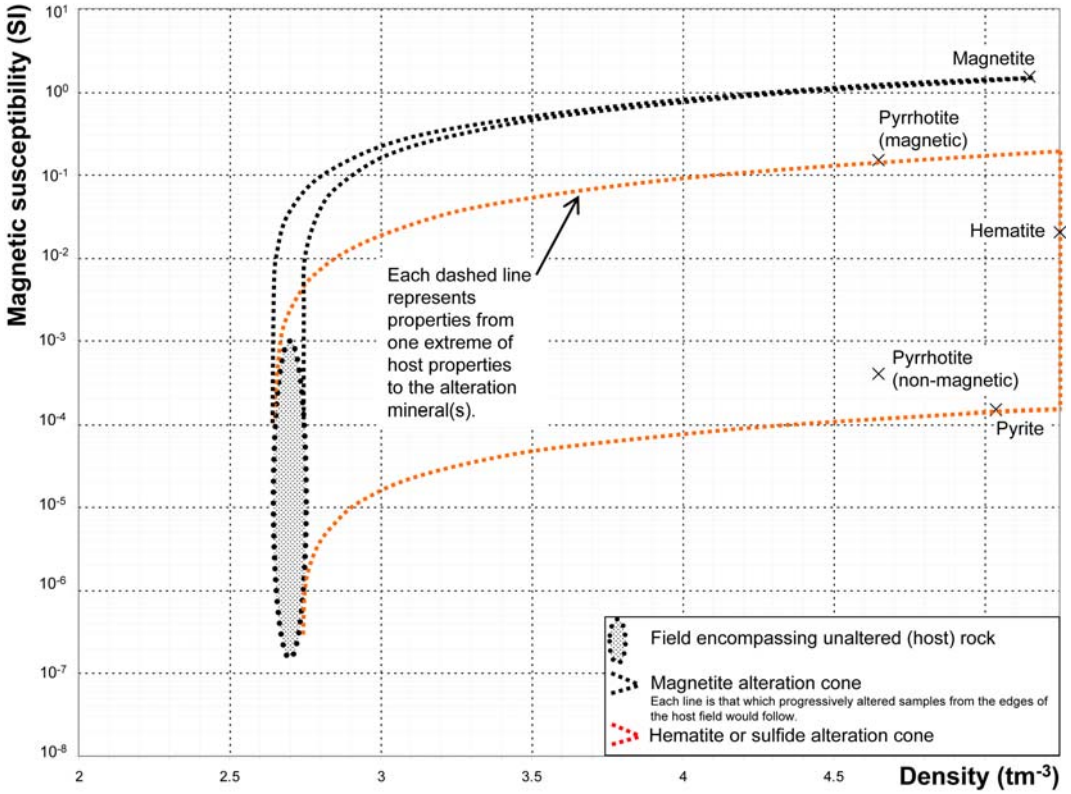

Figure 4.2.1: *Alteration trends to different end-member alteration minerals. In this example, alteration to magnetite versus alteration to either hematite or sulfides (such as pyrite or pyrrhotite) are shown.*

Examining Figure 4.2.1, it is obvious that there are regions of overlap between the alteration cones for magnetite and for hematite and sulfides. To simplify interpretation in this study, where very limited property contrasts between unaltered and altered rocks are observed, we calculate the Euclidean distance, in magnetic susceptibility-density space, to magnetite and hematite for each cell

in the inversion results. Cells which are altered, but plot within both alteration cones with properties closer to magnetite are thus attributed to be altered to magnetite, whereas cells with properties closer to hematite are attributed to be altered to magnetite or sulfides.

Quantitative method

The quantitative mineral estimates are obtained using a linear programming optimisation algorithm to solve a set of three linear equations, following the method described by Williams and Dipple (2007), based on the template outlined by Gordon and Dipple (1999). The three equations define the relationship between constituent component densities and susceptibilities and the total sample density and susceptibility, as described by Hanneson (2003):

$$\sum_{i=1}^{n} \kappa_i f_i = \kappa_{sample} , \quad 1$$

$$\sum_{i=1}^{n} \rho_i f_i = \rho_{sample} , \quad 2$$

$$\sum_{i=1}^{n} f_i = 1 , \quad 3$$

where κ_i and ρ_i are the magnetic susceptibility and density of the component i, f_i is the volume fraction of component i in the sample, n is the number of components in the sample, and κ_{sample} and ρ_{sample} are the magnetic susceptibility and density of the sample. The components on the left-hand side of the equations consist of the most common minerals expected to control the physical properties of the sample, plus one component that describes the properties of a barren silicate or carbonate host rock that contains none of the other component minerals.

These equations are modified to allow for uncertainty in each of the parameters by creating pairs of bounding inequality relations:

$$-\sum_{i=1}^{n} \kappa_i^{\max} \cdot f_i \le -\kappa_{sample}^{\min} \text{ and } \sum_{i=1}^{n} \kappa_i^{\min} \cdot f_i \le \kappa_{sample}^{\max} , \quad 4$$

$$-\sum_{i=1}^{n} \rho_i^{\max} \cdot f_i \le -\rho_{sample}^{\min} \text{ and } \sum_{i=1}^{n} \rho_i^{\min} \cdot f_i \le \rho_{sample}^{\max} , \quad 5$$

$$-\sum_{i=1}^{n} f_i \le -(1-\Delta v) \text{ and } \sum_{i=1}^{n} f_i \le (1+\Delta v) . \quad 6$$

Here, the superscripts max and min indicate the estimated maximum and minimum value for each parameter, and Δv is a small volume fraction that ensures that the solutions are only calculated to within an acceptable number of significant figures.

This set of equations can be solved for an arbitrary number of components using linear programming which seeks a solution to the set of equations 4-6 that satisfies:

$$\min_{\mathbf{x}} \mathrm{F}(\mathbf{x}) \text{ such that } \begin{cases} \mathbf{Ax} \le \mathbf{b} \\ \mathbf{lb} \le \mathbf{x} \le \mathbf{ub} \end{cases} , \quad 7$$

where F(**x**) is an objective function of the unknowns, **x**, of the form:

$$\mathrm{F}(\mathbf{x}) = \mathbf{c}^{\mathrm{T}}\mathbf{x} = c_1 x_1 + c_2 x_2 + \ldots + c_n x_n . \quad 8$$

where c_i is either -1 to maximise component i, or +1 to minimise component i. The vectors **lb** and **ub** contain the lower and upper bounds on the abundances of each component i. There will not be a

unique solution to the set of equations 4-6 as there are more unknowns than equations, so an objective function is chosen that minimises the possible amount of alteration in a sample. The solution that minimises the amount of alteration provides a useful conservative estimate of the abundance of each component in the sample, and is used throughout the rest of this study.

The densities in each inversion cell were assigned an uncertainty of ±0.03 g.cm-3, equal to 1 standard deviation of densities in the model, and the magnetic susceptibility was assigned an uncertainty of ±50 %.

To enhance the reliability of the solutions additional constraints based on geological or petrological relationships can be included directly in equation 7. These relationships take the form $f1 \geq f2$ to indicate that the volume fraction of component 1 ($f1$) is always greater than or equal to the volume fraction of component 2 ($f2$). Together, these relationships, and the mixing trends from sample to alteration minerals, provides the basis for the linear programming solution for the mineralogy for every inversion cell (Figure 4.2.2).

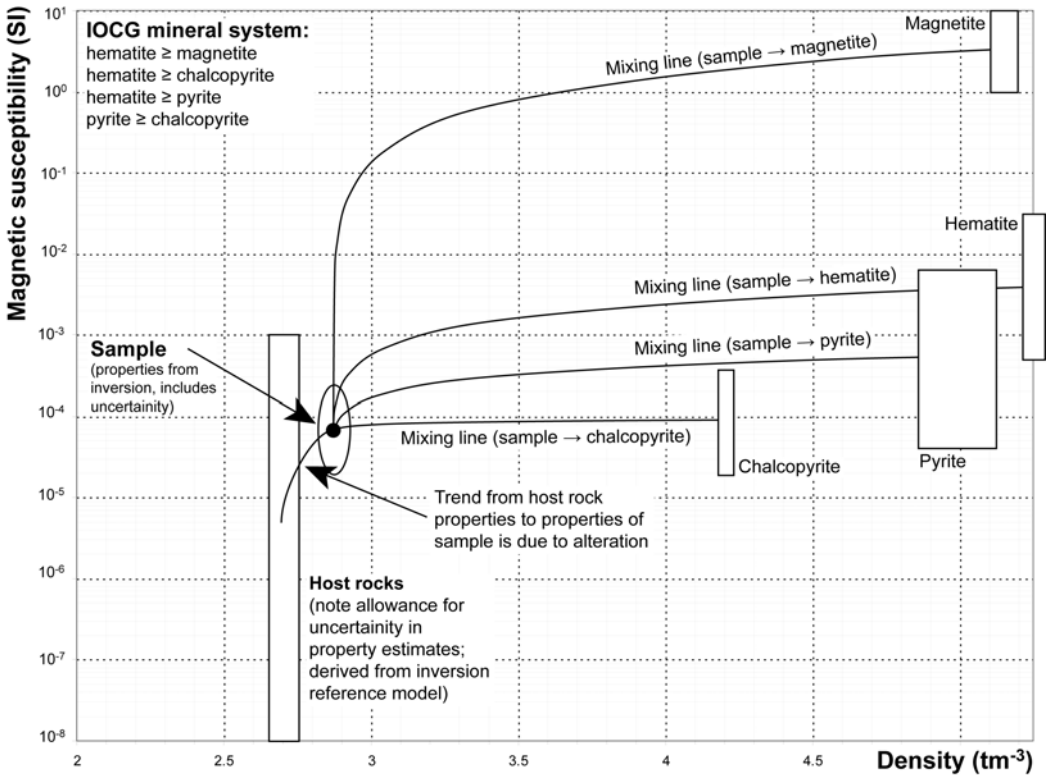

Figure 4.2.2: *Schematic representation of the relationship between the unaltered host rocks (the inversion reference model), a recovered sample (inversion cell properties), and alteration minerals. Constraints on the linear programming system used to solve for sample mineralogy are derived from studies of IOCG deposits in the North Queensland region. Effectively, the quantitative method seeks to resolve the difference between the sample and the reference properties in terms of the addition of alteration minerals. Although trend lines between the properties of the sample are shown in this diagram, in reality, an infinite number of mixing lines are present and the optimisation routine seeks to find the mixing trends that best explain the physical properties of the sample and minimise the amount of alteration predicted.*

In the North Queensland region, a solution based on the mineralogy expected for IOCG deposits, such as Ernest Henry, is obtained. Based on published descriptions of deposits in the area, this solution calculates the abundances of magnetite, hematite, chalcopyrite, pyrite, sericite, and barren host rock in each inversion cell, with constraints that magnetite ≥ hematite and pyrite ≥ chalcopyrite (Williams, 1998; Oliver et al., 2004). Published literature physical properties were used to establish the likely range of properties for each end-member minerals. For both the 3D map and Cloncurry model areas the inversion reference model of expected properties was used to define the barren host rock properties.

Mineralogy linked strongly to IOCG deposits is used because altered and mineralised rocks associated with IOCG deposits tend to have much higher contents of magnetite, hematite, and sulfide minerals, which contribute to stronger gravity and magnetic responses, making these minerals more amenable to predictive methods based on potential field data. Only the largest and richest Pb-Zn deposits will have significant gravity and magnetic anomalies over large enough areas to be reproduced within the coarse models used for this study.

Results

Qualitative method

As noted in the method section, qualitative interpretation of alteration trends for this study will involve significant overlap between fields expected for inversion cells showing alteration trends to magnetite and cells showing alteration trends to hematite or sulfides. To reduce this ambiguity, the Euclidean distance (in magnetic susceptibility-density space) to magnetite and hematite (the expected dominant alteration mineral in the hematite-sulfide field) was calculated. This was then used to discriminate between hematite or magnetite alteration, as well as define thresholds regarding the distance to either magnetite or hematite expected for altered cells (Figure 4.2.3).

Although the potential field inversions in the 3D map region extend to a depth of 25 km, analysis of alteration was only performed for cells to a depth of 4 km (Figure 4.2.4). The maximum depth of investigation of 4 km was used for this study as, although it is beyond the depth for exploration, the additional cells included by increasing the depth of interest of this study provides a better measure of the properties expected for unaltered rocks.

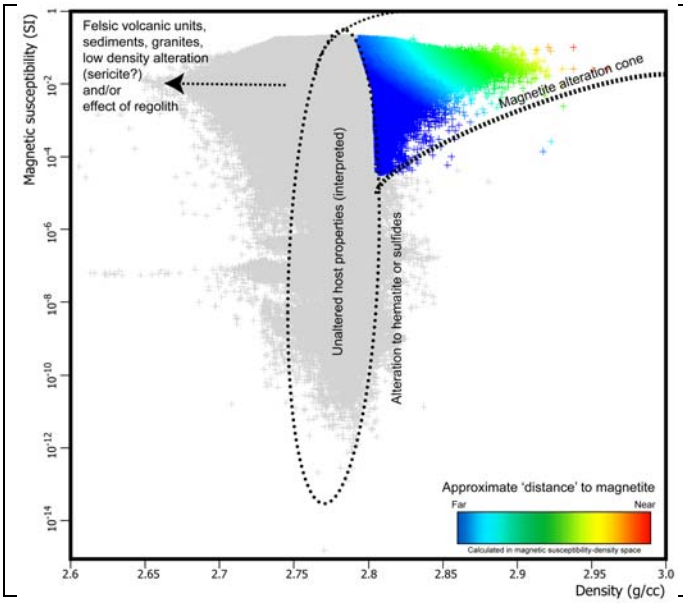

Figure 4.2.3: *Magnetic susceptibility-density for inversion cells in the Mount Isa Province, with cells plotting within the magnetite alteration cone coloured by their approximate distance to magnetite. Analysis for distance to hematite (not shown) was also performed, to distinguish between the two alteration types.*

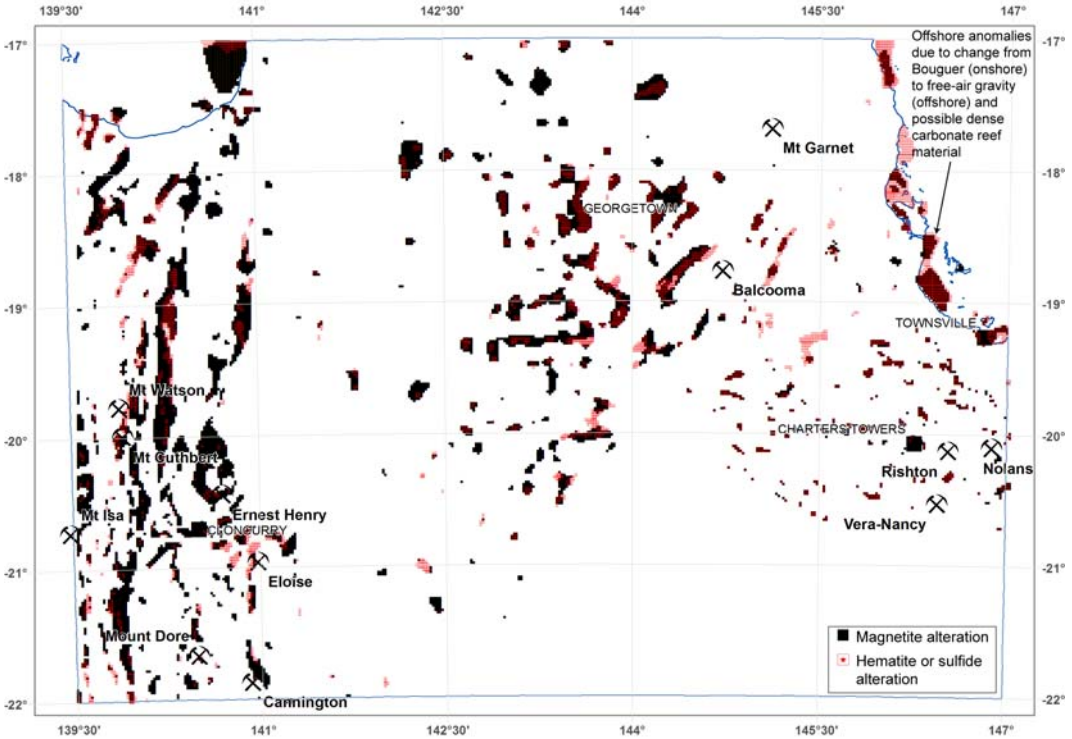

Figure 4.2.4: *Results of the qualitative alteration mapping in the 3D map area, to a depth of 4 km. Filled black squares denote alteration to magnetite; red squares with red stars indicate hematite alteration. Overlapping hematite and magnetite alteration occurs in regions where there is a change in alteration type with depth. Many of the IOCG deposits, such as Ernest Henry and Eloise, are mapped by this analysis. Note that a large number of mapped alteration, especially magnetite, are of a scale more typical of lithological features rather than alteration systems and thus may be mapping more mafic units in each of the provinces, rather than mapping alteration.*

Quantitative method

As for the qualitative alteration mapping, all calculated sulfide abundances are combined with hematite to create a total abundance of "sulfides plus hematite", which represents the most-dense, least-magnetic alteration assemblages. Note that quantitative alteration mapping produces abundances of alteration minerals across the region; for display here we use contours from the inversion volume of predicted magnetite, and hematite or sulfides (Figure 4.2.5).

South Cloncurry inversion

The south Cloncurry inversion (Section 3.4), as opposed to the 3D map inversion, had no prior constraints provided, and thus the recovered properties are significantly more speculative than the 3D map inversion results. Prominent alteration anomalies present in the 3D map qualitative results are not as apparent in the south Cloncurry inversion results (Figure 4.2.6). As the properties are less reliable than those for the 3D map inversion results are, the discussion here will centre around the qualitative alteration results only, and how they compare to the results from the 3D map region; the quantitative alteration results show very similar results to the qualitative alteration mapping results. Furthermore, as the depth of cover increases to the south in the south Cloncurry inversion, less alteration is mapped. This is due to the attenuation of the recovered properties because of the effect of thicker sediments of the Eromanga Basin. As the inversion cells are 1 km tall, 500 m of sediments of the Eromanga Basin will serve to significantly reduce the density in the topmost inversion cells, which will then serve to mask any signatures of alteration.

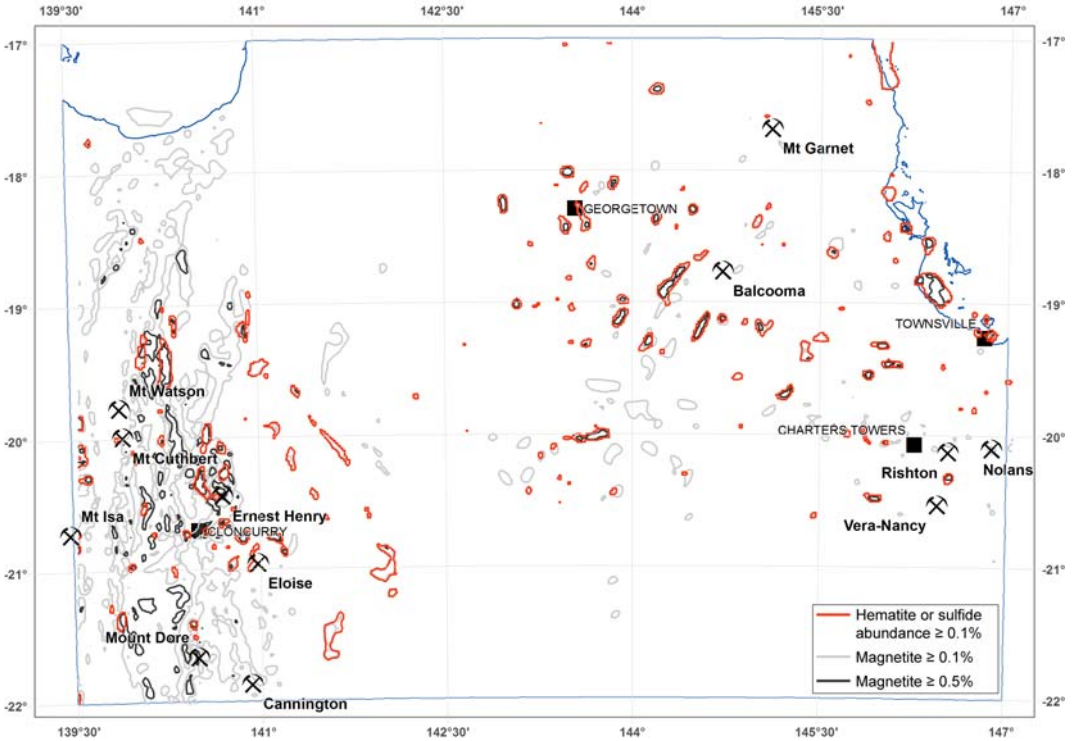

Figure 4.2.5: *Results of the quantitative alteration mapping in the 3D map area, for a depth slice between 0 and 1 km. Light grey lines indicate magnetite abundance ≥ 0.1% per 4 km^3, and dark grey lines indicate magnetite abundance ≥ 0.5% per 4 km^3. Red lines indicate hematite or sulfide abundance ≥ 0.1% per 4 km^3. This technique maps many of the IOCG deposits, such as Ernest Henry or Eloise. Note that a large number of mapped alteration, especially magnetite, are lithological in scale and thus may be mapping more mafic units in each of the provinces, rather than mapping alteration.*

Discussion and conclusions

As expected, given the complex geology and poor prior knowledge of the distribution of geological units, the areas predicted to contain anomalous sulfides and oxides could correlate strongly with the inferred distribution of geological units. This results commonly in the predicted volumes of alteration minerals being much larger than any likely alteration system. Such volumes are more likely to represent gaps in our understanding of the geology of the host rock, and likely indicate the presence of host rocks with more anomalous properties than anticipated, such as magnetic granites and gneiss, or denser mafic rocks. Only the smaller anomalies are candidates as possible hydrothermal alteration systems.

Some deposits, including significant deposits such as Cannington, are not associated with any predicted mineralogy anomalies (Figure 4.2.4 and 4.2.5). This is due to two reasons: firstly, the alteration at some deposits is insufficient in abundance to produce a noticeable physical property contrast against the background host rocks, and secondly, all of these interpretations seek to minimise the amount of alteration interpreted or recovered. More anomalous regions are able to be defined, either by adjusting the cut-offs of mineral proportions or reducing the expected unaltered host rock properties. These will provide more anomalous volumes at the expense of additional false positives as well as mapping features due to lithologies rather than alteration systems.

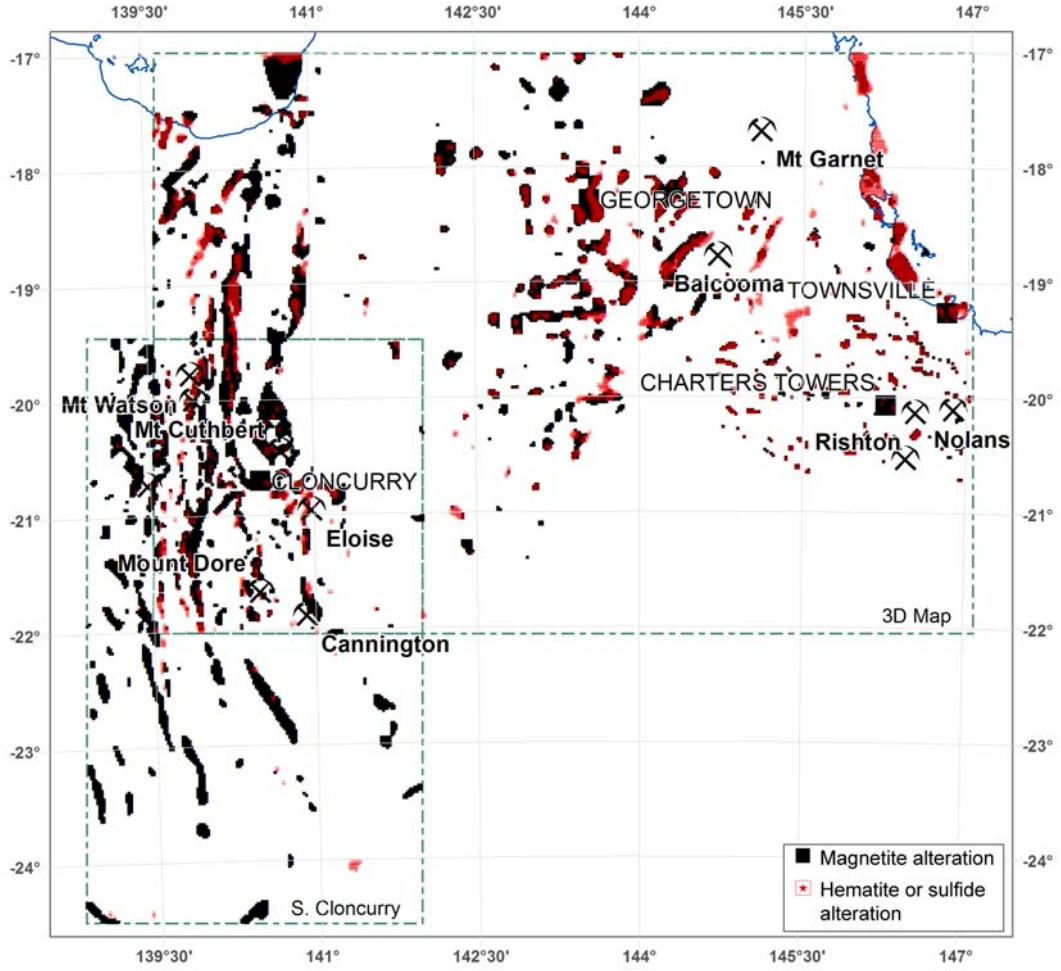

Figure 4.2.6: *Qualitative alteration mapping results for both the 3D map and south Cloncurry areas. Although similar alteration patterns are recovered where the two inversions overlap, the alteration anomalies in the south Cloncurry inversion generally are smaller in volume, reflecting the more attenuated properties of the unconstrained inversion. Added to this, as the depth of younger cover increases to the south, less alteration is predicted due to the reduction in density caused by the thicker sediments of the Eromanga Basin overlying the basement.*

The Eloise and Ernest Henry IOCG deposits lie along the margins of large coincident volumes of predicted anomalous sulfides and magnetite (Figure 4.2.7). Ernest Henry lies along a small finger of predicted sulfide and hematite on the flank of a voluminous magnetite anomaly. Eloise lies adjacent to another large predicted sulfide and hematite anomaly, with some association with magnetite. The size of these volumes suggests that they are beyond the scale of hydrothermal mineralising systems and may indicate an association with a particular host unit. This association is with a host rock, which is either with dense host rocks or with host rocks associated with reverse polarity remanent magnetisation that would act to reduce the strength of the predicted magnetic anomaly. An element of hydrothermal alteration is most likely present but unable to be discriminated from lithological responses, given the poor prior 3D geological knowledge. Discrimination of alteration systems from lithological features may be possible with a more detailed 3D geological model.

The Eloise and Ernest Henry IOCG deposits are also able to be mapped with the south Cloncurry inversion although the alteration signatures, especially the hematite or sulfide signatures, are reduced and interpretation is more difficult (Figure 4.2.8).

The Mount Elliott ICOG deposit is associated with a predicted sulfide and hematite anomaly, which is small enough that it could be wholly explained by the presence of alteration (Figure 4.2.9). This feature sits within a larger magnetite anomaly. Similar anomalies are predicted 10 km and 25 km north of Mount Elliott, the northernmost correlating with the location of the early 20th century Cu-Au Hampden and Kuridala mines. Although not shown in Figure 4.2.9B, the hematite or sulfide concentration at the Hampden-Kuridala area is approximately 0.07% per 4 km^3, just below the 0.1% per 4 km^3 contour cutoff that was used. The Starra and Mount Dore deposits, 14 km south of Mount Elliott, are associated with magnetite; the qualitative alteration mapping also indicates a possible presence of hematite or sulfides, although, these hematite or sulfide anomalies are borderline with magnetite anomalies.

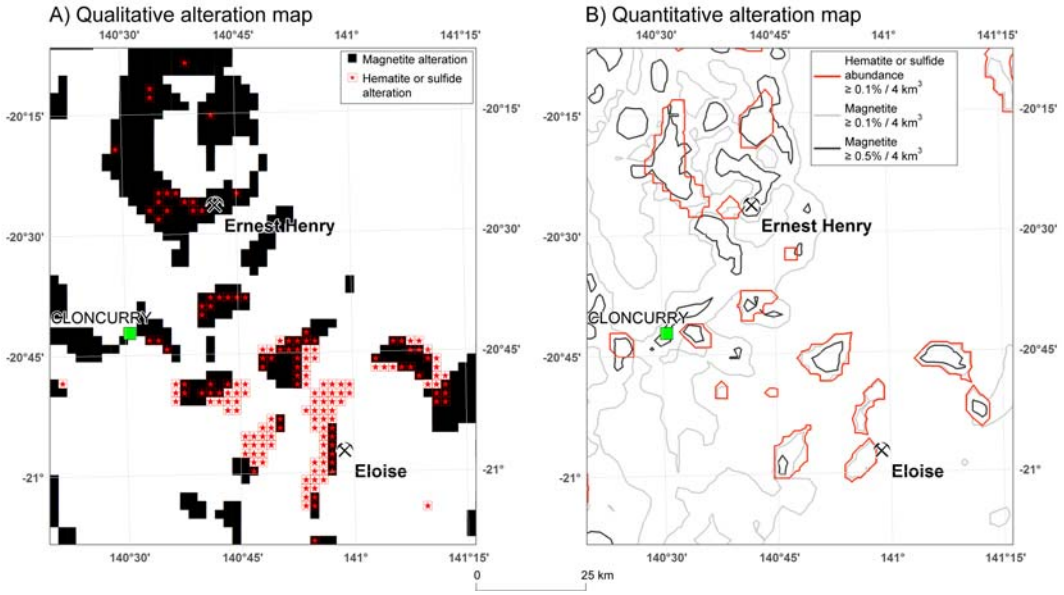

Figure 4.2.7: *Comparison between (A) qualitative alteration mapping and (B) quantitative alteration mapping over the Ernest Henry and Eloise deposits.*

Mapping of features due to anomalies dense or magnetic lithologies as mineralogical anomalies is perhaps the biggest downside to applying this technique to regional-scale models. Distinguishing these lithological features from alteration generally requires a robust geological model at a scale that is far more detailed than is feasible for regional-scale work. Alternatively, one can interpret lithological features due to their scale, which is often far in excess of that expected for the footprint of a hydrothermal system. Even so, these results indicate that some of the lithological-scale features also are associated with mineralisation. Successful targeting using this technique requires careful teasing out of the lithological from the alteration anomalies.

The alteration mapping work here also indicates that, for the best possible alteration mapping results, one requires the best physical property resolution available from the region. This implies the use of geologically constrained inversions. Traditionally, a constrained inversion is viewed as a product where a strong geological model is utilised as the reference property model; modern techniques allow for the inclusion of any geological knowledge such as outcrop geology, drillholes and depth to crystalline basement, assuming appropriate knowledge of physical properties. These modern techniques, demonstrated by Williams (2009), do not require building of a full geological model, but still serve to increase the physical property resolution of the recovered inverse models.

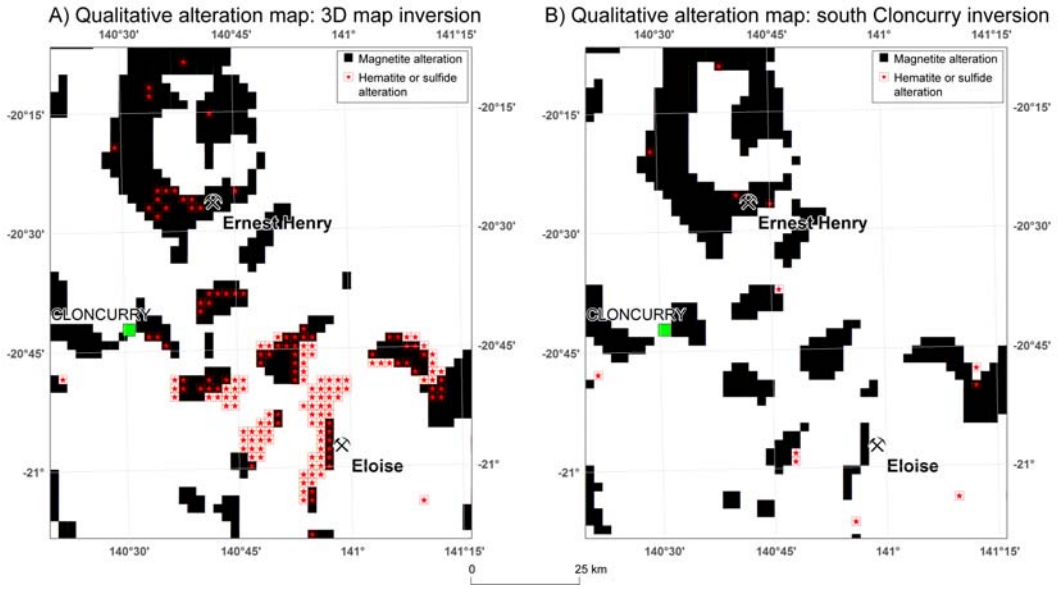

Figure 4.2.8: *Comparison between qualitative alteration interpreted from (A) 3D map inversion, which was constrained by properties for each province in the 3D map and (B) the south Cloncurry inversion, which was run as an unconstrained inversion.*

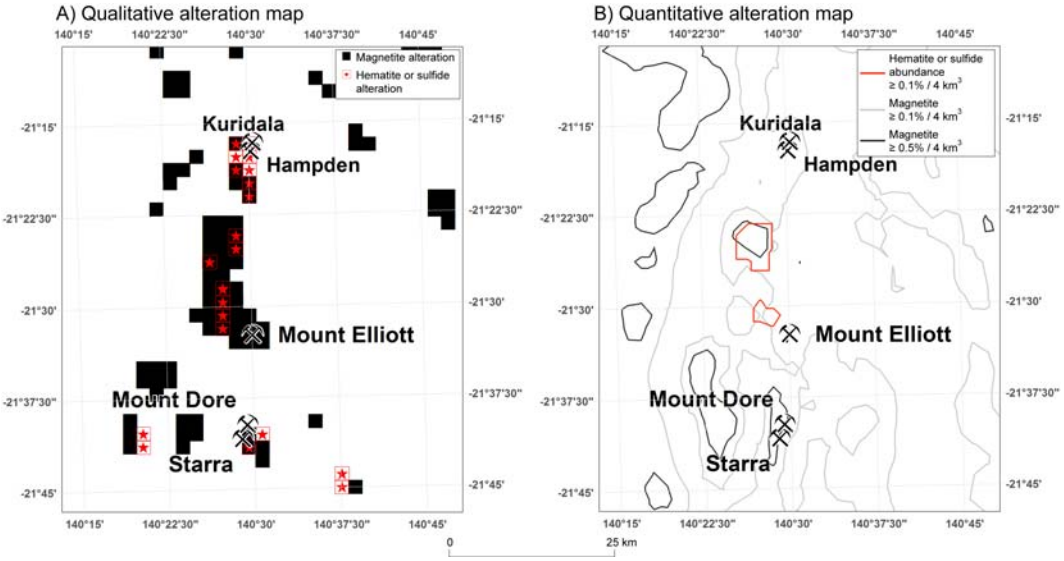

Figure 4.2.9: *Comparison between (A) qualitative alteration mapping and (B) quantitative alteration mapping over the Mount Elliott, Mount Dore and Starra regions. Also depicted are the locations of the early 20th Century Hampden and Kuridala mines.*

The results in this region are also limited by the available gravity data (Section 2.2). The inversions require downsampling of the magnetic data to ~ 2 km data, whereas the gravity data are sampled at an average of 4 km station spacings across the region, because, in some areas stations are up to 11 km apart. Better gravity coverage would provide for better inverse results, and hence better alteration mapping results.

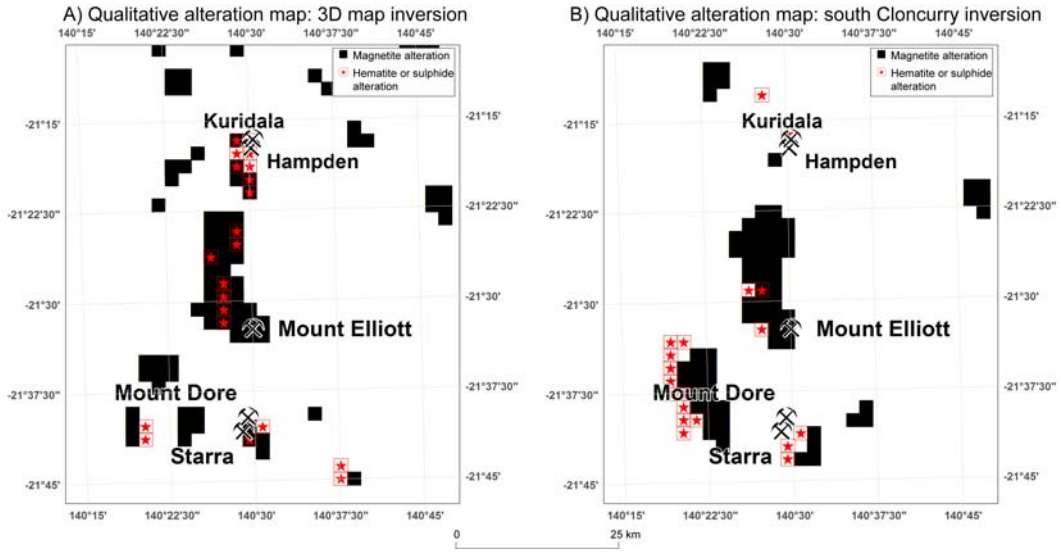

Figure 4.2.10: *Comparison between qualitative alteration interpreted for a common area from (A) 3D map inversion, which was constrained by geological provinces and (B) south Cloncurry inversion, which was run as an unconstrained inversion. Note that some deposits, such as Kuridala and Hampden, are able to be resolved by the constrained inversion, but not by the unconstrained inversion.*

Suggestions for future work

Alteration mapping using inverse modelling results is a relatively new technique for regional mineral system mapping. From this study, the following suggestions for future work are evident:

- Integration of information such as outcrop geology, depth to basement, and rock properties, to constrain inversions such as the south Cloncurry inversion, and
- The use of more detailed geological models in provinces such as the Mount Isa Province to better distinguish alteration from lithology.

Ultimately, the success of alteration mapping by the methodologies presented here requires the following geological factors:

- Large homogenous rock packages to reduce lithological effects, or
- Host rocks with limited physical property contrasts to each other, or
- A robust geological model to reduce the mapping of lithology as alteration and vice-versa, and
- Alteration to assemblages which produce strong physical property contrasts to the host rocks.

The following geophysical factors also influence the success of these techniques:

- Geophysical data coverage at a resolution similar to that required for the inversions, such as gravity at ~ 2 km station spacings for these inverse results, and
- Better knowledge of the physical properties of unaltered host rocks, to provide for better constraints on the inversions, and to better define the properties of unaltered host rocks, which reduces ambiguity in the alteration interpretations.

References

Chopping, R. and van der Wielen, S.E., 2009. Querying potential field inversions for signatures of chemical alteration: An example from Cobar, NSW. Australian Society of Exploration Geophysicists, *Preview*, **138**, Proceedings of the 20th International Geophysical Conference and Exhibition, Adelaide.

Fowler, C.M., Stead, D., Pandit, B.I., Janser, B.W., Nisbet, E.G. and Nover, G., 2005. A database of physical properties of rocks from the Trans-Hudson Orogen, Canada. *Canadian Journal of Earth Sciences*, **42**(4), pp. 555-572.

Gordon, T.M. and Dipple, G.M., 1999. Measuring mineral abundance in skarn; II, A new linear programming formulation and comparison with projection and Rietveld methods. *The Canadian Mineralogist*, **37**(1), pp. 17-26.

Hanneson, J. E., 2003. On the use of magnetics and gravity to discriminate between gabbro and iron-rich ore-forming systems. *Exploration Geophysics*, **34**(1-2), pp. 110-113.

Oliver, N.H.S., Cleverley, J.S., Mark, G., Pollard, P.J., Fu, B., Marshall, L.J., Rubenach, M.J., Williams, P.J. and Baker, T., 2004. Modelling the role of sodic alteration in the genesis of iron oxide-copper-gold deposits, Eastern Mount Isa Block, Australia. *Economic Geology*, **99**(6), pp. 1145-1176.

Williams, N.C., and Dipple, G.M., 2007. Mapping subsurface alteration using gravity and magnetic inversion models. In Milkereit, B., *Proceedings of Exploration 07: Fifth Decennial International Conference on Mineral Exploration*, pp. 461-472.

Williams, N.C., 2009. An automated spare constraint model builder for UBC-GIF gravity and magnetic inversions. Australian Society of Exploration Geophysicists, *Preview*, **138**, Proceedings of the 20th International Geophysical Conference and Exhibition, Adelaide.

Williams, P.J., 1998. An introduction to the metallogeny of the McArthur River-Mount Isa-Cloncurry minerals province. *Economic Geology*, **93**(8), pp. 1120-1131.

4.3 PRELIMINARY INVESTIGATION OF GRANITES BENEATH THE MILLUNGERA BASIN

R. Chopping, I.G. Roy and D.L. Huston

Potential field inversions (Section 3.4) provide an insight into the physical properties, and hence the composition (e.g. lithology or alteration – see Section 4.2, above) of subsurface units, including those that do not crop out. The seismic interpretation for line 07GA-IG1 (Korsch et al., 2009) mapped four bodies located directly beneath the Millungera Basin, which have seismic character and geometries akin to that expected for granites.

The potential field inversion results suggest that these bodies have very different properties, especially their densities (Figure 4.3.1). The differences in properties are important in understanding the composition of the bodies, which, in turn, has implications for the geothermal potential of the Millungera Basin.

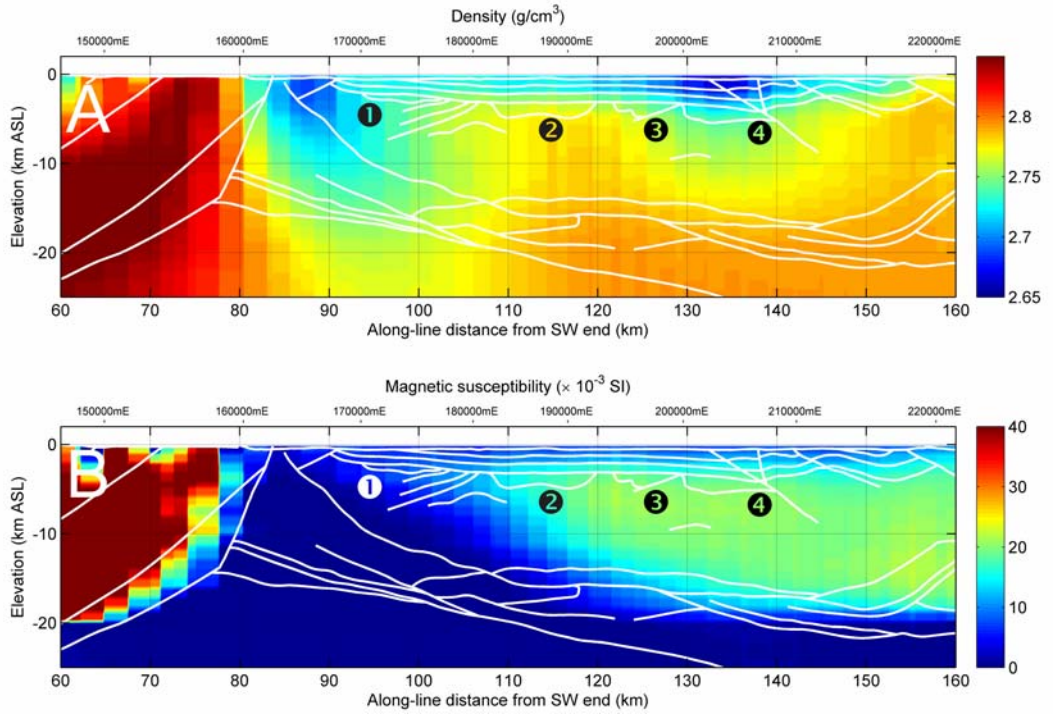

Figure 4.3.1: *The four bodies (labelled 1 through 4) beneath the Millungera basin, which show geometries expected for granites, show very differently physical properties in the inversion results (A – density along seismic line 07GA-IG1, B – magnetic susceptibility along seismic line 07GA-IG1).*

Of these bodies, the easternmost body (4 on Figure 4.3.1) shows the lowest density (~2.71 g.cm^{-3}) recovered in the inversion, followed by the westernmost body (1 on Figure 4.3.1, recovered density ~ 2.72 g.cm^{-3}). Body 2 shows the highest density – at approximately 2.78 g.cm^{-3}; it has a density more typical of an andesite (Telford et al., 1990). Furthermore, the inversion recovers densities that are smoothed out over a spatially larger area than the bodies themselves (Section 3.4), which will serve to reduce the amplitudes of the recovered densities. As bodies 1 and 4 show densities lower than the average surrounding densities, a less smooth inversion would reduce their densities below 2.7 g.cm^{-3}; and a less smooth inversion would increase the density of body 2 to above 2.8 g.cm^{-3}.

The magnetic susceptibilities of the bodies (Figure 4.3.1B) are less variable. Body 1 shows a low magnetic susceptibility; the other three bodies show higher magnetic susceptibilities. The broad magnetic susceptibility anomaly associated with the easternmost three bodies may reflect the magnetic susceptibilities of these bodies, or may also reflect the magnetic susceptibility of the Kowanyama Seismic Province that underlies the Millungera Basin.

Of these properties, density is more important in defining the primary lithology of the bodies. The lower density of bodies 1 and 4 suggest a felsic composition, and the higher density of body 2 is suggestive of a more intermediate to mafic composition. The magnetic susceptibilities of the bodies are not diagnostic of their composition: it is perfectly feasible to have felsic granites containing a small proportion of primary magnetite that would serve to produce a moderate magnetic susceptibility (Telford et al., 1990; Blevin, 2002). The magnetic susceptibility results, however, allow the recognition that bodies 1 and 4, although close in densities, and hence likely to be felsic in composition, are different: Body 4 is more likely to contain primary magnetite. This may then reflect a difference between a more oxidised (more likely to contain magnetite) and a more reduced (less likely to contain magnetite) granite (Blevin, 2002).

The composition of the bodies has significance for the geothermal resource in the Millungera Basin. Hot dry rock geothermal plays require a heat source, generally in the form of a high-heat producing (i.e. containing a high proportion of radioisotopes) granite, and blanketing sediments (preferably thick) with a low thermal conductivity (Baria et al., 1999). Heat production is a function of the concentrations of uranium, thorium and potassium, which are concentrated in felsic magmas compared with more mafic magmas (e.g. Plant et al., 1999)

Further work is required to define the geothermal resource of the Millungera Basin. More detailed and accurate inversions, including inversions with additional constraints to better define the physical properties of these bodies, are required along with studies targeted at characterising the sediments of the Millungera Basin.

References

Baria, R., Baumgärtner, J., Rummel, F., Pine, R.J. and Sato, Y., 1999. HDR/HWR reservoirs: concepts, understanding and creation. *Geothermics*, **28**(4-5), pp. 533-552.

Blevin, P., 2002. An Integrated Redox Classification Scheme for Granitic Rocks. In: Blevin, P, *Igneous Metallogenic Systems of Eastern Australia*, AMIRA P515 Final Report, AMIRA International, Melbourne, 36p.

Korsch, R.J., Withnall, I.W., Hutton, L.J., Henson, P.A., Blewett, R.S., Huston, D.L., Champion, D.C., Meixner, A.J., Nicoll, M.G., and Nakamura, A., 2009. Geological interpretation of deep seismic reflection line 07GA-IG1: The Cloncurry to Croydon transect. In: Camuti, K., and Young, D. (Eds.). *Northern Queensland Exploration and Mining 2009 and North Queensland Seismic and MT Workshop*. Australian Institute of Geoscientists Bulletin 49, pp. 153-157.

Plant, J.A., Simpson, P.R., Smith, B. and Windley, B.F., 1999. Uranium ore deposits: products of the radioactive earth. *Reviews in Mineralogy and Geochemistry*, **38**, pp. 255-319.

Telford, W.M., Geldart, L.P. and Sheriff, R.E., 1990. *Applied Geophysics (Second Edition)*. Cambridge University Press, Cambridge, 790p.

5. Conclusions

P.A. Henson and R. Chopping

5.1 CONCLUSIONS

The aim of this study was to utilise all the available data and integrate these data using 3D technologies. Combining the new and existing data in the North Queensland region has enabled a new understanding of the 3D architecture and geodynamics, as well as the mineralisation and energy potential, of the North Queensland region. These studies will provide valuable regional datasets that can be utilised by a variety of end users. Supporting geophysical studies, such as depth to basement modelling or forward and inverse modelling of potential field data, also shed light on the potential of the region.

The depth to basement modelling of the North Queensland and Georgetown region provides the most up to date assessment of this critical exploration parameter across a wide region of Queensland.

Geophysical studies, such as forward modelling of gravity data and inverse modelling of the gravity and magnetic data, allow the refinement of seismic interpretations and also allows the interpretation of geology in 3D, including in areas under significant cover. The inverse modelling also allows 3D alteration mapping to be performed. Worms, and fault length interpretations, are another interpretation that can indicate longer-lived or deeper penetrating structures.

Construction of 3D provinces has enabled a greater understanding of the depth component and relationships between different geological provinces. The architecture of the different provinces, defined on the seismic reflection lines, has been extrapolated over the region using a variety of different data. These geometries have been constructed to best fit all the available data and be internally consistent. The present-day architectures combined with structural, geochonological and lithological constraints have enabled a greater understanding of the evolution of the region and helped to unravel the series of geodynamic processes that have operated at different periods. These understandings have implications for targeting sites of mineralisation and energy potential.

The 3D provinces were used in conjunction with the potential field inversions to constrain the distribution of crustal regions and their different physical properties. In this way, direct linkages were made between the architecture derived from seismic reflection and other data with the observed potential field data. Furthermore, the use of the provinces to constrain the potential field inversions produces a more robust assessment of subsurface physical properties, allowing refined interpretation of the potential field inversion results to be made.

Alteration mapping, especially in the region of the 3D map, is able to locate many known IOCG deposits and can provide an assessment of additional targets. Although the alteration mapping results to the south of Cloncurry were more speculative, they provide some insight into the geometry of significant lithologies in an undercover region. Furthermore, integration of new geological data to better constrain potential field inversions will provide better assessments of the subsurface properties and hence allow more detailed and accurate alteration mapping to be undertaken.

Finally, the inversions provide a simple assessment of the properties, and hence composition, of the granites which occur beneath the Millungera Basin. Further work on these granites, including defining their geometries and further refining estimates of their composition and heat production capacity, will assist assessment of the geothermal potential of this region.